Development of LED-Based Instrumentation for the Monitoring of Water Quality Parameters

By
Thomas Murphy

A Thesis presented to
Dublin City University

For the degree of Master of Science

September 1995

School of Physical Sciences
Dublin City University
Ireland

Declaration

I hereby certify that this material, which I now submit for assessment on the programme of study leading to the award of M.Sc. is entirely my own work and has not been taken from the work of others, save and to the context that such work has been cited and acknowledged within the text of my work.

Signed: _____ **Date:** _____

Dedication

For Susanne and me Ma.

Acknowledgements

I would like to thank all at Aztec Ltd., firstly for making this project available and also for help with all the queries throughout the course of work. I would especially like to thank Neil Grant for his assistance with the chemistry and general information.

Al Devine, John Lynch, Joe Maxwell, Veronica Dobbyn and all the other technicians for their many and varied inputs.

For their comic relief, as much as technical assistance, I would like to thank the following people: Fergal Mc Aleavey, Ger O'Keeffe, Tom Butler, Des Lavelle, Aisling Mc Evoy, Fidelama Sheridan, John Maguire, Simon Mc Cabe, James Walsh and Fergus Connolly.

And finally, and most importantly, I would like to thank Dr. Brian Mac Craith. Thanks for all the patience and for giving me the opportunity to attempt this project.

Education is an admirable thing,
but it is well to remember from time to time,
that nothing that is worth knowing an be taught.

Oscar Wilde

Abstract

The development of LED based instrumentation for monitoring water quality is discussed. Many of the standard colorimetric tests for water quality monitoring coincide spectrally with widely available LED sources. Existing monitors use incandescent filament-based sources combined with narrow-band interference filters. Such systems suffer from problems of stability, bulk, cost and degradation with time. The replacement of such sources and filters with LED's overcomes many of these problems.

The initial experimental work involved identification of suitable LED's for detection of various analytes in water. In particular, LED's were selected on the basis of spectral match to standard colorimetric tests for species such as Fe, Al, Mg and P. Tests were carried out on a specially constructed bench-top system. Various path length cells were tested and based on these results, LED's were incorporated into existing on-line devices, replacing bulbs and filters. This involved the construction of the necessary electronics and changes to the resident software and mechanical design of the device.

The final part of the work involved construction of a prototype device capable of measuring concentrations of iron, aluminium, manganese and phosphate in drinking water as well as colour and turbidity. The device is portable, incorporates a full reagent mixing and delivery system and has limits of detection below EC directives for all the species listed above. This system was fully characterised in terms of limits of detection, linear ranges, accuracy, stability and repeatability.

Table of Contents

Chapter 1

Introduction to Water Quality Monitoring

1.1 Introduction

Over two thirds of the Earth's surface in covered by water. Over 70% of the human body consists of water. There is considerable concern over environmental issues, particularly with water quality, and this concern is reflected in increasingly rigid legislation governing the concentration of analytes in drinking water. This increased stringency on analyte levels is matched by the increased requirements on sensors to monitor these concentrations. For example, lowering the Guide Line concentration lowers the necessary Limit of Detection for a sensor. Investigative tests are often required at the site of the an environmental accident. It is therefore necessary to 'bring the lab to the sample' and this places further requirements on sensors in terms of portability, robustness and ease of use. In recent years, the trend in sensor design has been towards portability and versatility so as to meet these new requirements.

1.2 Constituents of Drinking Water

The main sources of drinking water are rivers, lakes, reservoirs and underground sources called aquifers. All naturally occurring water contains dissolved organic substances, large particles of biological origin, dissolved gasses and metals and suspended particles. The concentrations of these species depends upon location and climatic conditions. Water may also be classified in terms of colour, odour and turbidity. These also depend on the relative concentrations of the above constituents. The analyte concentrations, in the cases of reservoirs and underground sources, are generally slowly varying with time. With rivers and lakes these parameters may vary over periods as short as thirty minutes.

1.3 EC Guidelines for Water Quality

The quality of drinking water supplied to the public is subject to increasingly stringent regulations stipulated by the European Community, (EC) [1]. They govern the maximum admissible concentrations (MACs) and guide-line concentrations for all water quality parameters. Included below are some of the guidelines stipulated by the EC. Some possible sources for that particular parameter are also shown:

	Guide Line	MAC	Possible Source
Aluminium	50 $\mu g\ L^{-1}$	200 $\mu g\ L^{-1}$	Water treatment
Colour	1 Hazen	15 Hazen	High Fe/Mn Content
Iron	50 $\mu g\ L^{-1}$	300 $\mu g\ L^{-1}$	Water treatment, water pipes
Manganese	20 $\mu g\ L^{-1}$	50 $\mu g\ L^{-1}$	Water treatment
Phosphorus	0.4 $mg\ L^{-1}$	5.0 $mg\ L^{-1}$	Cleaning agents
Turbidity	1 NTU	5 NTU	Suspended matter

1.4 Water Quality Monitoring

A large number of techniques exist for the determination of the various parameters governing water quality. Each technique has its own particular advantages and disadvantages. When choosing the most suitable technique and apparatus for a particular situation the performance characteristics should be considered as well as cost and size. Some of the techniques used to test water quality are:

Ion Selective Electrodes: Electrodes are coated with ion selective resin and the voltage developed is a measure of the concentration present.

Atomic Methods: The sample is aspirated into a flame and atomized. In Atomic Flame Photometry the amount of light emitted is measured and the intensity at characteristic wavelengths gives the concentrations of the various metallic constituents. In Atomic Absorption Spectrometry a light beam is directed through the flame, into a monochromator, and onto a detector that measures the amount of light absorbed by the atomized elements in the flame [2].

Fluorescence Measurements: Fluorescence is excited in the sample using an external source. The intensity of the emitted fluorescence signal, at a characteristic wavelength, relates to the concentration of analyte in the sample. Another fluorescence method is where the intensity of emission of a fluorescing dye is reduced by the presence of the analyte. This is known as Fluorescence Quenching.

Filtration Methods: The sample is filtered through membrane filters of varying porosity. The mass deposited on the filter is then determined. This method determines the content and size distribution of suspended solids within the sample.

Colorimetric Determinations: The colour of a sample is photometrically determined. This can be done directly when sample Colour and Hue are required. Alternatively, colour determination may take place after the addition of specific reagents. The added reagent complexes with the analyte in the sample and colour forms at a particular wavelength region. The amount of colour developed relates to analyte concentration.

There are two main ways in which water quality tests are carried out: Sampling and In-situ Monitoring.

1.4.1 Sampling

Samples of water are obtained at the point of interest and taken back to the laboratory to be tested. This is an unsatisfactory approach as it may be labour intensive if a large number of samples are involved. The composition of a sample may change between extraction and testing. There is also a time interval between taking the sample and

obtaining the result. This is particularly relevant in a water treatment process where the result forms part of the feed-back loop, e.g. the aluminium content at the output of a coagulation process.

1.4.2 In-situ Monitoring

The required measurements are generated at the point of interest. The sample integrity is maintained and results are rapidly obtained. The sensor may also be *on-line* which means that the parameter is monitored continuously. This helps in the prevention and or control of transient pollution incidents, the gathering of detailed trend data for water management and the need to ensure that industrial discharges and abstracted, potable and treated waters conform to the required standards [3].

1.4.3 Sensor Characterisation

In the context of the work performed here the following are important in system/sensor characterisation [4]:

(i) Range: The range of a sensor may be defined as the range of the measurand values over which the sensor gives an unambiguous signal.

(ii) Sensitivity: The sensitivity of a sensor is a measure of the incremental change in output for a given change in the measurand. For a sensor having a linear response the sensitivity is the slope of the calibration curve in the linear region.

(iii) Resolution: The resolution is defined as the ability of a sensor to distinguish between closely adjacent values of the measurand. This can be calculated as 2 standard errors from the indicated value.

(iv) Repeatability: Repeatability is a measure of the agreement between a number of consecutive measurements of a chosen value of the measurand. Repeatability is expressed in terms of a parameter called the confidence interval. The confidence interval is a range

within which one may reasonably assume that the true value of a quantity being measured will be found. The 95% confidence interval is given by the equation:

$$\mu = \alpha \pm t\,(s.e)$$

where μ is the true value, α is the average value, t is a constant obtained from statistical tables and s.e. is the standard error. The value of t compensates for the uncertainty introduced by using a sample size less than infinity.

(v) Limit of Detection: The limit of detection is defined as the analyte concentration giving a signal equal to the blank signal plus three standard errors of the blank.

(vi) Accuracy: Accuracy describes the closeness of a measured value to the actual value of the measurand. The accuracy of a sensor is usually quoted in terms of the maximum error between the actual and measured values of a quantity.

(vii) Response Time: The response time can be defined as the time interval from the instant a step change occurs in the measurand to the instant when the change in the indicated value passes and remains beyond 90% of its steady state amplitude difference.

1.4.4 Portable Sensors

Because of the possibility of short-term changes in water quality, for instance due to storm events or point discharges, it is important to be able to rapidly detect water quality parameters along rivers and lakes. Hence it is necessary to have sensors which are portable and rugged enough to operate in the field. Many sensor techniques, such as Atomic Flame Photometry yield very accurate results in terms of number of constituents and their concentrations. However, the apparatus involved is not portable. In well characterised situations, such as point discharges, the sensor is only required to rapidly monitor a single parameter.

Many portable sensors currently available require considerable sample preparation before measurement and are hence slow and difficult to use. Others, although portable, still have a considerable amount of instrumentation and cost involved.

1.5 Objective of Project

This project arose from problems experienced with an existing commercial on-line monitor for iron and aluminum. The monitor uses a colorimetric technique with an interference filter and filament bulb as a source. The stability of the monitor is affected by variations in output from the bulb. Filter delamination and short Mean Times Between Failures (MTBF) for the bulbs increase the maintenance costs of the monitor. The filament within the bulb itself can also move and this can change the optical alignment over a period of time. It was noticed that the bulk optical components of this device could be replaced with a single LED and that this would overcome a number of the problems associated with the monitor. LED's have the advantages of long life-times, stable outputs, small size and low price. The incorporation of the LED into this system led to the examination of LED's in conjunction with other colorimetric tests and this in turn led to the design and construction of a portable system for monitoring water quality parameters. This sensor was designed with the requirements of ease of use and versatility in mind.

1.6 Structure of Thesis

Initially, the operating principles and performance characteristics of an LED are examined. Examples of current uses of LED's in chemical sensing are given. Colorimetric techniques are then examined in detail and the suitability and limitations of LED's as sources are discussed. Methods of determining sample turbidity are also outlined. The initial experimental sections describe experiments conducted on specific colorimetric tests using LED's as sources. Based on these tests, the filter and bulb of the previously mentioned on-line monitor were replaced with an LED and a description the of necessary changes and a comparison of performances, with both sources, is given. Next is the introduction of a modular design cell for the measurement of sample absorbance and scatter. The versatility of this cell allows it to be used for a range of colorimetric tests and also for determining sample colour and turbidity. Finally the construction of a portable system is discussed. Tests were conducted with the sensors configured to measure aluminium, iron, manganese and phosphate and sample colour and turbidity.

Chapter 2

LED Technology

2.1 Introduction

Traditionally, light sources for chemical sensing are broad-band sources with filters or narrow-band lasers. There are inherent problems associated with these sources. For example, laser sources are often bulky and expensive. Incandescent filament sources have stability problems, they generate a lot of heat and are generally bulky and movement of the actual filament within the bulb can cause changes in the optical alignment of the system. The interference filters often used with these sources are also very temperature sensitive and the layers forming the filter can separate over a period of time (i.e. delamination), causing a change in the optical transmission characteristics of the device. Light Emitting Diode (LED) sources can overcome a number of these problems. Their narrow bandwidths means that they can often be used without filters. They are small in size, have a low power consumption, they have a stable output and they are cheap in cost.

2.2 LED Technology

The next two sections discuss the operating principles of LED's and how these principles give rise to the advantageous features of these sources. An LED is basically a p-n junction diode operated under forward bias. A schematic diagram representing the band structure across a p-n junction is shown in Fig. 2.2.a

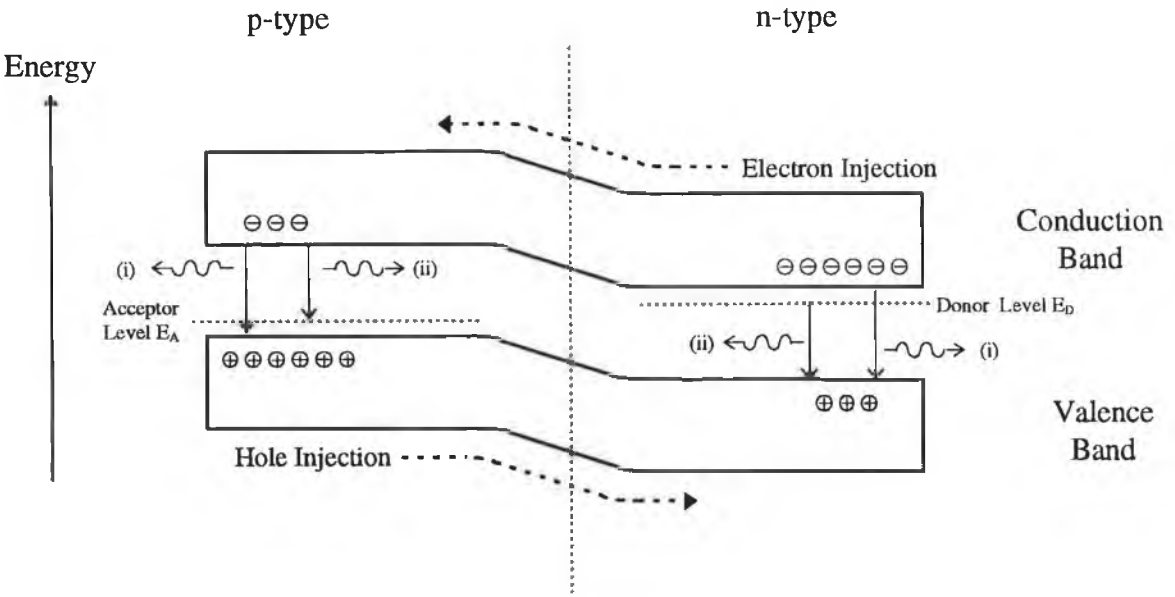

Fig. 2.2.a P-N JUNCTION OF LED UNDER FORWARD BIAS, (I) INTERBAND TRANSITIONS AND (II) IMPURITY CENTRE RECOMBINATIONS.

When an external voltage is applied to the junction, under forward bias, (p connected to positive terminal, n to negative), holes are injected from the p-type to n-type region and electrons from n to p-type. These charge carriers are replaced by the external circuit. The electron in the p-type conduction band recombines with a hole in the valence band and similarly the hole in the n-type combines with an electron from the conduction band. If the semiconductor material in question allows direct bandgap transitions [1], this may produce an emitted photon. The electron loses energy in this transition and the energy of the photon is the difference in electron energy before and after recombination. This is the basis of injection luminescence. Ideally, every injected charge carrier takes part in a radiative recombination and hence gives rise to an emitted photon. In the above example the electron goes from the conduction band to the valence band in an interband transition, (transition (i) in Fig. 2.2.a) [2]. In this case the wavelength of the emitted photon is related to the energy gap between conduction and valence bands, E_G:

$$E_G = E_C - E_V \qquad \text{Eq. 2.1}$$

$$\lambda = hc / E_G \qquad \text{Eq. 2.2}$$

E_C is the energy of the electron in the conduction band, E_V the energy in the valence band and E_G is the band gap energy. In Eq. 2.2, h is Planck's constant ($6.63 * 10^{-34}$ J s) and c is the speed of light in a vacuum ($3.0 * 10^8$ ms^{-1}). Doping the semi-conductor introduces impurity energy levels above and below the valence and conduction bands [3]. In the p-type region an acceptor level, E_A, exists just above the valence band and in the n-type region a donor level, E_D, just below the conduction band. These bands may also take part in recombination, so called impurity center recombination, (transition (ii) in Fig. 2.2.a), and the emitted photon has a wavelength longer than that of interband recombination, i.e.:

$$\lambda = hc / (E_C - E_A) \qquad \text{Eq. 2.3}$$

or

$$\lambda = hc / (E_D - E_V) \qquad \text{Eq. 2.4}$$

The positions of these impurity energy levels depend upon the manufacturing process and the dopants used. Other recombination processes such as exciton recombination, isoelectronic traps are also relevant [4]. When impurity centre recombinations dominate, the energy of the emitted photons differs from that of the energy gap, E_G, of the semi-conductor. The emission wavelengths for this situation are generally longer than those for the interband transitions as the impurity levels lie between the valence and conduction bands and the energy transitions are smaller.

2.3 Characteristics of LED's

The output spectrum of an LED is centered around the energy of the main recombination process for that particular p-n junction. This feature gives rise to two of the most important characteristics of LED's as light sources. The first is the narrow bandwidth of the output spectrum compared with broad-band sources. The emitted photons arise from a single recombination process and hence have a narrow band of energies centered around this transition level. The second feature is that LED output spectra cover almost the entire

visible and near-IR spectrum. By selection of semi-conductor material, dopant impurities, dopant concentrations and manufacturing techniques, LED's can be made to emit in specific wavelength bands. Because of the finite number of semi-conductor materials, (i.e. E_g values), not every wavelength region is available with LED's. However new materials and processes are constantly being discovered. For example until quite recently high intensity blue LED's were not available. Early designs involved doping silicon carbide with aluminium, but these had low output powers. More recently gallium nitride has been doped to p-type producing a new range of high intensity LED's which emit in the near ultra-violet and blue regions [5].

Each emitted photon is generated by an injected electron from the external circuit. Hence the output intensity is easily modulated by controlling the externally supplied current. As the majority of semiconductor materials used in LED's are of the direct band-gap type, there is no heat released in the recombination process and hence no electrical heating in the device. As a result LED's have very large mean time between failures, (e.g. 10,000 hrs), compared with incandescent sources.

Advances in semiconductor manufacturing technology have improved the quality and reduced the cost of LED's. Large numbers of p-n junctions can be produced from a single wafer and this results in low costs for LED's. They are also easily manufactured to specific shapes and orientations which enables efficient coupling to fibre ends, for example, as in Burrus-type LED's [6].

2.4 Temperature Effects of LED's

A disadvantage of LED's is that their output is temperature sensitive. The peak wavelength of the output spectrum shifts to longer wavelengths with increasing temperature by typically 0.3 nm/K [7]. The output intensity also decreases with increasing temperature and aging [8]. The intensity L, at a particular wavelength λ and temperature T, is governed by the following equations [9]:

$$L(\lambda,T) = Po / 0.6\,\lambda_W\,(\pi)^{1/2} \cdot \exp(k_I \Delta T) \cdot \exp\{ -2.78\,[\,\lambda - \lambda_0(T)\,]^2 / \lambda_W\,(T)^2 \} \qquad \text{Eq. 2.5}$$

$$\lambda_0\,(T) = \lambda_0 + k_S \Delta T \qquad \text{Eq. 2.6}$$

$$\lambda_W\,(T) = \lambda_W + k_B \Delta T \qquad \text{Eq. 2.7}$$

$$\Delta T = T_A - 25 \qquad \text{Eq. 2.8}$$

Po is the Radiant Power, λ_0 is the Peak Wavelength, λ_W is the Spectral Bandwidth, k_I is the Temperature Coefficient of Light Intensity (usually -0.001 /K $\rightarrow$ -0.02 /K), k_S is the Temperature Coefficient of Spectral Shift (usually 0.1 nm/K $\rightarrow$ 0.6 nm/K), k_B is the Temperature Coefficient of Spectral Bandwidth (usually assumed to be 0) and T_A is the Ambient Temperature (25 °C). These equations were applied to a yellow LED using the following values: λ_0 = 592 nm, λ_W = 30 nm, k_I = -0.006 /°C, k_B = 0, k_S = 0.2 nm/°C, T = 0 $\rightarrow$ 75 in 15 °C steps and also showing the output at 25 °C . The output power P_0 = 1mW. The results are shown in Fig. 2.4.a. Included in this figure is the spectral attenuation of the dye 2,4,6-tripyridyl-s-triazine, (TPTZ), complexed with ferrous iron. TPTZ is a colorimetric dye reagent used for determining iron concentration. A yellow LED may be used to determine the absorbance, or optical density, of the sample and hence the iron content.

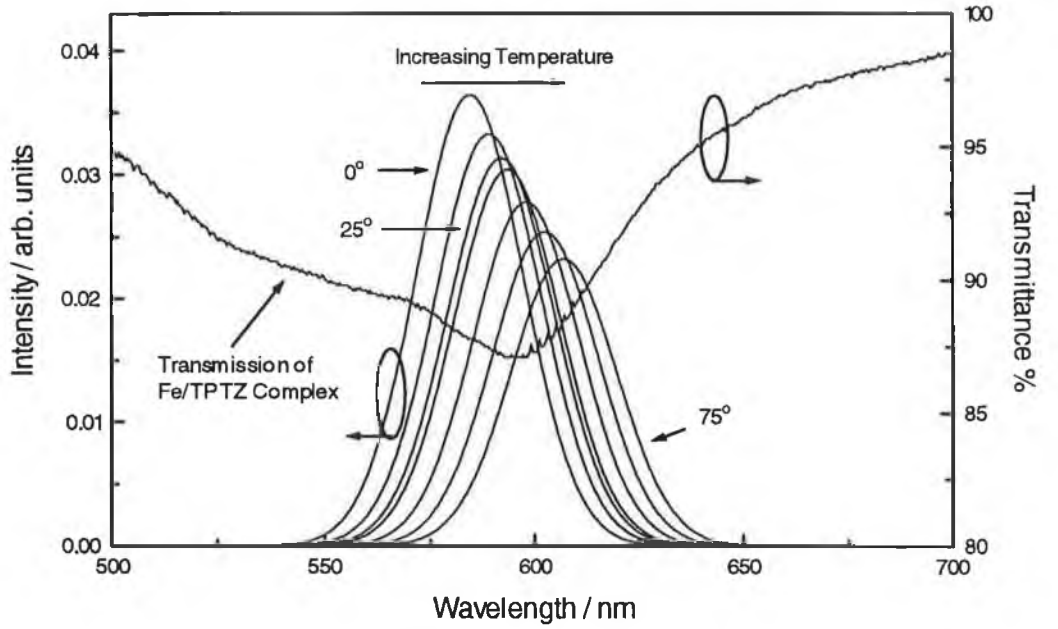

Fig. 2.4.a VARIATION OF LED OUTPUT WITH TEMPERATURE, 0→75 °C IN 15 °C STEPS

By combining the various LED spectra with the spectral attenuation curve, it is possible to determine the change in measured optical density with change in temperature. This is done using the following equations:

$$I_0 = \int_{\lambda_2}^{\lambda_1} L(\lambda, T) \qquad \text{Eq. 2.9}$$

$$I = \int_{\lambda_2}^{\lambda_1} T(\lambda) \,.\, L(\lambda, T) \qquad \text{Eq. 2.10}$$

$$OD = \text{Log}_{10} (I_0 / I) \qquad \text{Eq. 2.11}$$

$T(\lambda)$ is the spectral transmittance at wavelength λ, and λ_1 and λ_2 are chosen so that they span the full output of the LED. I is the initial intensity of the LED, and I_1 is the intensity after passing through the reagent/analyte sample. Hence, OD is the optical density of the

sample as measured using the LED as a source. Fig. 2.4.b shows the change in optical density with temperature. The percentage value, of the value at ambient temperature (25 °C), is also shown. It can be seen that the measured optical density changes with temperature. The magnitude and direction of this change depends upon the shape of the spectral attenuation curve, as well as the particular LED in question.

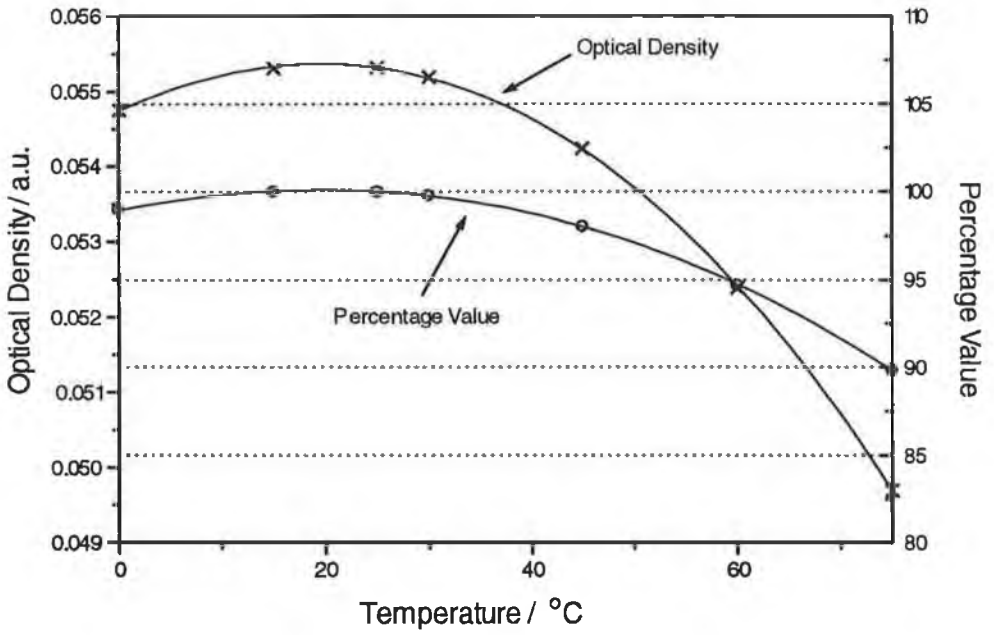

Fig. 2.4.b CHANGE IN MEASURED OPTICAL DENSITY WITH TEMPERATURE

It is possible to compensate for this temperature sensitivity in various ways. The LED can be operated at a controlled temperature. Alternatively, a fraction of the initial optical signal can be removed from the beam. This fraction can then be used as a reference for the final signal or to determine the feed-back in a closed loop control system [10]. This latter method is effective at controlling the output intensity of the LED. The shifts in spectral properties can also be compensated for by methods such as Wavelength Thermal Matching (WTM) [11]. When using WTM, a region of minimum variation with temperature on the LED spectrum is used for measurements.

2.5 LED's and Chemical Sensing

A recent review paper by Taib and Narayanaswamy details a number of LED-based systems for chemical sensing [12]. The most common use of LED's in chemical sensing has been with photometric methods, i.e. measurement of spectral attenuation of the LED by a sample. Traditionally incandescent sources and filters have been used for these tests. However this arrangement has inherent stability problems associated with filter degradation and bulb stability. Recently LED's have been favored, as alternative light sources, for the reasons outlined in section 2.3. Some examples of the use of LED's in various chemical sensor arrangements are described here.

Worsfold et al. have produced numerous papers outlining the incorporation of LED's into on-line flow injection analysis (FIA) systems [13-15]. The stability, long life and low power consumption of LED's make them ideal sources for on-line systems. Worsfold documents a nine month field trial of an on-line FIA system testing for nitrate in river water [16]. No problems were reported from the green LED used in this system. Kraus et al. utilise LED's in their photometric comparator [17]. This hand-held device provides a binary output which tells if a sample is above or below a certain threshold. Several LED's can easily be incorporated into a single FIA system to allow dual analyte detection, e.g. zinc & aluminium [18], dual wavelength referencing [19] and dual wavelength compensation for turbidity and refractive index effects [20]. Grattan et al. have also used dual wavelength referencing for their fibre optic based pH sensor [21]. Small size and low power consumption make LED's ideal sources for a portable pH sensor for entro-gastric reflux detection as outlined by Baldini et al. [22]. This fibre based device is inserted into the patients stomach via. the nasal cavity. The small size and low power consumption of the source allows the necessary instrumentation to be strapped to the patients body. Recently LED's have been used in a fluorometric process [23]. Here the LED excites fluorescence of a particular dye and then the concentration of analyte in the sample affects the intensity or lifetime of the emitted fluorescent intensity. Lasers were previously favored for fluorimetric techniques because of the high intensity and narrow bandwidths

required. However new high intensity LED's are now proving suitable and this allows considerable simplification of the necessary instrumentation.

2.6 Conclusion

The principal performance characteristics of LED's are their narrow bandwidth and stability compared to incandescent sources, their small size, long lifetimes and low power consumption. The output of LED's is temperature sensitive but there are methods of compensating for these variations. The main features of LED's mean that they are increasing used in favour of the traditional sources in chemical sensing applications.

Chapter 3

Water Quality Monitoring using LED's

3.1 Introduction

Chapter 2 contained a discussion of the operating principles of LED's and their performance characteristics. This chapter discusses colorimetric techniques in detail and outlines the use of LED's in these tests. The Beer/Lambert Law is discussed and this yields the equations necessary for calculating concentrations in a colorimetric method. It also gives the criteria for a suitable source in these tests. Details are also given on scatter and turbidity and a method of measuring turbidity is outlined.

3.2 The Beer/Lambert Law

When a beam of radiation passes through a sample, photons can be removed by absorption or scattering. Absorption occurs when the photon is removed and its energy converted to another form of energy. Absorption is the basis of colorimetric measurements and is discussed in the next section. The Beer/Lambert Law, or Beer's Law, describes the intensity of radiation as it passes through a sample. It can be stated in the following ways:

$$I = I_0\, 10^{(-abc)} \qquad \text{Eq. 3.1}$$

$$A = \mathrm{Log}_{10}(I_0/I) = abc \qquad \text{Eq. 3.2}$$

where I is the intensity after passing through the sample, I_0 is the incident intensity, a is the absorptivity (L g^{-1} cm^{-1}) of the sample, b is the path length (cm) of sample through which the radiation passes and c is the concentration (g L^{-1}) of the absorbing species contained in the sample. A is the absorbance or optical density, OD, of the sample itself. It can be seen from Eq. 3.2 that A increases linearly with concentration or path length Another parameter commonly used is the tranmittance T, and it is the ratio of the tranmitted power to incident power, or I/I_0.

In some situations absorbance varies in a non-linear manner with respect to concentration. True deviations from Beer's Law, where the absorptivity of the absorbing species in the sample actually changes, occur in systems where the concentration of the absorbing species is so high that the index of refraction for the absorbed radiation is changed [28] Apparent deviations occur when Beer's Law is not obeyed, although the absorptivity has not changed. Such apparent deviations may occur due to chemical limitations or instrumental limitations. Chemical limitations may occur at high concentrations as chemical composition of a sample may change, due to association, dissociation, or reaction of the absorbing species with the solvent, resulting in non-linearity in the measured absorbance [29]. There follows a discussion of instrumental limitations. Beer's law is strictly true only for monochromatic radiation. However, all optical sources are polychromatic to some extent. This fact causes an instrumental limitation to Beer's law. The extent of the deviation depends upon the source used, but also upon the attenuation spectrum of the sample in question. Consider the following example: [30]

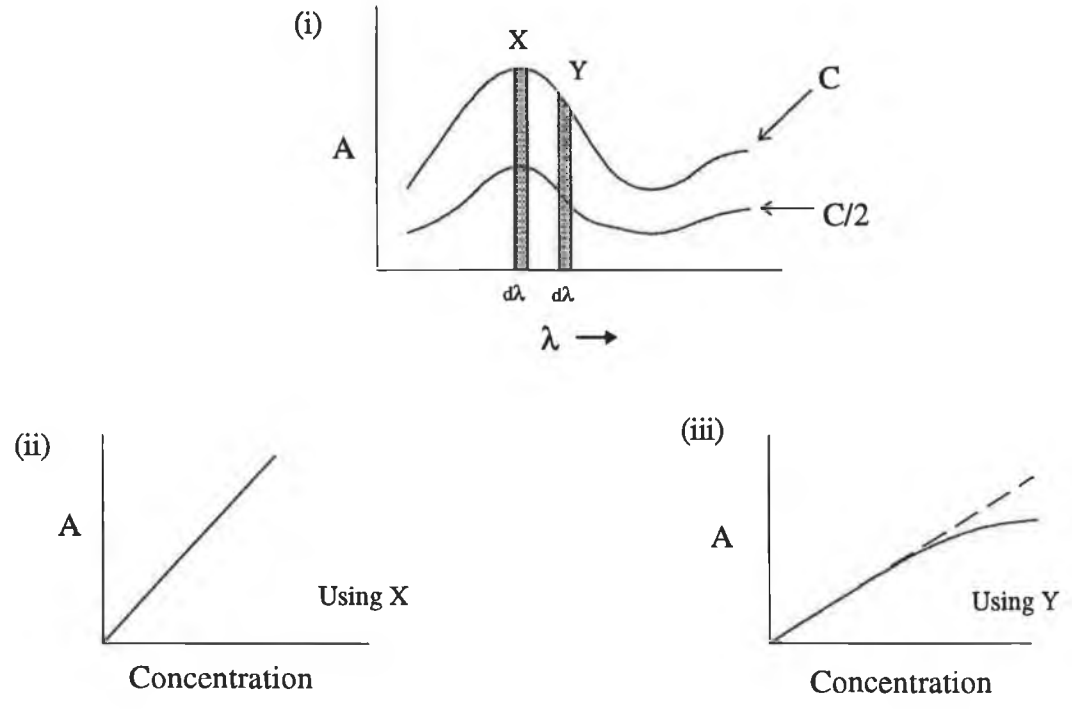

Fig. 3.2.a EFFECT OF FINITE BANDWIDTH ON MEASURED ABSORBANCE

In Fig. 3.2.a (i), a typical attenuation curve is shown where C/2 represents a sample half the concentration of C.

Consider a beam comprising of two wavelengths, λ' and λ''. Assuming that Beer's Law applies for each of these individually, the following equations hold [31].

$$A' = \log_{10}(I'_0/I) = a'bc$$
$$\text{or}$$
$$I'_0/I' = 10^{a'bc}$$

Similarly, for λ''

$$I''_0/I'' = 10^{a''bc}$$

where a' and a'' are the the absorptivities at wavelengths λ' and λ'', respectively. When an absorbance measurement is made with radiation comprising only these two wavelengths, the initial intensity of the beam is given by $(I'_0 + I''_0)$, and the intensity after passing through the sample is $(I' + I'')$. Therefore the measured absorbance A_M is:

$$A_M = \text{Log}_{10}((I'_0 + I''_0)/(I' + I''))$$

which can also be written as:

$$A_M = \text{Log}_{10}(I'_0 + I''_0) - \text{Log}_{10}(I'_0 * 10^{a'bc} + I''_0 * 10^{a''bc})$$

When $a' = a''$, this simplifies to $A_M = a'bc$, which is the case for monochromatic radiation, i.e. Beer's Law. However, the relationship between A_M and concentration is no longer linear when the absorptivities differ, and it has been shown by Skoog and West [32] that greater departures from linearity are experienced with increased differences between a' and a''. This derivation can be expanded to include additional wavelengths; the effect remains the same. Consider now the wavelength band X, of bandwidth $d\lambda$, in Fig. 3.2.a (i). As this band coincides with the peak of the absorption curve, the absorptivity is relatively constant across the band. When this band is used to measure the absorbance, there is little

deviation from Beer's Law and a linear calibration curve is obtained, as shown in Fig. 3.2.a (ii). Hence, for a polychromatic source, Beer's Law is closely approximated when the absorptivity does not vary considerably across the wavelength band. However, the absorptivity varies considerably across wavelength band Y, also of bandwidth $d\lambda$. When this band is used, at higher concentrations departures from Beer's Law occur and a typical resulting calibration curve is shown in Fig. 3.2.a (iii).

An additional advantage of using wavelength band X, as opposed to band Y, is that it coinincides spectrally with the absorbance peak of the sample and hence has a greater sensitivity compared to band Y.

When choosing a source for a colorimetric method, the most suitable source is one with maximium sensitivity, and minimum variation of the samples absorptivity across the bandwidth of the source. Consider again Fig. 3.2.a (i). This shows that to satisfy the above criteria, the most suitable source is one whose centre wavelength coincides with the peak of the absorption curve and whose bandwidth is less than the width of the absorption curve. In this way sensitivity is maximised and deviations from Beer's Law are minimised.

3.3 Colorimetric Techniques

3.3.1 Sample Treatment

Colorimetric techniques for water quality analysis were mentioned in section 1.4. The use of pyrocatechol violet (PCV) for the detection of aluminium is examined here as a representative test for water monitoring. PCV complexes with Al^{3+}, giving a colloidal lake which has an absorbance maximum at 589 nm [33]. Samples are generally pre-treated before PCV is added. Addition of acid to the sample brings all the aluminium present to the same oxidation state (i.e. Al^{3+}) and brings soluble aluminium such as residual floc into solution so that it can be measured. The interference of ferric iron can be masked by the reduction of Fe(III) to Fe(II), by the addition of hydroxylamine hydrochloride and by

subsequent chelation of Fe(II) with orthophenanthroline [34]. The colour developed by the PCV-Al complex depends also upon pH and the optimum value is 6.1. The acid treated sample is usually buffered to ensure the correct pH value.

The above chemicals can be diluted with de-ionised water to form reagent solutions. This simplifies the design of an on-line device for aluminium monitoring as reagents are more easily measured, delivered and mixed compared with solid chemicals. One such device is the RC100 on-line monitor for iron and aluminium produced by Aztec Environmental Control Ltd, Didcot, Oxon OX11 7HR, UK. The procedure used in this device for testing samples for aluminium content using PCV is as follows. Initially acid reagent is added to the sample. The acid reagent contains 5N hydrochloric acid, hydroxylamine hydrochloride, 1,10 phenanthroline and polyoxyethylene 23 lauryl ether. Buffer reagent, of pH 6.1, consisting of anhydrous acetate, sodium hydroxide and formaldehyde is then added. Finally the colour reagent is added. This contains pyrocatechol violet and formaldehyde. For the reagents used, a 5:1:1:1 volume ratio is required between the sample:acid:buffer:colour [35]. Hence, within this device, to 10 ml of sample, 2ml of acid reagent is added, then 2 ml of buffer reagent and then 2 ml of colour reagent [36]. Fig. 3.3.1.a shows the resulting spectral attenuation of two samples treated in this way. The blank is a sample of de-ionised water which is assumed to contain no aluminium. The standard is a sample containing 200 $\mu g\ L^{-1}$ of aluminium. Included in this figure is the spectral output of a yellow LED with its peak wavelength at 592 nm and spectral bandwidth of 30 nm.

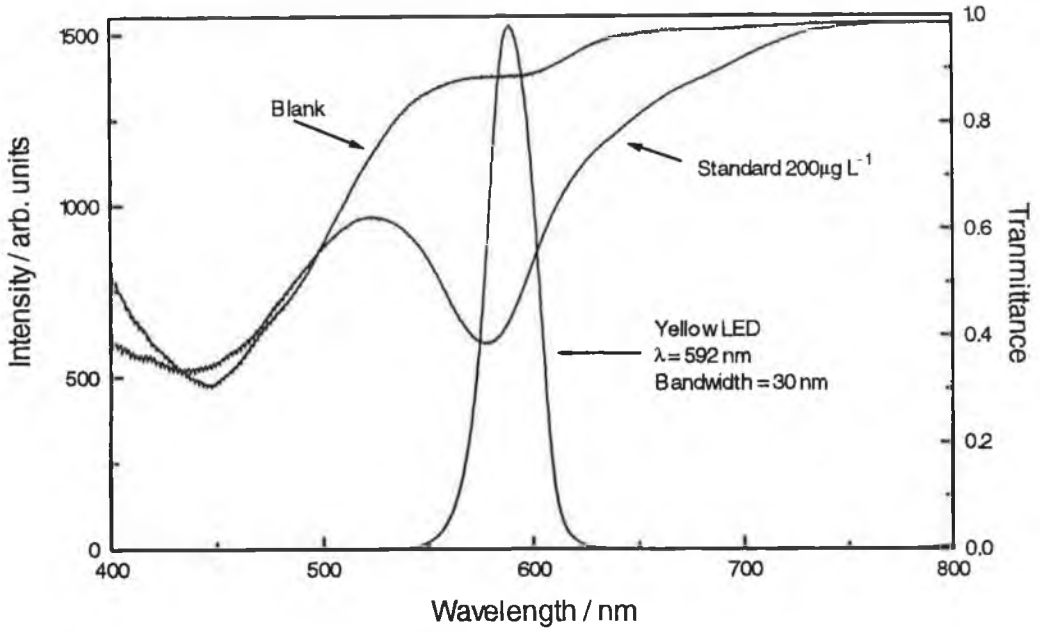

Fig. 3.3.1.a SPECTRAL ATTENUATION FOR TWO ALUMINIUM-PVC SAMPLES, TOGETHER WITH A YELLOW LED SPECTRUM

3.3.2 Calculating Concentrations

By measuring the optical density of the PCV-aluminium sample, at 589 nm, one can deduce the aluminium concentration from Beer's Law. The LED shown in Fig. 3.3.1.a has a peak wavelength sufficiently close to this point to make it a suitable source. It can be seen that the absorptivity varies across the bandwidth of the LED and one can expect deviations from Beer's Law when using this source. Once the optical density has been measured, the concentration c can be calculated from a knowledge of the path length b, and the absorptivity a. Another method, which does not require knowledge of the absorptivity value, is to use a calibration curve. Optical density is measured over a range of samples of known concentration. These values are then used to generate a regression equation which relates A to c. Knowledge of the optical density of an unknown sample can then yield the unknown concentration. If the optical density change is linear over a

certain range then two points can be used to generate this equation. This is known as a two point linear calibration.

A blank (BL) sample is usually the lower concentration of a two point calibration. The upper concentration, known as the standard (STD, 200 $\mu g\ L^{-1}$ in this case), must be chosen so that it lies within the linear range of the test in question. The following two equations yield the unknown concentration of the sample (SPL).[†]

$$S = K(OD_{SPL} - OD_{BL}) \qquad \text{Eq. 3.3}$$

$$K = \frac{200}{OD_{STD} - OD_{BL}} \qquad \text{Eq. 3.4}$$

where S is the concentration of analyte, in $\mu g\ L^{-1}$, in the unknown sample. K is known as the Calibration Constant and is the reciprocal of the slope of the calibration curve. OD_{SPL} is the optical density of the sample of unknown concentration and OD_{STD} & OD_{BL} are the optical densities of the standard and blank, respectively. The figure 200, in Eq. 3.5 corresponds to the 200 $\mu g\ L^{-1}$ concentration of the standard.

3.3.3 Other Colorimetric Tests

In sections 3.3.1 and 3.3.2 the used of a yellow LED to test for Al in the aluminium-pyrocatechol violet reaction was discussed. There are a large number of colorimetric techniques for monitoring water quality and many of these have absorption maxima which overlap LED output spectra. Included is a list of some examples:

[†] The full derivation of these equations is included in Appendix A

Analyte	Reagent	Wavelength /nm	Reference #
Al(III)	PCV	592 (Yellow)	37
Cu(II)	Neo-cuproine	440 (Blue)	38
Fe(II)	TPTZ	592 (Yellow)	39
Manganese	Formaldoxime	440(Blue)	40
Nitrate	NINED + sulphanilamide	565 (Green)	41
Phosphate	ANSA	660 (Red)	42
Zinc	Xylenol Orange	580 (Yellow)	43

The spectral attenuation curves for some of the above tests are shown in Fig. 3.3.3.a. These spectra were measured in the course of this project. In all cases, the blank is a de-ionised water sample containing no analyte and the standard is a sample of known concentration. Included with each example is the output spectrum of an LED suitable as a source for that test.

It can be seen that the phosphate reaction has a very broad attenuation spectrum. The choice of a red LED as a source is arbitrary. A different source (e.g. green or IR LED) would have a similar performance in this test. Sample colour is conventionally determined at 400 nm [44]. No reagents are required in this test. The calculations are the same as outlined by equations 3.4 and 3.5. Colour standards are conventionally prepared from platinum-cobalt and the units of colour are mg L^{-1} of Pt-Co, or Hazen. The LED shown in Fig. 3.3.2.a has a peak wavelength of 420 nm. As no LED with a peak at 400 nm currently exists, this is the most suitable LED as a source for colour measurement.

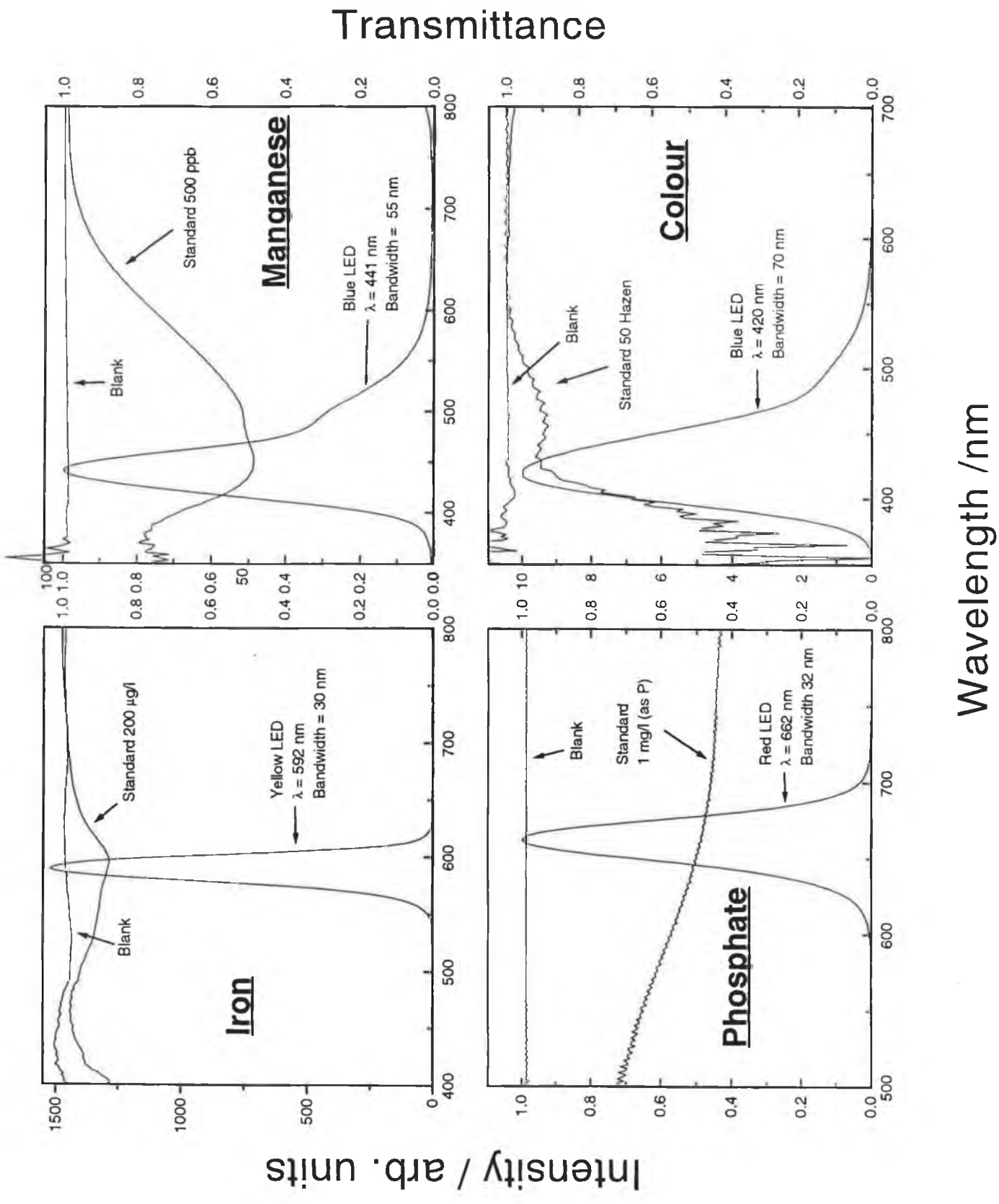

Fig. 3.3.3.a SPECTRAL TRANSMITTANCE & INTENSITY FOR LED VS. WAVELENGTH FOR VARIOUS COLORIMETRIC TESTS.

3.4 Turbidity Measurement

3.4.1 Scatter Theory

In section 3.2 it was stated that photons may be removed from a beam by either absorption or scattering. Scattering occurs when a photon interacts with a particle but the photon continues to propagate in a random direction after the interaction. The photon has been removed from the beam but may re-enter at a later stage. When absorption and scattering occur in a sample, Beer's law changes as follows:

$$I = I_0\, 10^{(-\alpha bc)} \qquad \text{Eq. 3.5}$$

$$A = \mathrm{Log}_{10}(I_0/I) = \alpha bc \qquad \text{Eq. 3.6}$$

$$\alpha = a + s \qquad \text{Eq. 3.7}$$

where α is the total attenuation coefficient, a is the absorptivity and s is the scatter coefficient. All other parameters have the same meaning, as outlined by Eqs. 3.1 to 3.3. The two main scattering processes are Rayleigh and Mie scattering.

Rayleigh Scattering: This process occurs when the size of the particles is much smaller than the wavelength of the light. In this case the scattered flux density is directly proportional to the fourth power of the driving frequency [45], or equivalently:

$$I \propto \frac{1}{\lambda^4} \qquad \text{Eq. 3.9}$$

In normal conditions, with real samples taken from rivers and lakes etc, the scattering particles are larger than the wavelength of radiation and Rayleigh scattering plays a small overall affect.

Mie Scattering: This type of scattering occurs when the particles are comparable in size to the wavelength of the radiation. Mie scattering is a more complicated phenomenon than Rayleigh scattering. Models have been derived which describe the scattering in a sample

due to equivalent spheres [46]. However, in a real sample the scattering particles are generally heterogeneous and non-spherical. This means that they scatter light in random directions because of their random shape and orientation.

3.4.2 Measuring Turbidity

Turbidity in samples is caused by suspended matter, such as clay, silt and particles of biological origin. Turbidity is an expression of the optical property that causes light to be scattered and absorbed rather than transmitted in straight lines through the sample [47]. Turbidity has a large positive interference in a colorimetric process as it increases the measured optical density due to the larger value of α, as described by Eqs. 3.6 and 3.9. The majority of samples have some level of turbidity and no standard method exists for the removal of, or compensation for this turbidity. Turbidity is generally measured by measuring the intensity of the light scattered in a particular direction, (e.g. forward/back scattered or scattered at right angles). However, because of the random nature of scattering from larger particles, the measured turbidity is very sensitive to the orientation of the optical components. This leads to poor reproducibility between turbidimeters of different designs. The standard design for turbidimeters for low turbidity measurement is the Nephelometric design as this configuration is relatively unaffected by small changes in design parameters [48]. In this method the scattered signal is measured at right angles to the direction of the incident beam. The unit of turbidity is the nephelometric turbidity unit, (NTU). Another problem giving rise to bad reproducibility is the difficulty in generating consistent standard solutions for turbidimeter calibration. Formazin is currently used to produce standards but at low levels (e.g. 10 NTU) the stability of these standards is less than one day. Recently a suspension of styrene divinylbenzene beads has been developed and this shows much improved stability and reproducibility [49]. The calibration and use of a turbidimeter is similar to that of a colorimetric device. However this time the scattered signal intensity is measured rather than the sample optical density. The following equations illustrate this point:

$$S = K(V_{SPL} - V_{BL}) \qquad \text{Eq. 3.10}$$

$$K = \frac{20}{V_{STD} - V_{BL}} \qquad \text{Eq. 3.11}$$

where S is the sample turbidity in NTU, K is the turbidity calibration constant, V_{SPL} is the scattered signal from the sample and V_{STD} & V_{BL} are the scattered signals from the standard and blank, respectively. The 20 in Eq. 3.11 represents the turbidity of the standard.

There is almost no wavelength dependence on the scattered signal from a real sample [50]. Hence an LED with any peak wavelength may be used to measure turbidity. For turbidity values below 5 NTU the scattered signal intensity is very low and in this situation a high intensity source is required. GaAs infra-red LED's with large output intensities (>100 mW) are relatively inexpensive and are therefore suitable.

3.5 Conclusion

Beer's law was discussed and a method derived for determination of analyte concentration in a sample when using a colorimetric process. Based on their spectral outputs, LED's were shown to be suitable sources in several of these tests. In certain tests deviations from Beer's Law may occur at high concentrations, due to the finite bandwidth of the LED. Scatter and turbidity were also discussed and a method of measuring turbidity, suitable for an LED source, was detailed.

Chapter 4

Experimental - Bench Top Measurements

4.1 Introduction

In Chapter 3 colorimetric techniques were discussed. LED's were discussed as suitable sources in these measurements. This chapter outlines a number experiments carried out to determine the performance characteristics of LED's as sources in monitoring water quality parameters. The tests were carried out on a bench top system and sample pre-treatment was performed manually. The final section discusses the incorporation of an LED into a commercial on-line monitor, replacing a filter and white light bulb. The performance characteristics of the monitor with both sources were compared.

4.2 Colorimetric Measurements

Results quoted in this section and section 4.3 do not include limit of detection or repeatability. These are omitted because manual sample preparation and treatment involve the largest errors in repeated measurements on a single sample. Therefore a limit of detection or repeatability measurement would reflect this error rather than a measurement variation due to instrumentation.

4.2.1 Bench-Top System

The two lenses used each had a focal length of 25 mm. The detector used was a medium area silicon photodiode. Cuvettes of varying path lengths (e.g. 1, 2 and 4 cm) were used, as required by the particular colorimetric reaction. The LED's were powered using a continuous current source and the detector was connected to a voltmeter.

The experimental set-up for absorption measurements is shown in Fig. 4.2.1.a.

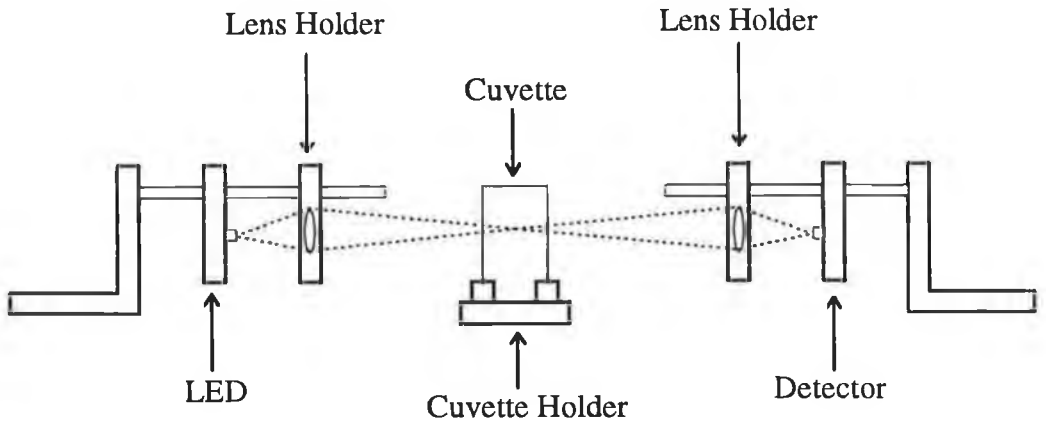

Fig. 4.2.1.a LED SYSTEM FOR ABSORPTION MEASUREMENTS

4.2.2 Sample Preparation and Treatment

All reagent used were provided by Aztec Environmental Control Ltd. The test samples were prepared from 1000 ppm stock solutions. For example, a stock solution of aluminium nitrate nonahydrate in a nitric acid base, ($Al(NO_3)_3.9H_2O$ in $HNO_3(0.6M)$), was used to prepare aluminium standard solutions. The procedure was as follows. Given that 1 mL of 1000 ppm solution has an Al content of 1 mg, 10 mL of this solution diluted with de-ionised water to 1 L gives a solution of 10 mg L^{-1}. If 20 mL of this solution is further diluted to 1 L, this gives a 200 $\mu g\ L^{-1}$ solution. Samples of varying concentrations were prepared in this manner.

Using aluminium as an example again, the procedure for treating the above samples was as follows. Using individual pipettes, 40 mL of sample was added to a beaker. Then 8 mL of acid, buffer and colour reagent were added in turn. In this way the required 5:1:1:1 volume ratio between sample and reagents was achieved. Colour was allowed to develop in the sample for ten minutes.

4.2.3 Evaluation of Yellow LED as Source for Aluminium Measurement

Cuvettes were filled with the samples treated as outlined in the last section, and their optical densities were measured using the LED system. A typical calibration curve obtained for aluminium samples prepared and treated in the above manner is shown in Fig. 4.2.3.a.

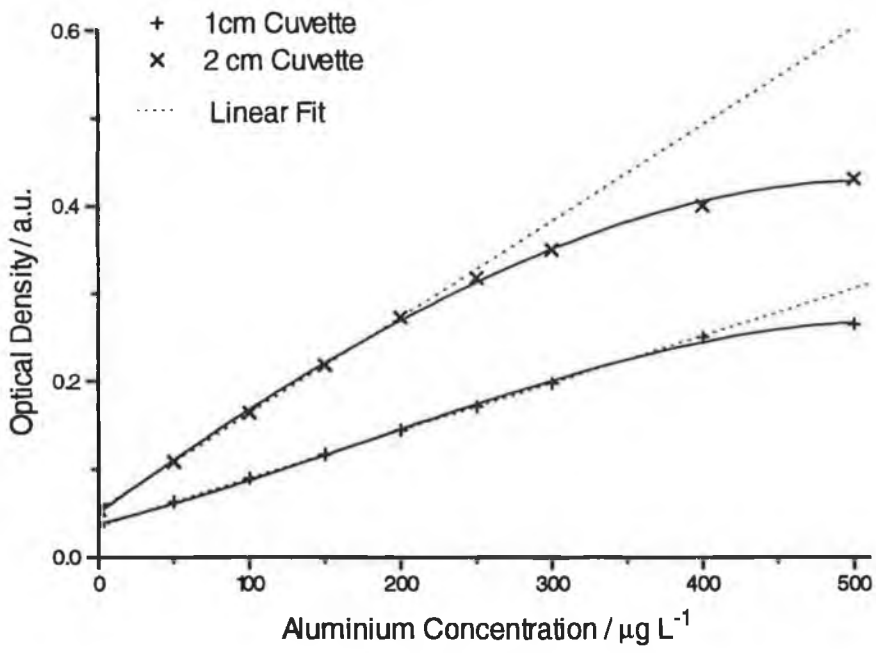

Fig. 4.2.3.a CALIBRATION CURVES FOR ALUMINIUM USING 1&2 CM PATH LENGTHS.

It can be seen that both curves become non-linear at higher concentrations, for reasons outlined in section 3.3. The Linear Fit lines represent a linear fit to the initial linear part of each curve. The larger slope of the 2 cm cuvette indicates the greater sensitivity for longer path lengths accompanied however, by a corresponding reduction in linear range. Hence there is a compromise between sensitivity and linear range. The measured optical densities were then applied to Eqns. 3.4 and 3.5 and a comparison of calculated and actual concentrations is plotted in Fig. 4.2.3.b.

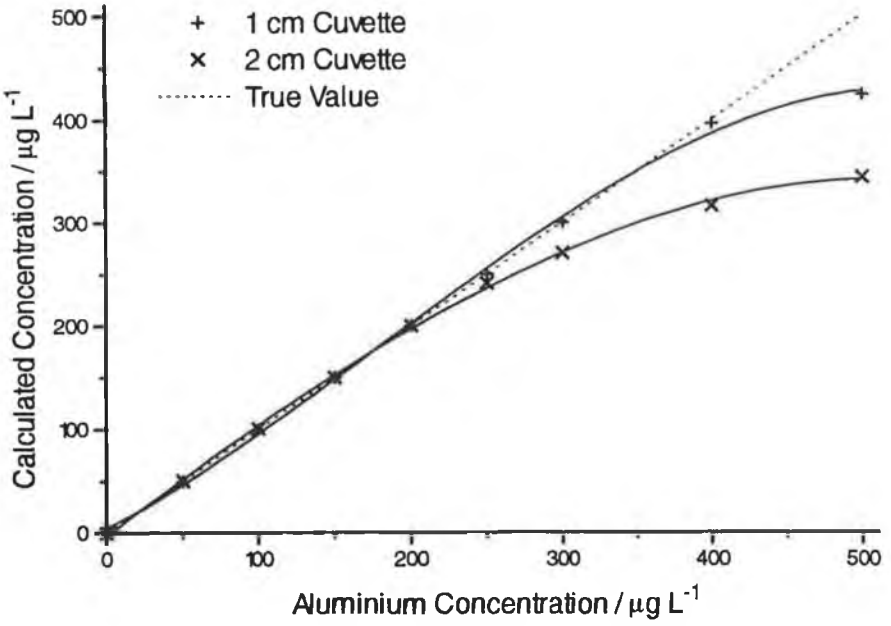

Fig. 4.2.3.b CALCULATED CONCENTRATION VS. ACTUAL CONCENTRATION FOR ALUMINIUM SAMPLES, USING 1 & 2 CM CUVETTES.

In Chapter 3 it was stated that deviations from Beer's Law can be expected at high concentrations when using certain sources in certain colorimetric tests. This deviation from linearity can be seen in Figs. 4.2.3.a and 4.2.3.b. In Chapter 3 equations were also given for calculating concentrations in a colorimetric test based on a linear two point calibration, (i.e. Eqs. 3.3 and 3.4). Figs. 4.2.3.a shows that using the yellow LED as a source, the measured optical density changes linearly, up to a certain sample concentration. For both path lengths used the concentration of the standard (i.e. 200 µg L^{-1}) was within the linear range. Hence, when using a two point linear calibration, within a certain concentration range a yellow LED is a suitable source for quantitative analysis of aluminium in samples using a pyrocatechol violet colorimetric technique.

4.2.4 Other Colorimetric Tests

Experiments similar to those outlined in the last two sections were also carried out on the iron, manganese, phosphate and colour tests. A brief summary of these results follows.

Iron

The yellow LED used for aluminium measurements was also used for iron. A 2 cm cuvette was used. The three reagents used were acid reagent (R1), buffer reagent (R2) and colour reagent (R3). The reagent/sample volume ratio, between sample:R1:R2:R3, was 5:1:1:1. Colour developed instantly on addition of the colour reagent. The resulting calibration curve is shown in Fig. 4.2.4.a.

Manganese

A blue LED with a peak wavelength of 450 nm and a bandwidth of 55 nm was used for manganese measurements. A 4 cm cuvette was used. The three reagent used were alkali reagent (R1), complexing reagent (R2) and colour reagent (R3). The reagent/sample volume ratio, between sample:R1:R2:R3, was 20:3:1:1. Colour developed in two minutes. The resulting calibration curve is shown in Fig. 4.2.4.b.

PHOSPHATE (AS P)

A red LED with a peak wavelength of 662 nm and a bandwidth of 32 nm was used for phosphate measurements. A 2 cm cuvette was used. The three reagents used were acid reagent (R1), conditioning reagent (R2) and colour reagent (R3). The reagent/sample volume ratio, between sample:R1:R2:R3, was 5:1:1:1. Colour developed in ten minutes. The resulting calibration curve is shown in Fig. 4.2.4.c.

Colour

A blue LED with a peak wavelength of 420 nm and a bandwidth of 70 nm was used for colour measurements. A 4 cm cuvette was used. No reagents are required for colour measurement. Samples were not filtered before measurement. The resulting calibration curve is shown in Fig. 4.2.4.d.

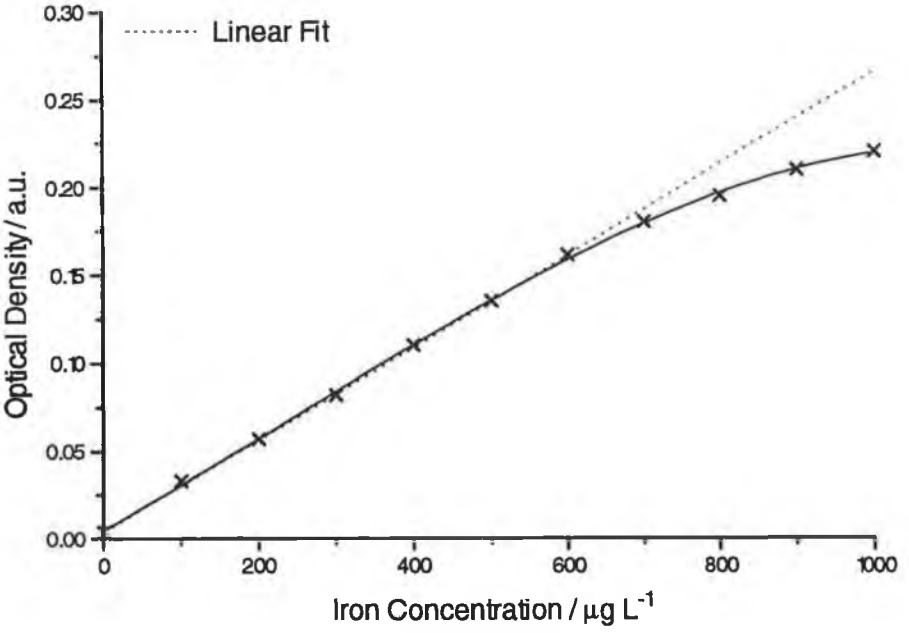

Fig. 4.2.4.a CALIBRATION CURVE FOR IRON, 2 CM CUVETTE, YELLOW LED AS SOURCE

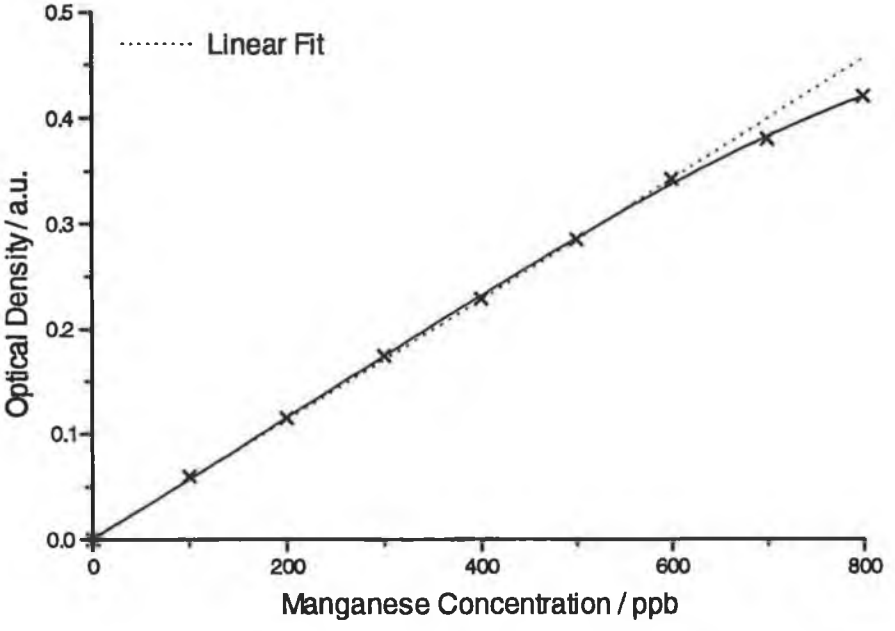

Fig. 4.2.4.b CALIBRATION CURVE FOR MANGANESE, 4 CM CUVETTE, BLUE LED AS SOURCE

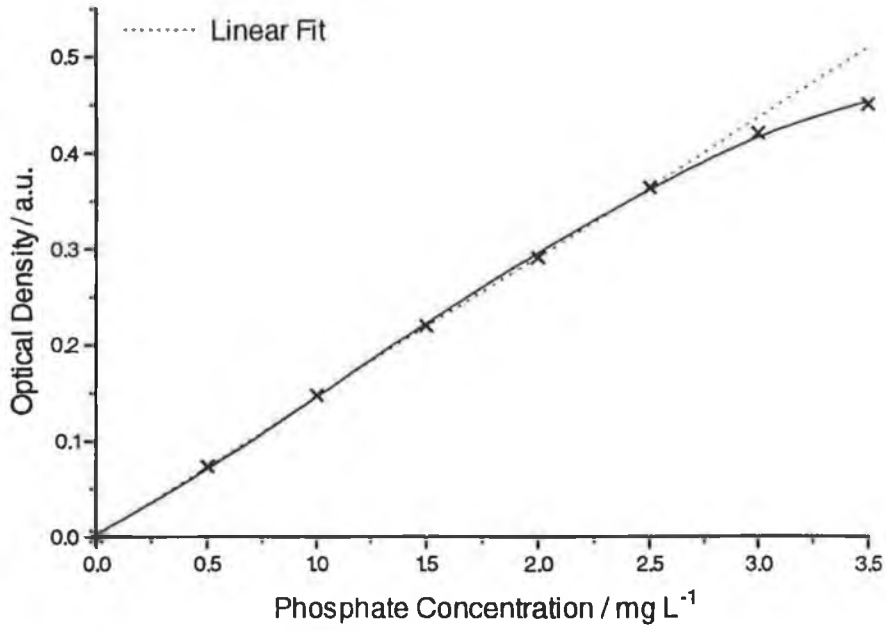

Fig. 4.2.4.c CALIBRATION CURVE FOR PHOSPHATE (AS P), 2 CM CUVETTE, RED LED AS SOURCE

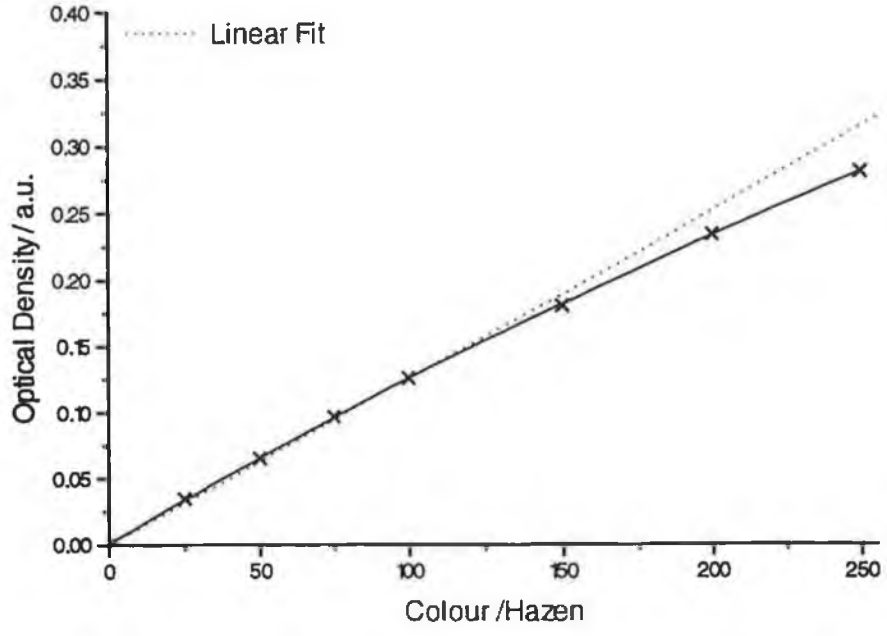

Fig. 4.2.4.d CALIBRATION CURVE FOR COLOUR, 4 CM CUVETTE, BLUE LED AS SOURCE

The following table summarises the results of the previous three sections.

	Sensitivity	Linear Range
Aluminium	$1.15 * 10^{-3}$ a.u./μg L^{-1}	0→230 μg L^{-1}
Colour	$1.3 * 10^{-3}$ a.u./Hazen	0→160 Hazen
Iron	$3.0 * 10^{-4}$ a.u. /μg L^{-1}	0→750 μg L^{-1}
Manganese	$5.7 * 10^{-4}$ a.u. /μg L^{-1}	0→75 μg L^{-1}
Phosphate	$1.49 * 10^{-4}$ a.u. /μg L^{-1}	0→$2.25 * 10^{-3}$ μg L^{-1}

The above table and preceding graphs show the linear range and sensitivities of LED's as sources in various colorimetric tests. Based on these results it was decided to design a sensor system for monitoring water quality parameters, incorporating a range of LED sources and using colorimetric tests for the above parameters. The design and testing of this system is discussed in the next two chapters. In the next chapter a modular sensor head is introduced and the above figures were relevant in choosing the range of path lengths when designing the cell.

4.3 Turbidity Measurements

4.3.1 Bench-Top System

The experimental set-up for turbidity measurements is shown below in Fig. 4.3.1.a.

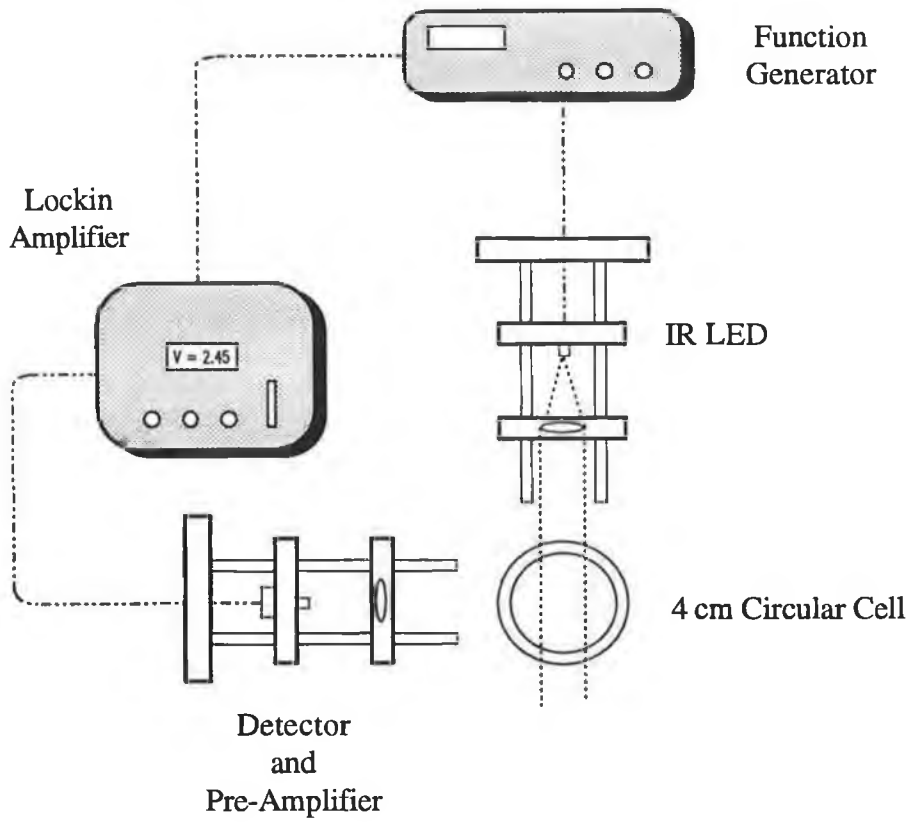

Fig 4.3.1.a LED SYSTEM FOR TURBIDITY MEASUREMENT

The collimating and collection lenses each had a focal length of 25 mm. The sample cell used was a glass walled circular cell with 4 cm internal diameter. The LED used was of GaAs type with a peak wavelength of 880 nm and a maximum output power of 20 mW. The LED was modulated at 450 Hz using a function generator and a lockin amplifier was used at the detection stage. This was nesessary because of the low intensity of the scatter signals from samples of low turbidity. The detector used was a medium area silicon photodiode. The detector and its pre-amplifier were combined onto a single PCB

board so as to reduce electrical noise pick-up between detector and lockin amplifier. The detection optics were enclosed to prevent scattered light, other than that from the sample, reaching the detector. Even with this precaution, a small amount of stray scattered light did reach the detector and this can be seen, in Fig. 4.3.1.b, in the non-zero scattered signal value for a sample with no turbidity , i.e. 0 NTU.

Two stock solutions were used to prepare samples. Formazine was used to prepare samples of turbidity 10 NTU and greater. Because of the instability of formazine solutions, especially at low NTU values, AEPA-1 stock solution from Advanced Polymer Systems [51], was used for the preparation of samples of turbidity 5 NTU and lower. The stock solutions had turbidity values of 4000 NTU and 200 NTU, respectively. For example 5 mL of 4000 NTU stock solution was diluted with de-ionised water to 1 L to produce a 20 NTU sample.

The response of the LED system to increasingly turbid samples is shown in Fig. 4.3.1.b.

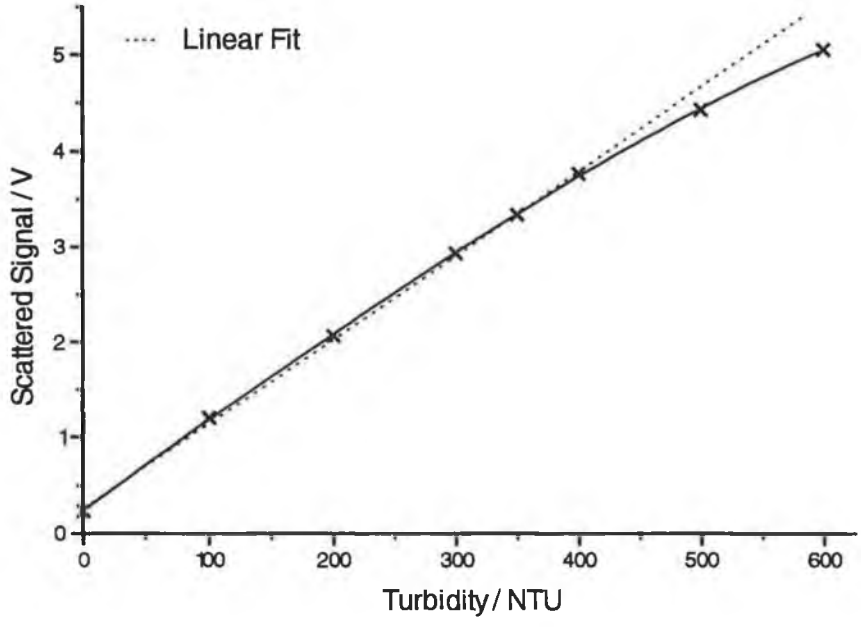

Fig. 4.3.1.b SCATTERED SIGNAL VS. TURBIDITY FOR LED SYSTEM

It can be seen that the detected signal becomes non-linear above 400 NTU. This occurs because the scattered signal is increasingly attenuated by the sample as the turbidity increases and hence the detected signal decreases. Samples of turbidity less than 1 NTU were also tested and the smallest turbidity change measureable was 0.1 NTU.

For absorption measurements, the sensitivity and limit of detection is influenced by the path length of cell used. For turbidity measurements, however, these factors are mainly influenced by the intensity of the source. For example, increasing the source output increases the scattered signal for a particular intensity. This effectively raises the sensitivity as a bigger scattered signal change occurs. It also increases the signal-to-noise ratio (and reduces the standard deviation) of a blank signal and hence lowers the limit of detection.

4.4 Combined Colour and Turbidity Measurements

Any sample has two associated colour values which are called the apparent and true colour. The true colour is that which is measured after the turbidity has been removed, usually by filtration to remove suspended solids. If the initial sample has very low turbidity then the true and apparent colour are the same. As already mentioned in section 3.3.1, turbidity has a large positive influence on a colorimetric process. Later in the chaper in section 4.5, colour correction is discussed as a method of overcoming natural colour or turbidity in samples. This section discusses experiments made to investigate the interference of turbidity on colour measurements, and vice versa.

4.4.1 Bench-Top System

The experimental set-up for combined colour and turbidity measurements is shown in Fig. 4.4.1.a. The set-up for turbidity measurements was the same as previously outlined in the last section. A blue LED was placed in line with the detector to enable sample colour to

be determined. Both LED's were modulated and lockin detection was used. The switch was used to select the LED required and, as only one LED was on at any one time, there was no interference between the two sources.

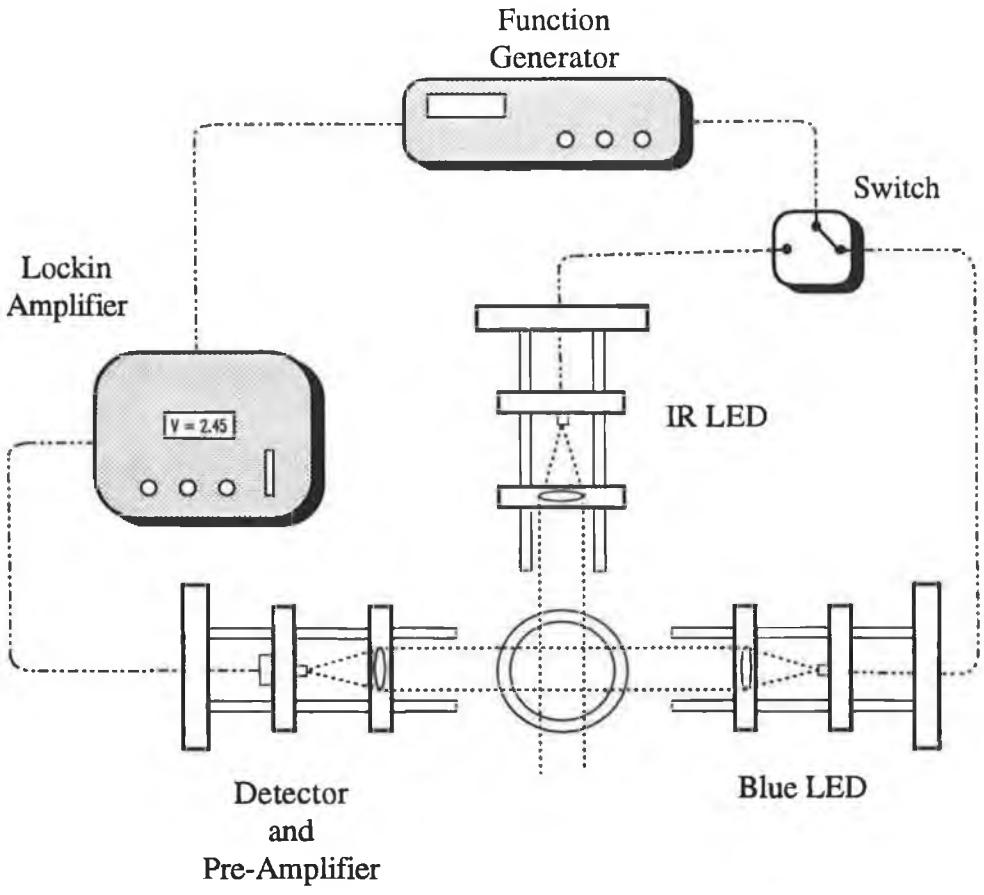

Fig. 4.4.1.a EXPERIMENTAL SET-UP FOR COMBINED COLOUR AND TURBIDITY MEASUREMENTS

4.4.2 Interference of Colour on Turbidity

A colour sample was prepared and placed in the cell and the signals from the blue and IR LED's recorded. Increasing amounts of formazine (4000 NTU stock solution) were then added to the sample to raise its turbidity and the colour and turbidity signals were recorded

at each point. As very small volumes of formazine were required, the dilution of the colour sample was ignored. This was repeated for different colour samples.

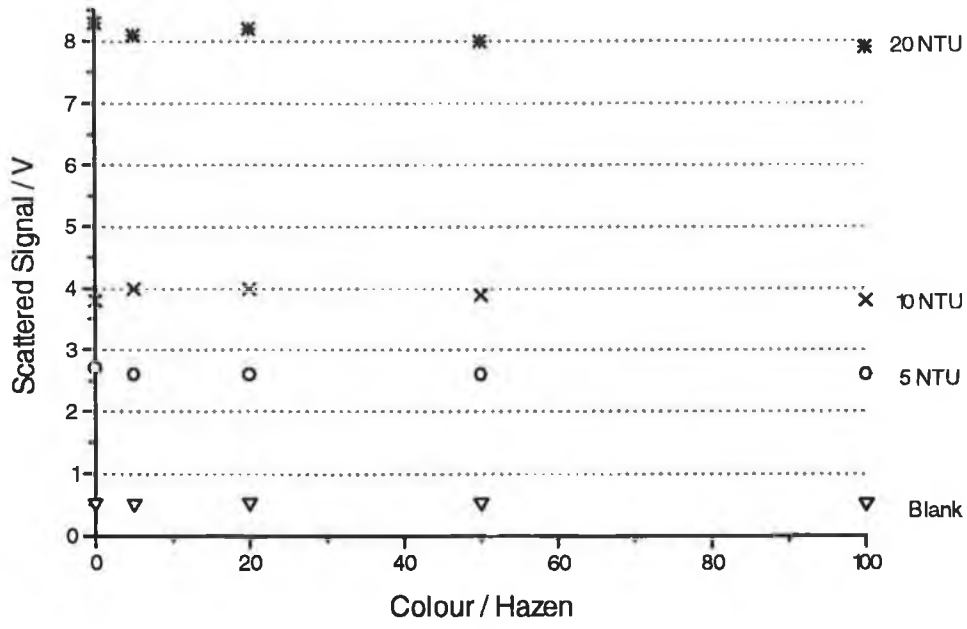

Fig. 4.4.2.a INTERFERENCE OF COLOUR ON TURBIDITY SAMPLES

Fig. 4.4.2.a shows the effect of increasing colour in turbidity samples. It can be seen that the scattered signal from each sample, (i.e. 0, 5, 10 & 20 NTU), remains approximately constant as the colour of that sample is increased from 0 Hazen to 100 Hazen. Colour samples have zero attenuation in the infra-red (see Fig. 3.3.3.a) and hence the infra-red signal is un-attenuated by the increasing colour.

4.4.3 Interference of Turbidity on Colour Measurement

In Chapter 3 it was stated that turbidity has a large positive interference on absorption measurements and this effect is investigated in this section. The sample preparation and experimental procedure were similar to those outlined in section 4.4.2 in that, while

measuring colour and turbidity, the turbidity of a colour sample was gradually increased by the addition of turbidity stock solution. The results are shown in Fig. 4.4.3.a.

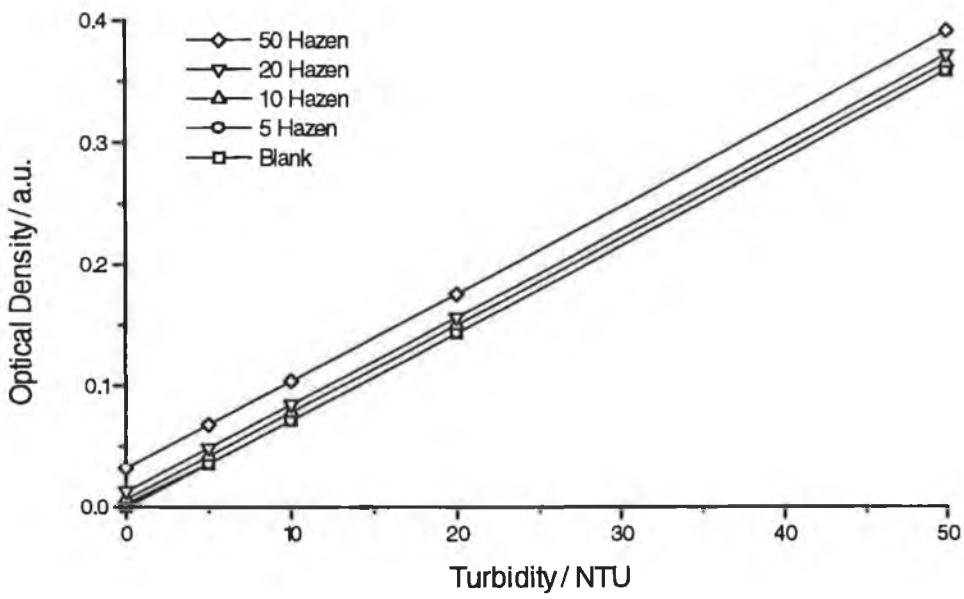

Fig. 4.4.3.a INTERFERENCE OF TURBIDITY ON COLOUR MEASUREMENT

It can be seen from Fig. 4.4.3.a that the optical density of a sample changes linearly as the turbidity is increased. The large positive interference of turbidity on colour can be seen in the dramatic increase in sample optical density with increasing sample turbidity. Therefore a small increase in turbidity causes a large increase in the apparent colour of a sample.

4.4.4 Turbidity Compensated Colour Measurements

The results presented in the last two sections showed that a sample's optical density increases linearly with increasing turbidity and that turbidity is relatively independent of colour. These facts may be used to compensate for turbidity in colour measurements. Consider a sample which has both colour and turbidity. When the optical density of this sample is measured it has both a colour and turbidity contribution. By subtracting the turbidity contribution, the turbidity-compensated-colour, or true colour, can be obtained.

This calculation requires three calibration constants: one for colour and turbidity as outlined in Eqs. 3.5 and 3.12, and a third which converts a turbidity to an optical density. This is done by measuring the optical density of a sample of known turbidity. This optical density is then scaled by the turbidity of subsequent samples. By making the following measurements and then applying Eqs. 4.1 to 4.6, this procedure can be implemented.

	Measured Signals	
	Blue LED	*IR LED*
Blank	V_1	V_2
Colour Standard (50 Hazen)	V_3	-
Turbidity Standard (20 NTU)	V_4	V_5
Sample	V_C	V_T

$$K_C = \frac{50}{\text{Log } V_1 - \text{Log } V_3} \qquad \text{Eq. 4.1}$$

$$K_T = \frac{20}{V_5 - V_2} \qquad \text{Eq. 4.2}$$

$$K_{CORR} = (\text{Log } V_1 - \text{Log } V_4) / 20 \qquad \text{Eq. 4.3}$$

$$C = K_C.(\text{Log } V_1 - \text{Log } V_C) \qquad \text{Eq. 4.4}$$

$$T = K_T.(V_T - V_2) \qquad \text{Eq. 4.5}$$

$$C_{CORR} = K_C.((\text{Log } V_1 - \text{Log } V_C)-(K_{CORR} * T)) \qquad \text{Eq. 4.6}$$

where K_C is the colour calibration constant, K_T is the turbidity calibration constant, K_{CORR} is the turbidity correction constant, C is the calculated colour, T is the calculated turbidity and C_{CORR} is the calculated corrected colour.

In Eq. 4.6, the (K_{CORR} * T) term is the contribution to optical density of turbidity in the sample. This is subtracted from the measured sample optical density to give the corrected colour value. These equations were applied to the samples mentioned in section 4.4.3 and the result is shown in Fig. 4.4.4.a.

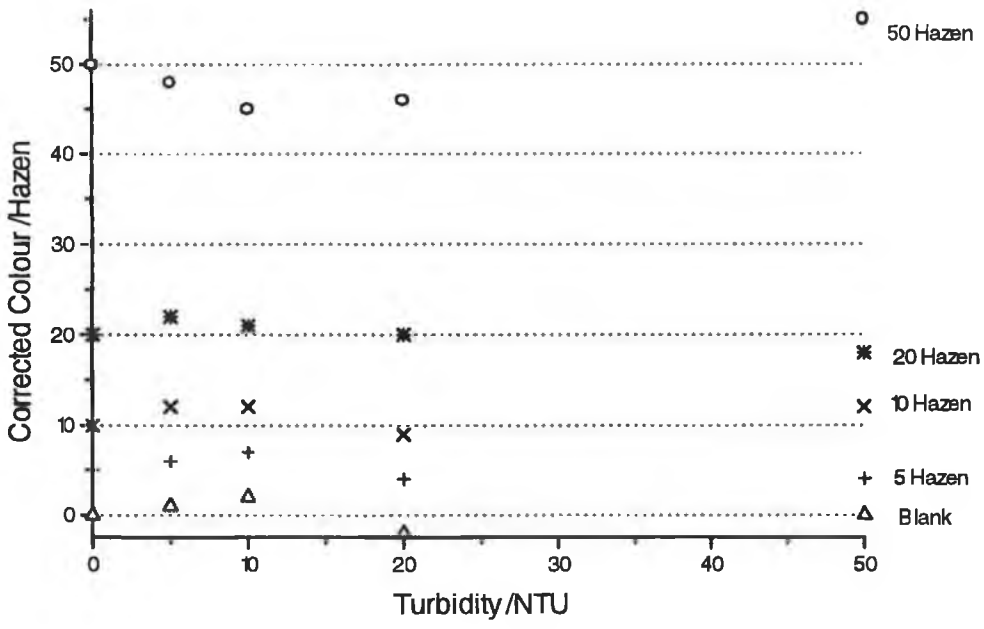

Fig. 4.4.4.a TURBIDITY COMPENSATED COLOUR MEASUREMENTS

Fig. 4.4.4.a shows that the corrected colour remains relatively constant as turbidity is increased. Fig. 4.4.3.a shows the change in optical density of these samples with increasing turbidity, and the above figure shows that this interference has been reduced considerably. Errors in this method arise from the much larger contribution to optical density of turbidity compared with true colour. This can be seen in the variation in corrected colour for all the samples.

4.5 Incorporation of LED into an Existing On-line Monitor

A schematic diagram of the RC100 Residual Coagulant Monitor for aluminium or iron is shown in Fig. 4.5.a. This device is produced by Aztec Environmental Control Ltd.

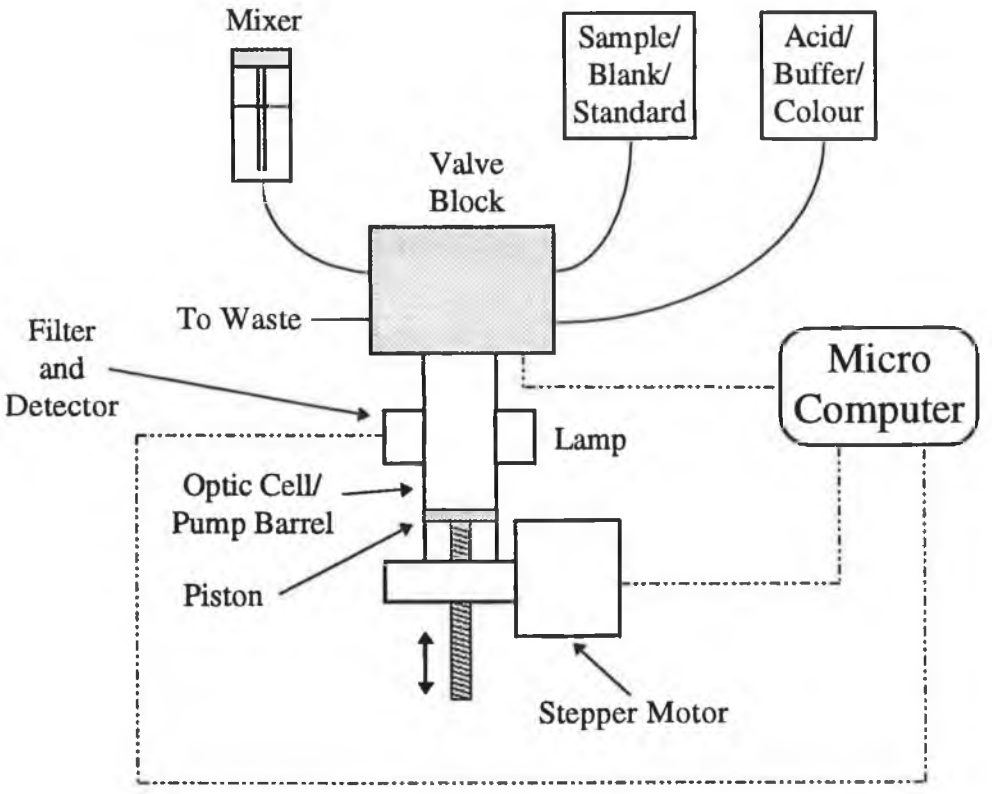

Fig. 4.5.a SCHEMATIC DIAGRAM OF ON-LINE MONITOR FOR ALUMINIUM OR IRON

The optic cell/pump barrel is a cylindrical glass walled cell with 2 cm internal diameter. The piston moves up and down the pump barrel or optical cell. By opening or closing selected valves in the valve block, sample/reagents can be drawn individually into the cell or the cell contents pumped to or from the mixers. The required volume ratio between sample and reagents is achieved by controlling the distance the piston moves and hence the amount of sample/reagent drawn into the cell. The treated sample is mixed for ten minutes

while colour develops. It is then drawn into the optical cell where its absorbance is measured. The monitor has an automatic two point calibration. For iron and aluminium, the lower concentration is a blank and the upper concentration is a 200 $\mu g\ L^{-1}$ sample. Eqs. 3.4 and 3.5 are then used to calculate the aluminium concentration in a sample. The onboard micro-computer controls the hardware and carries out the necessary calculations.

As the optical cell is also the pump barrel, the moving piston continually wipes the walls of the optic cell. Hence the device has in built cleaning which is important for long term on-line operation. The monitor also incorporates automatic sample dilution. Fig. 4.2.2.a shows that the Al-PCV reaction becomes non-linear at a certain point. This point for the filter and bulb used in the RC100 is ~330 $\mu g\ L^{-1}$. When the micro-computer detects a sample concentrations above this point, sample dilution is introduced. The sample is then diluted 2:1 with de-ionised water before being treated in the normal way. The calibration constant is automatically scaled by three to compensate for the dilution. This extends the linear range of the monitor to 1000 $\mu g\ L^{-1}$, roughly three times the value it would be without sample dilution. The monitor also incorporates colour correction. This is a method of compensating for any natural colour or turbidity in the pre-treated sample. It is achieved in the following way. The optical density of the untreated sample is measured. The reagents are added and the optical density again measured. The sample optical density (OD_{SPL} in Eq. 3.4) is defined as the difference between these two values. Therefore, only colour developed in the Al-PCV reaction is used in the calculation, and any natural colour present in the sample is omitted.

The optical source used is a white light incandescent bulb together with an interference filter. The optical components are shown in (i) of Fig 4.5.b. White light is passed through the sample with the filter allowing only the required bandwidth reach the detector. Positioning screws allow x-plane alignment of the detector and y-plane alignment of the bulb. The filter has a peak transmission wavelength of 592 nm and a bandwidth of 10 nm. There are several problems inherent in this optical configuration. Firstly the filter can delaminate over a period of time. This is the separation of the layers that form the filter

and it results in a change its optical transmission characteristics. The output of the bulb decreases over its lifetime. The filament inside the bulb can also move with a resulting change in alignment of the optical system. A number of these problems would be overcome by replacing the bulb and filter with an LED. Hence the yellow LED mentioned earlier was incorporated into this monitor and the resulting performance characterised.

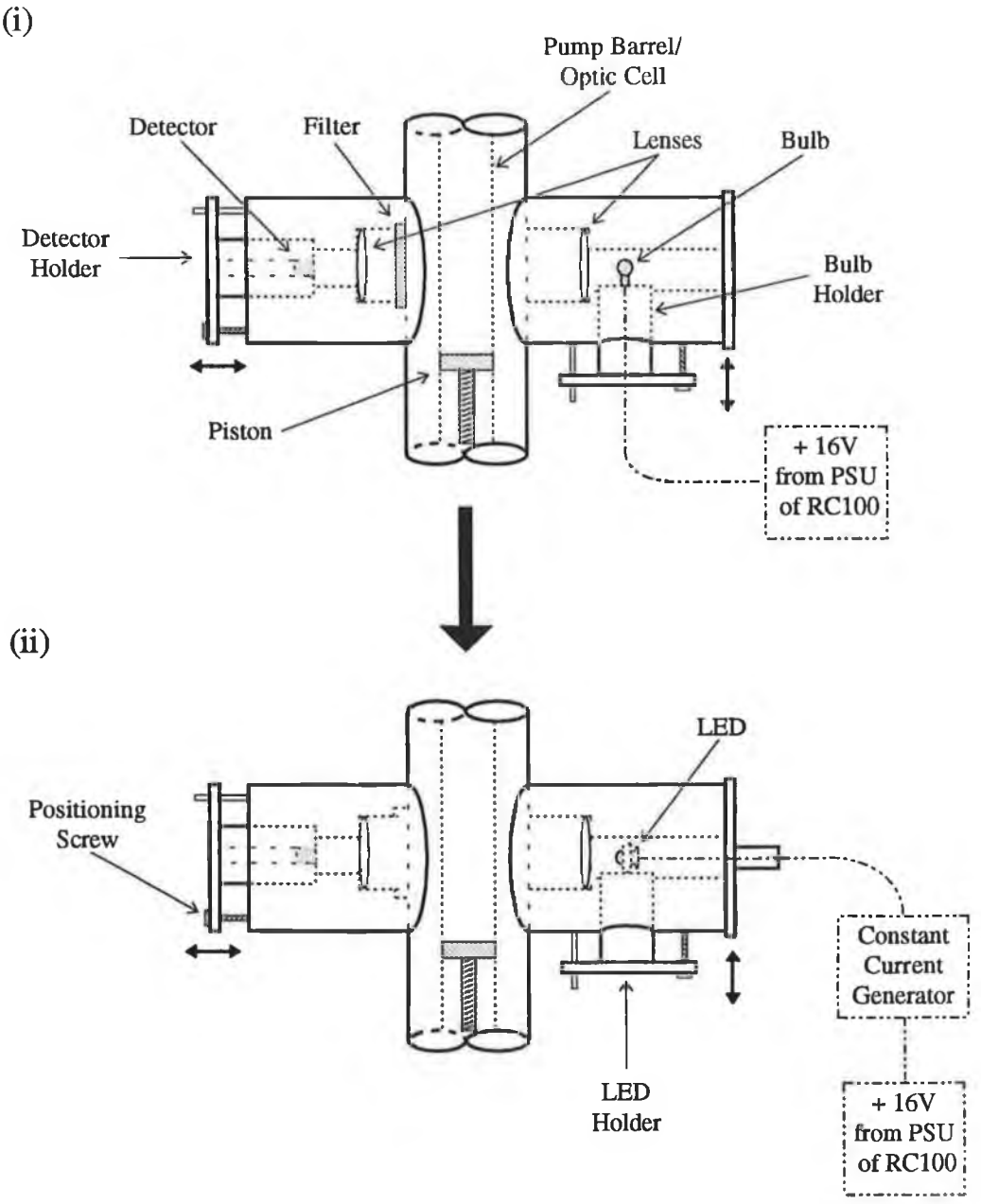

Fig. 4.5.b INCORPORATION OF YELLOW LED INTO RC100 MONITOR, (I) WITH FILTER & BULB, (II) WITH LED

A holder was constructed so that the position of the LED in the sensor head corresponded with the former position of the bulb, as shown in Fig. 4.5.b (ii). This meant that no additional lenses were required to complete the optical system. The filter was removed from the sensor head. The power supply for the bulb (+16 V) was used to power the LED. This voltage was converted to a constant current using a constant current regulator (LM317).

The bandwidth (10 nm) of the filter used in the RC100 is narrower than the output spectrum (30 nm) of the yellow LED. This means that the calibration curves of the two sources differ for reasons outlined in section 3.2. The calibration curves for the RC100 with filter and bulb and LED sources are shown in Fig. 4.5.c.

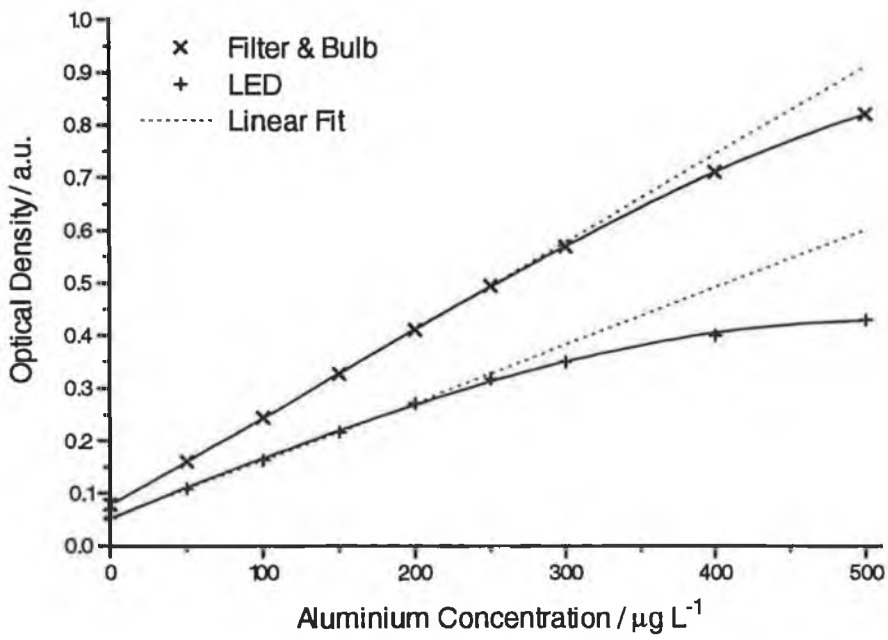

Fig. 4.5.c CALIBRATION CURVES FOR RC100 WITH FILTER & BULB AND LED AS SOURCES

It can be seen from Fig. 4.5.c that the filter and bulb has a higher sensitivity and higher linear range than the LED. However the increased output stability of the LED over the filter and bulb helps compensate for this reduced sensitivity and the overall performance is

not adversely affected. The lower sensitivity of the LED also means a higher value for the calibration constant outlined in Eq. 3.5. The RC100 has several automatic tests incorporated into its operating software. One of these tests checks that the calibration constant is within a certain range. The calibration constant required for operation with the LED is outside this range and hence the operating software was changed to allow for this larger value. Fig. 4.5.d shows the output from the RC100 in both configurations. In addition, when using the LED, the operating software was adjusted to change the point at which switch over to sample dilution occurred from 330 μg L^{-1} to 230 μg L^{-1}.

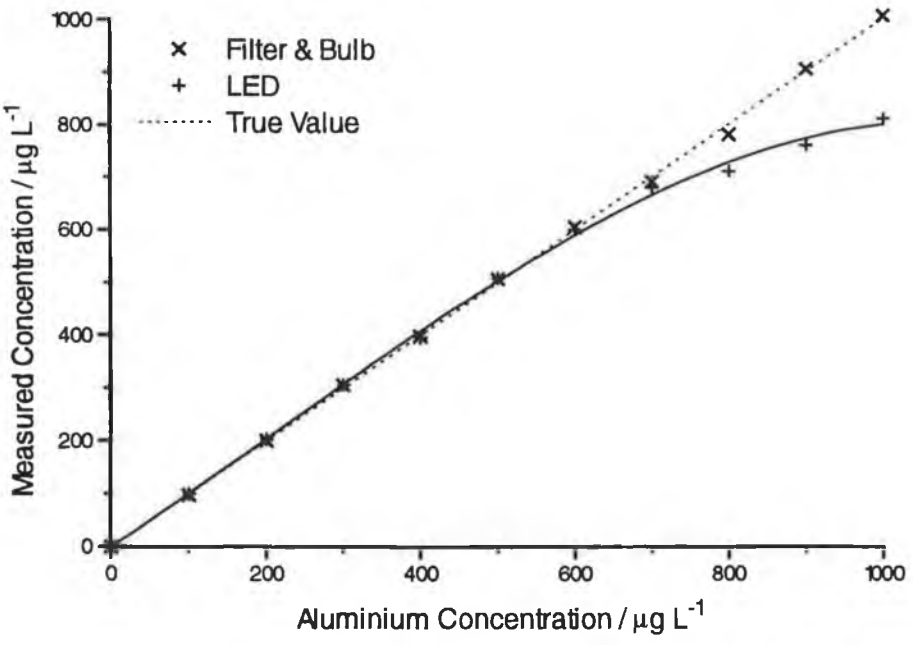

Fig. 4.5.d RESPONSE OF RC100 WITH FILTER & BULB AND LED AS SOURCES

It can be seen from Fig. 4.5.c that the measured values from the RC100 with LED are almost equal to the true values, in the range 0 → 600 μg L^{-1}. Beyond this point the system becomes non-linear. The linear range could be further extended by increasing the sample dilution ratio or by a reduction of the path length of the cell.

Tests were also carried out with the system testing for iron. Again the LED showed a lower sensitivity and shorter linear range compared with the filter and bulb. However, as with aluminium, the performances of the system in both configurations compared favorably.

Independent tests were carried out by Aztec Ltd. at their site in Didcot. They replaced the filter and bulb arrangement in an RC100 and carried out long term stability tests on aluminium samples. The monitor ran continuously for a ten day period. Over this time it took one measurement per hour. All measurements were made on one sample of concentration 198 $\mu g\ L^{-1}$. The results are shown in Fig. 4.5.e.

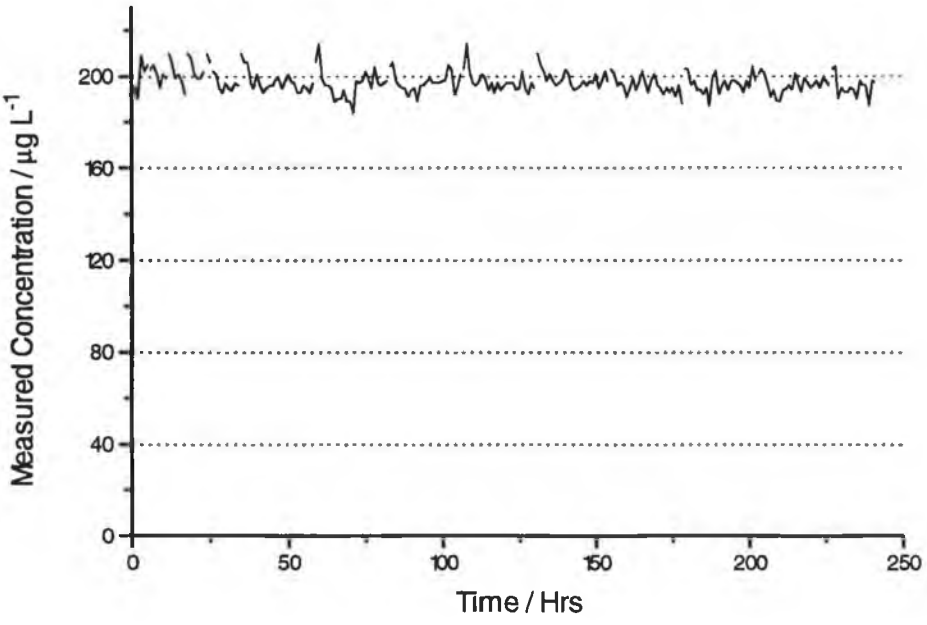

Fig. 4.5.e LONG TERM STABILITY TESTS OF LED IN RC100, TESTING FOR ALUMINIUM

The results shown in Fig. 4.5.e show a repeatability of 2% and a resolution of 0.3%, (see section 1.4.3). These figures are approximately equal to the technical specifications of the RC100 when operating with filter and bulb. The quoted figures for repeatability and

resolution are 2% and 0.5% respectively. These results show that the LED could replace the filter and bulb source of the RC100.

4.6 Conclusion

LED's were tested as sources in colorimetric tests for aluminium, iron, manganese, phosphate and colour. These tests revealed the linear range and sensitivity of LED's as sources in these tests. In certain cases the linear range and sensitivity of the LED were lower than those of the conventional filter and bulb sources, but the LED was still deemed to be a suitable source within the linear range of concentrations. An infra-red LED was also used to measure turbidity by means of scatter from samples. The intensity of the LED used was not as high as white light bulbs conventionally used to measure turbidity. For turbidity measurement sensitivity is related to intensity, hence, the LED was less sensitive than the conventional source, but the increased stability of the LED compensates for this loss of sensitivity. Investigations were made into the interference of colour in turbidity measurement and turbidity in colour measurement. Equations were derived for the compensation of turbidity in colour measurement. Finally, an LED was incorporated into an existing on-line colorimetric monitor and the performance of this system, with the LED source was determined. There was a reduction in linear range compared with the existing source. However other performance characteristics were not adversely affected by the incorporation of the LED. Problems of reduced linear range could be overcome by use of shorter path lengths. Hence LED's were shown to be suitable sources for colorimetric tests and their incorporation into on-line monitors would overcome several of the problems associated with the existing sources, i.e. bulb and filter instability and filter delamination.

Chapter 5

Modular Sensor Head

5.1 Introduction

In Chapter 4 a set of experiments which showed the suitability of LED's as sources in a number of colorimetric tests was described in detail. In addition the performance of an LED which was tested in an on-line commercial colorimetric monitor was reported. Based on the results of these experiments it was decided to design a modular sensor head with a view to its use in a miniature system for monitoring a range of water quality parameters. This cell was tested in a computer-controlled system. The object of these tests was to determine the feasibility of using miniature optical components and a flow through cell to measure the absorbance of treated samples.

5.2 Modular Cell Design

The on-line system examined in Chapter 4 is limited to a single path length cell and a single source. Because the cell has a large volume it has considerable reagent consumption. It was shown in the last chapter that because of the different sensitivities of the various colorimetric tests, a range of possible path lengths would be necessary in a sensor employing all of these tests. Each test has its own source and a multi-analyte sensor would also have to incorporate a range of different sources. Miniaturisation of the sensor head allows miniaturisation of the complete sensor system, as well as reducing the amount of sample and reagents consumed and hence reduces the operating costs of the system. These were the motivations behind the design of the sensor head described here.

The range of path lengths was achieved by the modular design of the components making up the sensor head. The LED sources were incorporated into the control electronics and an optical fibre was used to deliver light to the sensor head. In this way, a range of sources was available by simply changing the fibre to the relevant LED connection at the

control electronics. Miniaturisation was assisted by use of miniature lenses. The modular design of the sensor head is shown in Fig. 5.2.a.

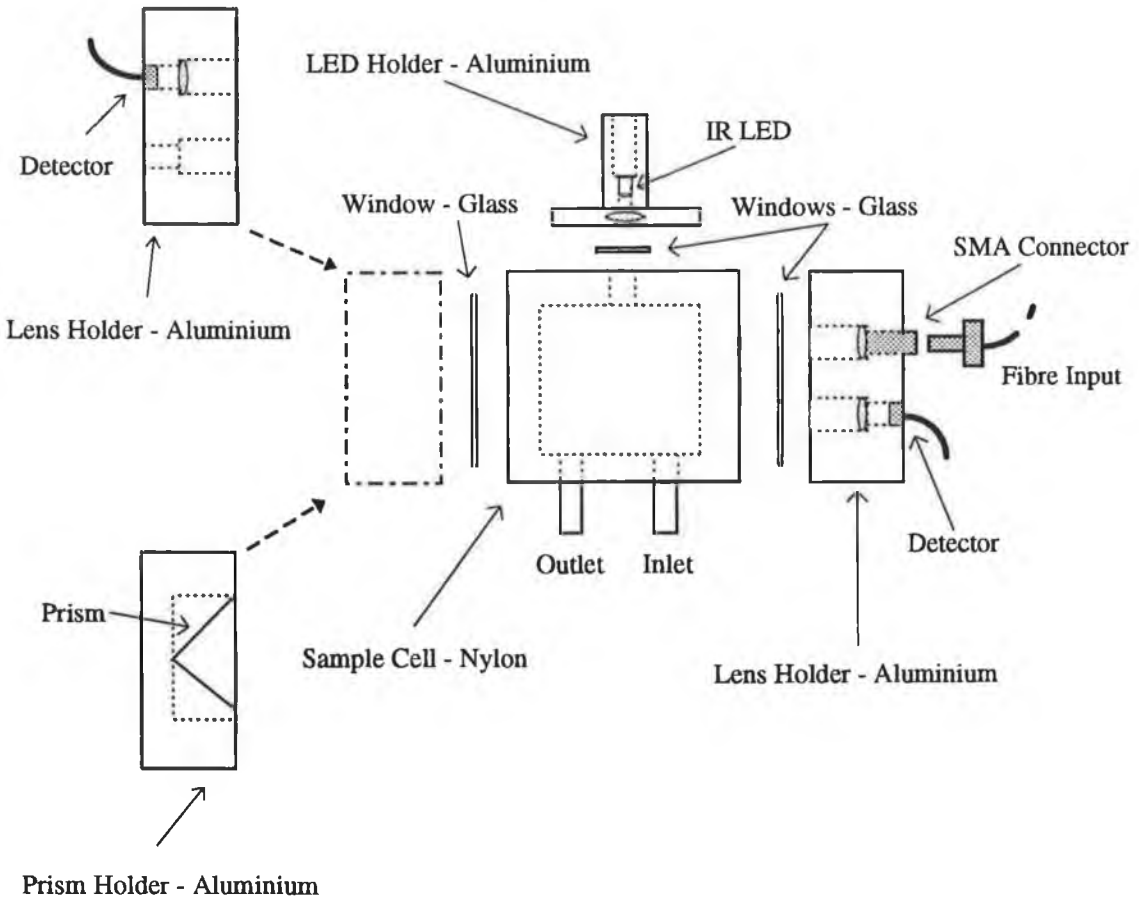

Fig. 5.2.a MODULAR DESIGN OF SENSOR HEAD

Three sample cells were constructed from nylon. The cell shown in Fig. 5.2.a has a path length of 4 cm for straight through transmission, without the prism, and is used for colour and turbidity measurements. Cells were also constructed of path length 2 and 1.5 cm. These cells were designed for absorption measurements only. Optional incorporation of the prism doubled the effective path length of each cell. In this way, the range of total path lengths available was 1.5, 2, 3, 4 and 8 cm. This range was chosen based on the sensitivities and linear ranges for the various tests as determined in Chapter 4. The sample

outlet in the 1.5 cm cell was positioned directly opposite the inlet hole. This improved bubble rejection in the cell as bubbles floated to the top of the cell and out through the outlet. Glass windows were used between the sample cell and the lens or prism holders. Hence the sample encountered no metal parts in the sensor head. This is particularly relevant for the prevention of interferences when detecting metal ions in water. Rubber 'O-Rings' on both sides of the glass windows were used to seal the cell.

5.3 Description of Computer-Controlled System

A schematic diagram of the computer-controlled system is shown in Fig 5.3.a with the sensor head configured for colour and turbidity measurements.

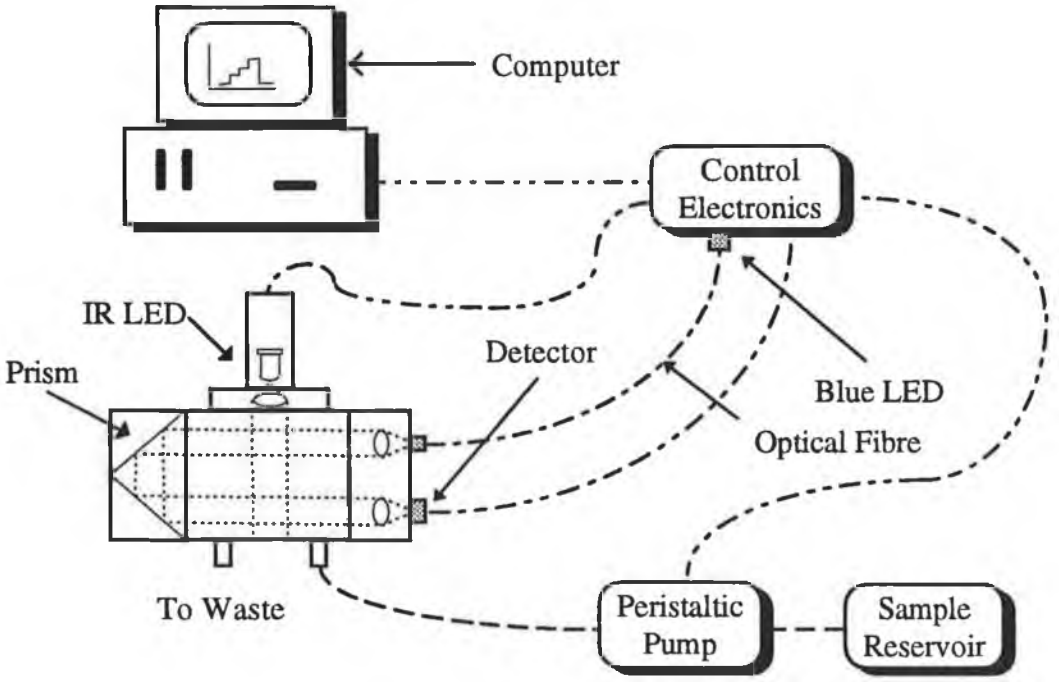

Fig. 5.3.a SCHEMATIC DIAGRAM OF COMPUTER CONTROLLED SYSTEM CONFIGURED FOR COLOUR AND TURBIDITY MEASUREMENTS

There follows a description of the other components used in the computer-controlled system.

5.3.1 Optics

Each of the three lenses used was of the plano-convex type, with a focal length of 8 mm and diameter of 8 mm. The optical fibre used to deliver light from the LED's to the cell had a glass core with a diameter of 1 mm and a numerical aperture of 0.49. The fibre was SMA-terminated and the cell had an SMA connection. An infra red LED (RS# 585-242) with a peak wavelength of 880 nm, a bandwidth of 20 nm and an output power of 20 mW was used for turbidity measurements. A blue LED (Ledtronics, California, U.S.A.) with a peak wavelength of 420 nm, a bandwidth of 70 nm and an output intensity of 1 mW was used for colour measurements. A high intensity source is necessary to measure the scattered signals from samples of low turbidity, hence the infra red LED was incorporated into the sensor head, overcoming losses due to fibre coupling. The blue LED was located with the control electronics and the fibre was used to deliver the light to the cell. The prism used was a glass, right angle (90°) total internal reflection prism.

5.3.2 Sample Delivery

A peristaltic pump, Gilson Minipuls 3, was used to deliver samples to the cell. The sample delivery time of the system was ~90 seconds which corresponded to pumping 30 mLs of sample through the system. The volume of the sensor head itself is smaller than this required sample volume. The larger volume is required to flush the old sample from the cell. Reducing the cell volume would lower the response time and sample volume required. Increasing the pump rate would also decrease the response time.

5.3.3 Electronics

A full description of the LED driver circuit is given in Appendix B. This circuit operates one of three LED's at a time as determined by the computer. The current to the operating LED is modulated and a lockin amplifier is used at the detection stage. A full description of the detection circuit is given in Appendix C. The output from this circuit goes to the Analog to Digital Converter (ADC) of the Input/Output (I/O) card of the computer, a Bytronic MPIBM3 Multifunction I/O Card.

A software routine was written to measure the long term stability of the electronics. The sensor head was assembled but no sample was placed in the cell. The routine operated in the following way. The blue LED was switched on, and its intensity measured three times over a three minute interval. The blue LED was then switched off and the IR LED switched on and its intensity measured over a three minute interval. The values were written to a file and the whole procedure was repeated over a twenty four hour period. The relative standard deviations (RSD) of the blue and IR LED's were 0.4% and 1.0%, respectively.

5.3.4 Software

The control software for the system was written in TurboC++. A listing is included in Appendix D. The software turned on/off the various LED's. The computer also switched on/off the pump, and read the signal values from the detection circuit. The calculated values were displayed, in the form of a graph, on the computer screen and also saved to disk. Calculations of sample colour, turbidity and corrected colour were performed, based on the method outlined in sections 3.3.2 ,3.4.2 and 4.4.4. Fig. 5.3.4.a shows a flow chart of the control software for the combined colour and turbidity measurement system.

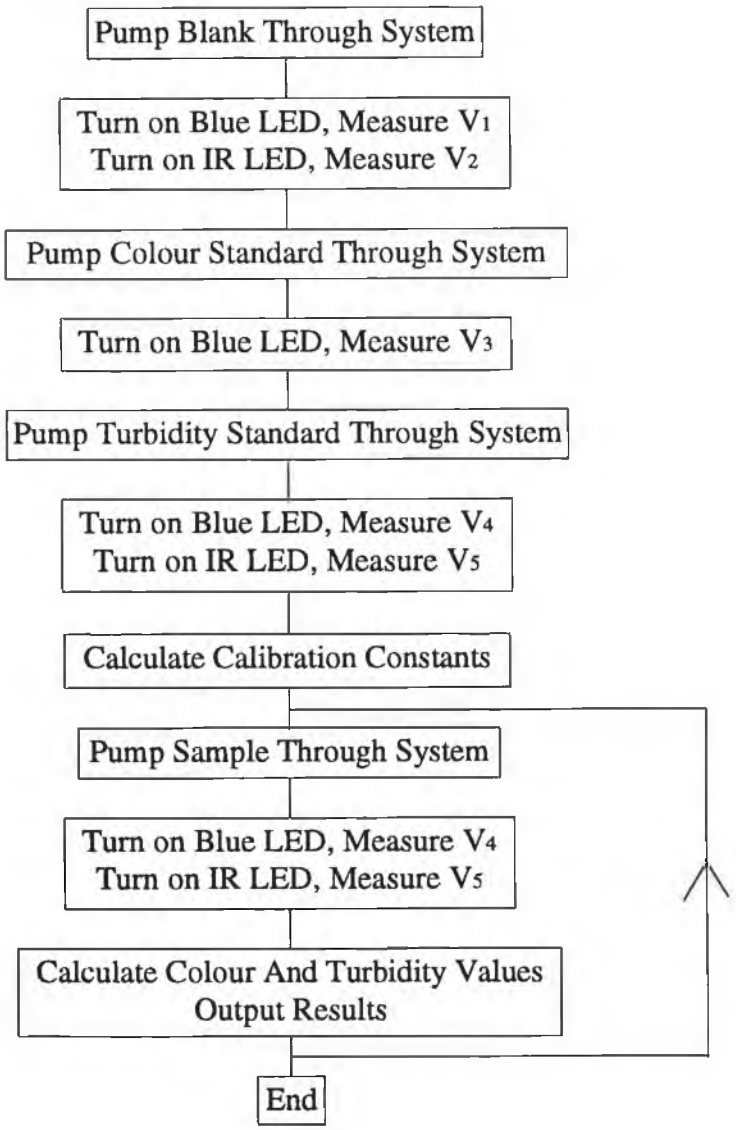

Fig. 5.3.4.a FLOW CHART OF COMPUTER SOFTWARE

5.4 Results

All reagents used were provided by Aztec Environment Control Ltd. A de-ionised water blank sample, a 50 Hazen colour standard and a 20 NTU turbidity standard were used to calibrate the system for colour and turbidity measurements.

5.4.1 Colour Measurements

Colour samples were prepared by dilution of a 500 Hazen stock solution as outlined in the last chapter. The sample colour was incremented by 10 Hazen at each change. The system response to colour is shown in Fig. 5.4.1.a. Colour samples have a low optical density and in order to maximise sensitivity the longest path length was used, i.e. 8 cm.

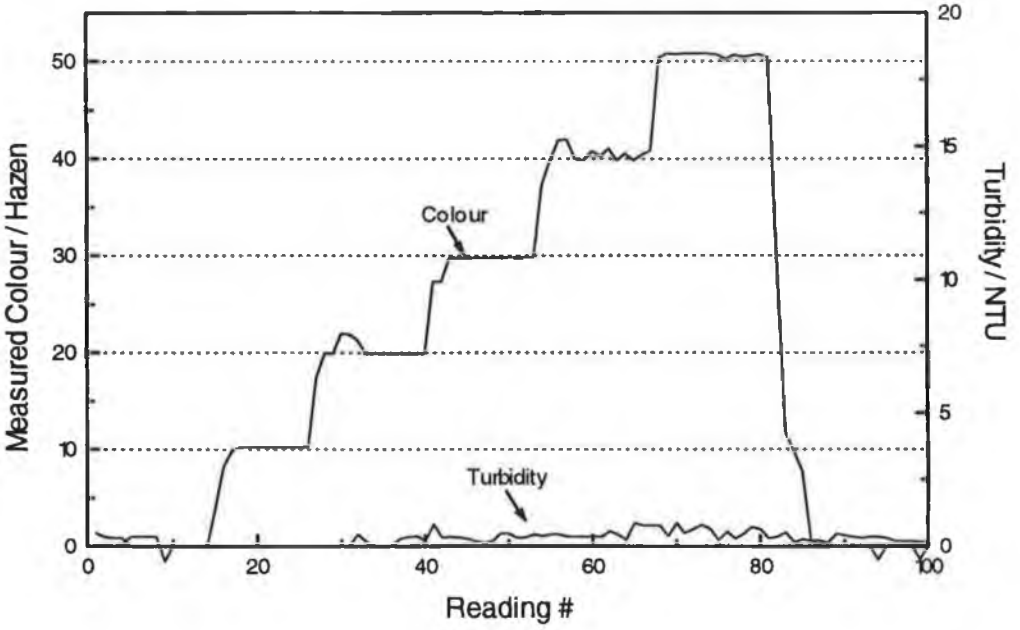

Fig. 5.4.1.a SYSTEM RESPONSE TO COLOUR

The variations on the signal in Fig. 5.4.1.a, are due to air-bubbles in the cell. Air-bubbles entered the cell, obstructed the optical beam and therefore increased the measured colour until they were ejected from the cell. Without the interference of air-bubbles the system output is relatively steady, as can be seen from the 10, 30 and 50 Hazen regions. At a later

stage in the experimental work it was discovered that this problem could be reduced considerably by proper sealing of the tubes comprising the deliver system, and by reduction of the internal diameters of the delivery tubes. The linear range for colour was found to be 80 Hazen with a limit of detection of 0.5 Hazen, a resolution of 1% and a repeatability of 1%. The measured turbidity is also included in Fig. 5.4.1.a. It can be seen that the turbidity remains approximately zero as the sample colour is increased. This shows that sample turbidity is almost independent of colour, as stated in section 4.4.2.

5.4.2 Turbidity Measurements

Turbidity samples were prepared by dilution of a 4000 NTU turbidity stock solution as outlined in the last chapter. The turbidity increments were 5 NTU. The system response to turbidity is shown in Fig. 5.4.2.a.

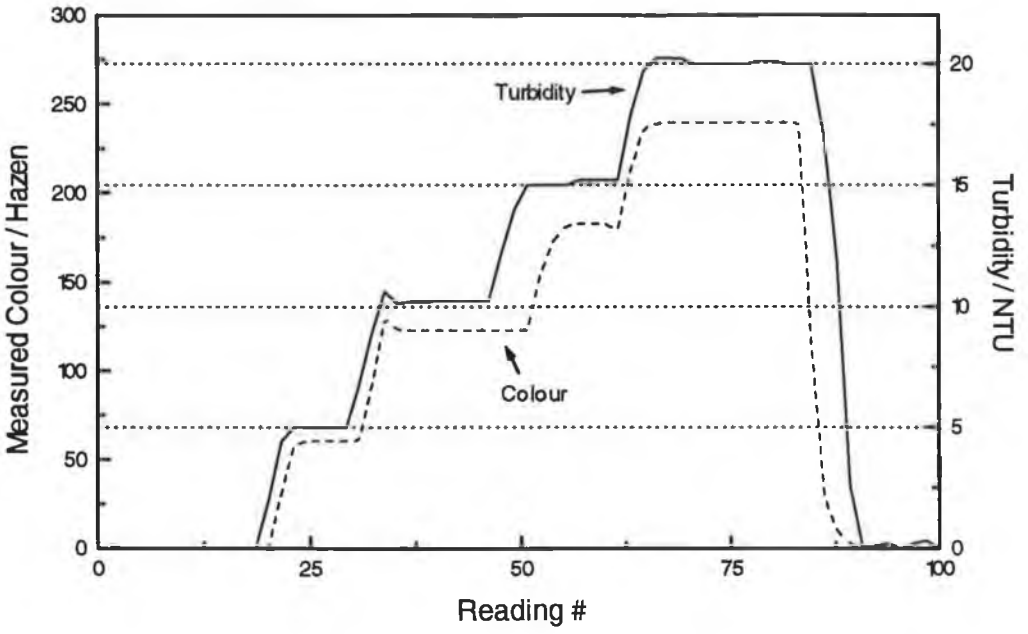

Fig. 5.4.2.a SYSTEM RESPONSE TO TURBIDITY

Included in Fig. 5.4.2.a is the measured colour. It can be see that the measured colour value increases dramatically as the sample turbidity increases. For example, for a sample turbidity of 20 NTU, the measured colour is 240 Hazen. This positive interference of turbidity on colour measurements was discussed in section 4.4.3 and a method of compensating for the interference was derived. This approach was pursued here and the outcome is described in section 5.4.3. The linear range for turbidity was found to be 50 NTU with a limit of detection of 0.3 NTU, a resolution of 1% and a repeatability of 0.5%. In the last chapter in section 4.3 using the bench-top system, the linear range for turbidity was found to be 400 NTU. The reason for this large difference in linear range between the two systems is unknown by the author. The two systems have different optical configurations. For example, in the bench-top system the lenses used had a focal length of 20 mm and a diameter of 25 mm. This meant a beam width ~15 mm in the sample and the equivalent collection optics dimensions. However in the configuration discussed here, the beam width and collection optics had a dimension of ~4 mm. Hence the sensing area in the sample was smaller and this may account for the reduced linear range.

5.4.3 Turbidity Compensated Colour Measurements

In section 4.4.4 equations were derived for the compensation of turbidity in colour measurement. These equations were incorporated into the control software for the system. This section investigates this compensation by measuring the colour of an increasingly turbid colour sample. A 20 Hazen solution was prepared and placed in the sample reservoir. The system was started and as colour and turbidity was measured, increasing amounts of 4000 NTU stock solution were added to the sample to increase its turbidity. The results from this test are shown in Fig. 5.4.3.a

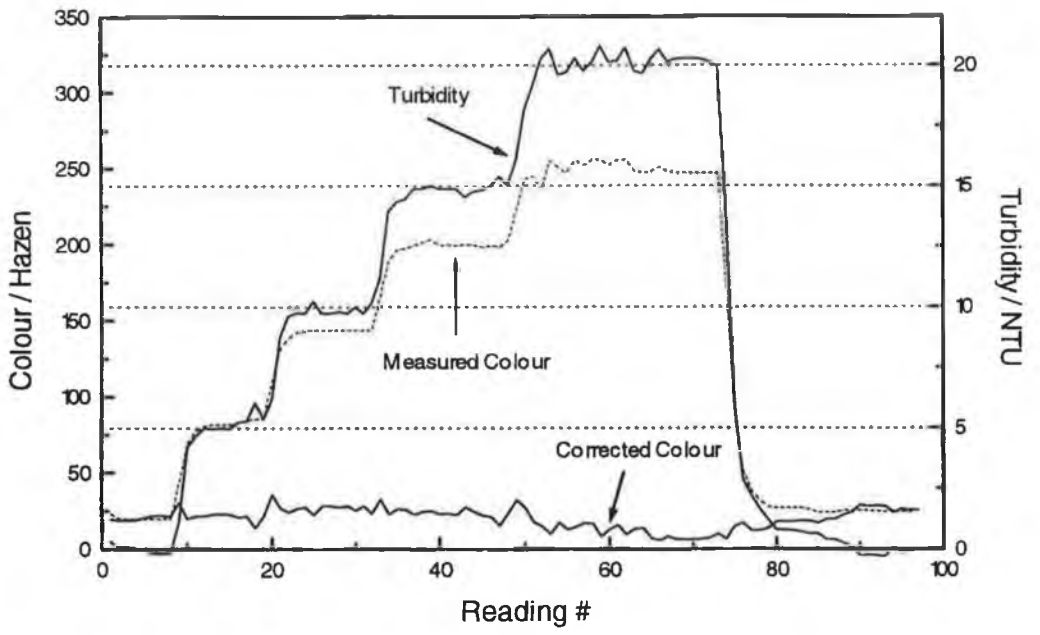

Fig. 5.4.3.a TURBIDITY COMPENSATED COLOUR MEASUREMENTS

Again, the variation on the signals in Fig. 5.4.3.a is mainly due to air bubbles in the cell. At a turbidity of 20 NTU, the measured colour is ~250 Hazen. Using the compensation approach the corrected colour is recorded to be ~15 Hazen, a discrepancy of 5 Hazen from the known value. When the sample turbidity value is zero, the measured colour and corrected colour have the same value. The approximately constant value of corrected colour in Fig. 5.4.3.a show that the interference of turbidity on colour measurements can be reduced considerably.

5.4.4 Additional Colorimetric Tests

The last section showed that the modular cell could be used to measure colour and turbidity. Experiments were also carried out with the cell on the colorimetric tests for iron and aluminium. This required the use of different path lengths and changing the LED source. The IR LED was removed and the yellow LED mentioned in the previous chapter

replaced the blue LED. The software was changed so that the yellow LED remained 'on' throughout the measurement procedure. No switching between LED's was required. All samples were pre-treated manually, as outlined in section 4.2.2. An typical system response is given in Fig. 5.4.4.a. These results were obtained for iron samples. The concentration increment at each point was 100 μg L^{-1}. A 4 cm cell was used, based on the sensitivity of this reaction as determined in Chapter 3.

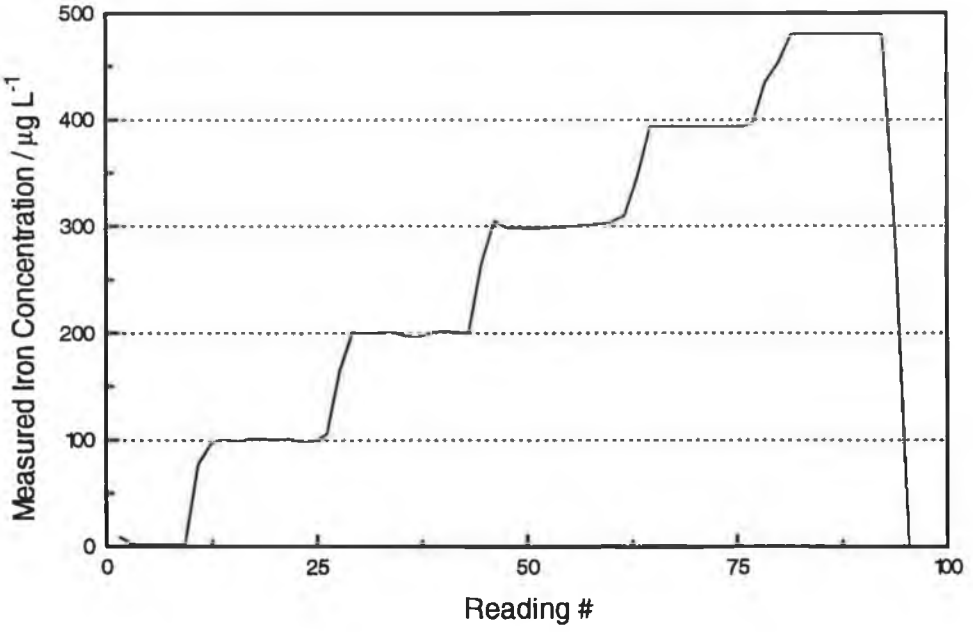

Fig. 5.4.4.a SYSTEM RESPONSE TO IRON SAMPLES, YELLOW LED AS SOURCE, 4 CM CELL

It can be seen from Fig. 5.4.4.a that at a concentration of 400 μg L^{-1} the system output is ~390 μg L^{-1}, that is, the system is becoming non-linear. The limit of detection was measured to be 8 μg L^{-1} with a repeatability and resolution of 1.5% and 1.5%, respectively. The tests were repeated using a 2 cm path length cell. This doubled the effective linear range but increased the limit of detection, repeatability and resolution.

5.4.5 Summary of Results

The following is a summary of results obtained from the computer based sensor system outlined in this chapter.

	Path Length/cm	Limit of Detection	Linear Range	Repeatability / %	Resolution / %
Colour	8	0.5 Hazen	80 Hazen	1	1
Turbidity	-	0.3 NTU	50 NTU	0.3	1
Iron	2	14 $\mu g\ L^{-1}$	750 $\mu g\ L^{-1}$	2	2
	4	8 $\mu g\ L^{-1}$	400 $\mu g\ L^{-1}$	1.5	1.5
Aluminium	2	6 $\mu g\ L^{-1}$	200 $\mu g\ L^{-1}$	2	1.2

5.5 Conclusion

In this chapter a modular design flow through cell was introduced. Using a computer based system, the cell was tested for absorption and scatter measurements. The modular cell achieved most of its objectives, i.e. versatility and miniaturisation. Measurements were made using a range of path lengths and colorimetric tests requiring different sources were tested with the cell. The sensor head was also miniaturised. However compared to the sensor head of the on-line monitor presented in Chapter 4, the sample volume required was not reduced considerably. Although the volume of the sensor head was reduced, an amount of sample volume is required to flush the old sample from the cell. In the next chapter this sensor head will be used in a portable stand alone system capable of monitoring a range of water quality parameters.

Chapter 6

Portable LED-Based System

6.1 Introduction

In the last chapter the use of a modular sensor head was described. These experiments showed that the combination of miniature optical components, fibre optic links and LED's could produce a compact, versatile flow through sensor head for absorption and turbidity measurements. As a further development of this it was decided to miniaturise a complete system and to produce a fully portable, versatile, stand-alone unit. This system incorporates a full sample/reagent delivery system based around a four channel peristaltic pump. System control and calculations of analyte concentrations are performed by dedicated electronics. The sensor performance was characterised for measurement of aluminium, iron, manganese, phosphate and sample colour and turbidity.

6.2 Description of Set-up

A schematic diagram of the portable LED based system is shown in Fig. 6.2.a.

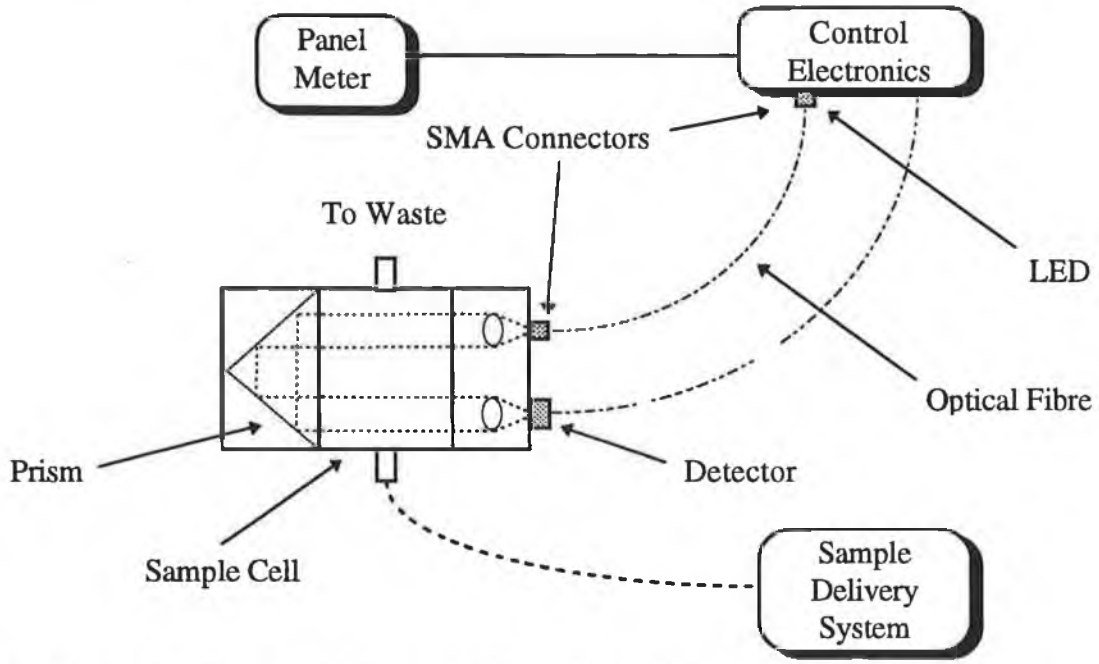

Fig. 6.2.a SCHEMATIC DIAGRAM OF PORTABLE LED-BASED SYSTEM

In the last chapter the modular sensor head was tested in a computer controlled system. The computer controlled the hardware and carried out the necessary calculations. Samples were pre-treated manually and delivered to the cell using a single channel peristaltic pump. There follows a description of the additional components introduced to the system to produce a portable sensor. A photograph of the sensor is shown in Appendix E.

6.2.1 Delivery System

A schematic diagram of the delivery system used is shown in Fig 6.2.1.a. The peristaltic pump used was an Ismatec Mini-S Cartridge pump with a fixed speed of 40 r.p.m. The pump was powered from the mains supply. When using a peristaltic pump, for a fixed head rotation rate, different flow rates are achieved by using pump tubes of varying internal diameters (I.D.). To ensure correct pH values and maximum colour development, the reagents used for the different tests require a 5:1:1:1 ratio between sample and the three reagents and this was achieved by choosing a pump tubing internal diameter of 1.09 mm for the reagents and 2.79 mm for the sample. This gave a delivery rate of 16 mL/min. for the sample and 3 mL/min. for the reagents. In this way the required ratio was approximately achieved. The tubing used to form the mixing coils and deliver the sample to the cell was tygon tubing of I.D. 0.89 mm. The mixing coils were achieved by wrapping the tubing ~7 times around a rod of diameter 1 cm. This induced swirling in the sample and caused it to mix.

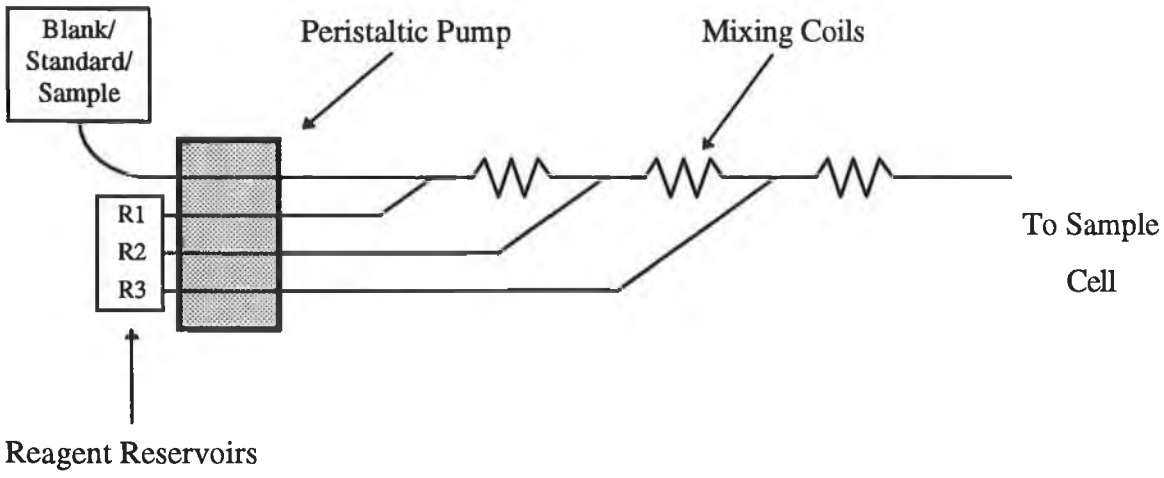

Fig. 6.2.1.a SCHEMATIC DIAGRAM OF DELIVERY SYSTEM

With the pump on, the sample and three reagents are pumped continuously. The sample and first reagent (R1) combine, the two mix and then the second reagent (R2) is added and so on. In this way the three reagents are sequentially added to the sample.

6.2.2 Electronics

The dedicated electronic circuits replaced the computer used in the system detailed in Chapter 5. The principle electronic circuits required were the LED driver circuit, which allowed selection of a source from a range of LED's and the detection and log-amp circuit. These were constructed on two separate PCB's. A detailed description of these two circuits is given in Appendices F and G, respectively. A block diagram of the detection electronics is shown in Fig. 6.2.2.a

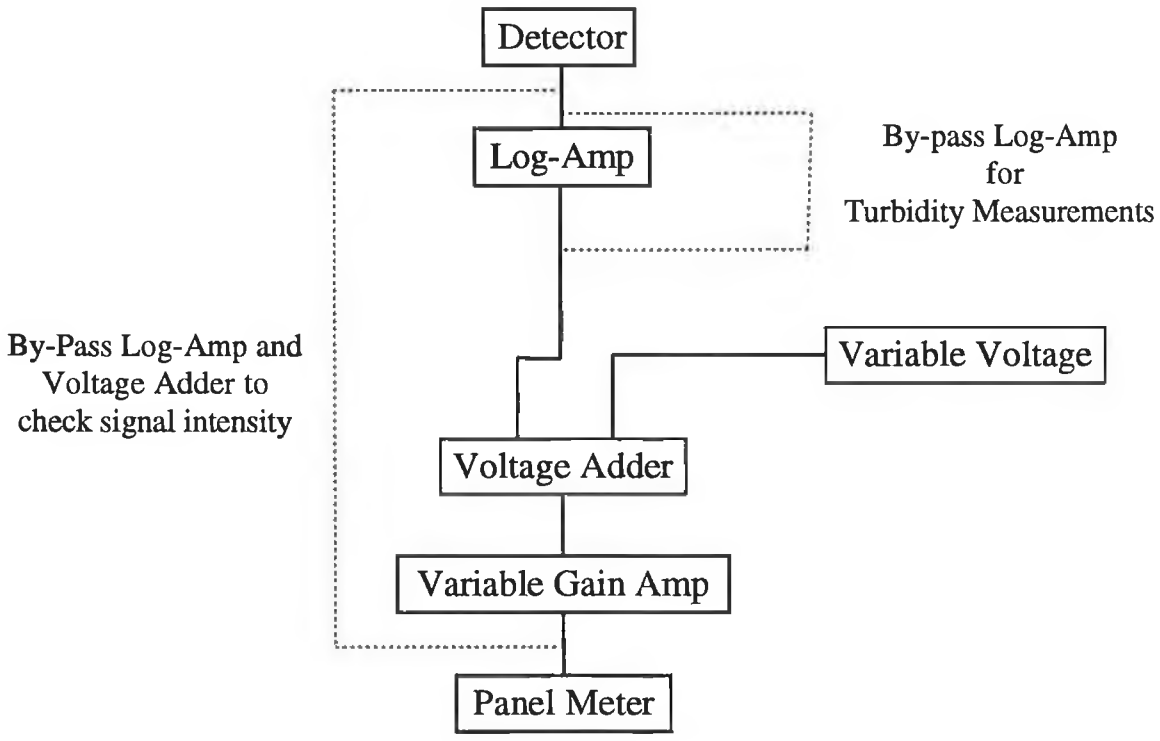

Fig. 6.2.2.a BLOCK DIAGRAM OF DETECTION ELECTRONICS

The block diagram in Fig. 6.2.2.a shows schematically how the detection electronics generates analyte concentrations from signal intensities. The signal from the detector goes to the logarithmic-amplifier, (log-amp). The log amplifier converts the detector output to a voltage which corresponds to the log of the signal intensity. Conversion of the signal intensity to log allows optical densities to be generated. In this way the system converts the logarithmic changes in the treated sample's optical density to linear changes in sensor output. The voltage from the log-amp then goes to the voltage adder. The other input to the adder is a variable voltage. When a blank has been generated by the system, this voltage is adjusted, (by adjustment of the Zero Adjust), until the adder output is zero. Hence the blank value is effectively subtracted from subsequent measurements. The output from the voltage adder goes to a variable gain amplifier. When a standard has been generated, the gain of this amplifier is adjusted, (by adjustment of the Gain Adjust), until the value displayed by the panel meter corresponds to the concentration of the standard. For turbidity measurements the log amplifier is by-passed and the signal intensity may be checked by by-passing the log-amp and voltage adder.

The long term stability of the electronics was tested in the following way. The system was assembled with a yellow LED selected on the LED driver circuit. A data logger was used to record signal values. The data logger used was a SmartReader self-powered device. It has an 8 bit ADC and a memory capacity of 36000 points. The data logger also recorded temperature. On the detection and log-amp circuit, voltages were recorded at two points. The output signal from the detector was connected to the data logger. This voltage corresponded to the signal intensity of the LED. The output to the panel meter was also recorded. This corresponded to the variation in the output signal of the complete system. A reading was taken every eight seconds over a twenty-four hour period. The relative standard deviations in the signal intensity, panel meter output and temperature were 0.4%, 5% and 0.8%, respectively.

6.2.3 Measurement Procedure[†]

The first step is to choose the path length appropriate for the measurement required. This is determined by the analyte of interest but also by the limit of detection and linear range required. The sensor head is then assembled using the appropriate modules. The required LED is chosen on the LED driver circuit and the detector circuit is configured for attenuation or turbidity measurements, as required. The free end of the reagent pump tubes are placed in the relevant reagent reservoirs. A sample is inserted into the system by placing the free end of the sample pump tube into the sample. A blank sample is inserted. The pump is turned on for ~2 minutes. In the case of colorimetric measurements, colour is allowed to develop in the cell, the time required depending upon the analyte in question. The Zero Adjust is changed until the panel meter reads zero. A standard sample is then inserted and the pump turned on. After two minutes the pump is stopped and colour allowed to develop. The Gain Adjust is changed until the panel meter reads the appropriate concentration, (e.g. 0200 for an iron standard of 200 $\mu g\ L^{-1}$ concentration). The sensor is now calibrated and ready for use. Samples of unknown concentration are inserted and pumped through the system. The panel meter value corresponds to the concentration of analyte in the sample.

A typical response from the sensor system is shown in Fig. 6.2.3.a. These measurements were taken with the device configured for manganese measurement. The path length was 3 cm and the LED used had a peak wavelength of 450 nm. Samples were prepared from 1000 ppm stock solution as outlined in section 4.2.2.

[†] A more detailed set of User Instructions is given in Appendix H

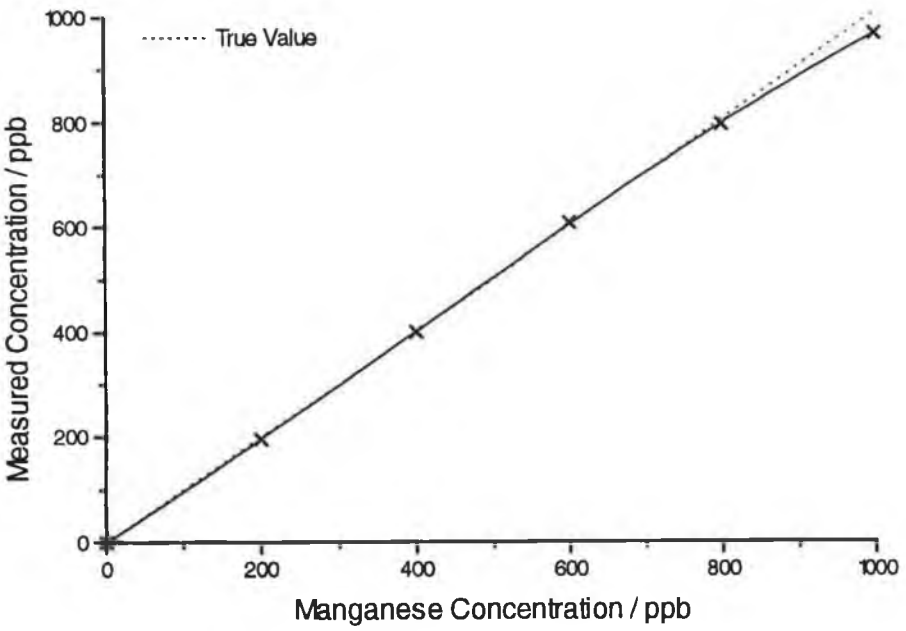

Fig. 6.2.3.a SENSOR RESPONSE TO MANGANESE SAMPLES, 3 CM CELL, $\lambda = 450$ NM

It can be seen that the sensor has a linear output in the range 0→800 ppb of manganese. Repeated measurements were made on a blank sample, and a sample of known concentration, to determine the limit of detection and repeatability. These were found to be 5 ppb and 3% respectively.

Tests were also carried out on several river samples. These samples were also tested, using standard test procedures, on a spectrophotometer. The samples were pre-treated manually and Eqs. 3.4 and 3.5 used to calculate concentrations. Sample turbidity was measured on the apparatus outlined in section 4.4.1. The results of these tests are shown in the following tables.

Didcot Stream

	Al /μg L^{-1}	*Colour /Hazen*	*Fe /μg L^{-1}*	*P /mg L^{-1}*	*Turbidity /NTU*
Sensor	3	18	3	97	47
Spectrophotometer	4	16	2	96	50

Didcot Bore Hole

	Al /μg L^{-1}	*Colour /Hazen*	*Fe /μg L^{-1}*	*P /mg L^{-1}*	*Turbidity /NTU*
Sensor	0	0	0	4	0.2
Spectrophotometer	0	0	0	3	0

River Thames

	Al /μg L^{-1}	*Colour /Hazen*	*Fe /μg L^{-1}*	*P /mg L^{-1}*	*Turbidity /NTU*
Sensor	2	22	4	80	60
Spectrophotometer	2	20	3	83	67

The above tables show a good agreement between the results from the standard procedure and those from the sensor system. This shows that the system developed is suitable for measurements on real river samples.

6.3 Additional Features of Sensor

6.3.1 Sample Dilution

Sample dilution enables linear range to be extended without reducing the path length of the cell used. This was discussed in section 4.5, in relation to the RC100 on-line monitor for iron and aluminium. The RC100 monitor automatically dilutes samples of high concentration, thus extending the linear range of the device. This technique can also be used with the portable sensor under consideration. Dilution can be performed manually before sample treatment or automatically by the introduction of an additional stream into the delivery system. Fig. 6.3.1.a shows how automatic sample dilution may be achieved.

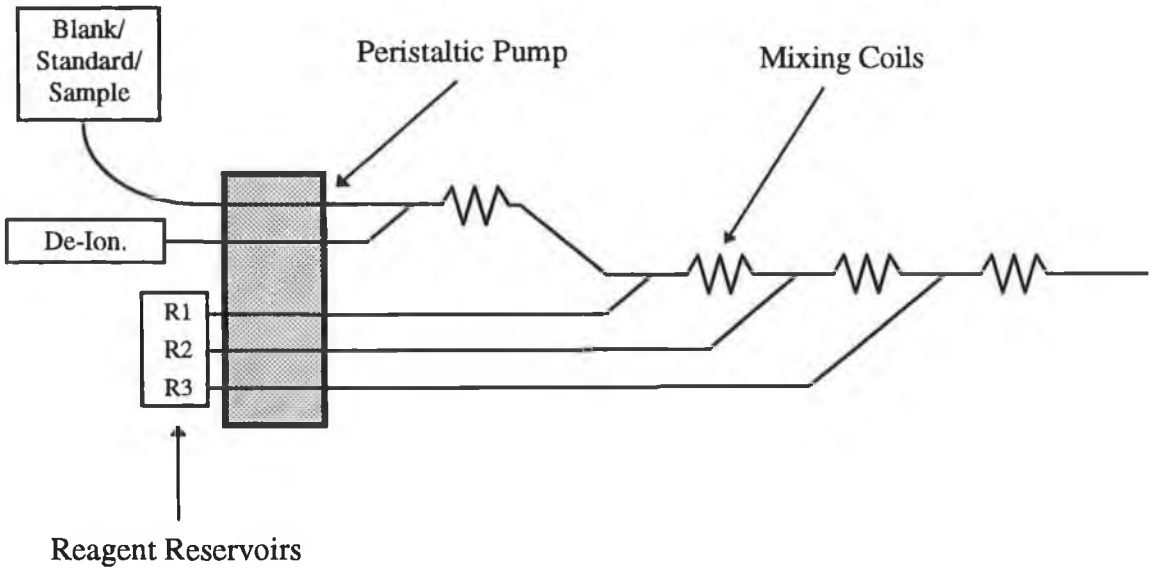

Fig. 6.3.1.a SCHEMATIC DIAGRAM OF DELIVERY SYSTEM WITH SAMPLE DILUTION

In this case the sample is mixed with de-ionised water before addition of the reagents. The sample dilution ratio depends upon the I.D.s of the tubes chosen but the combined volumes from both sample and de-ionised water must satisfy the required 5:1:1:1 ratio between treated sample and reagents. If sample dilution is introduced then the values displayed by the panel meter are scaled by the dilution ratio. For example, if the dilution ratio is 1:1 then the values displayed by the panel meter will be halved. Alternatively, the system can be recalibrated and operated as normal. Sample dilution requires the introduction of an additional channel to the delivery system and pump tubes of varying I.D.s. Shown in Fig. 6.3.1.b is an example of where sample dilution is used to extend the linear range of the sensor in the iron measurement configuration.

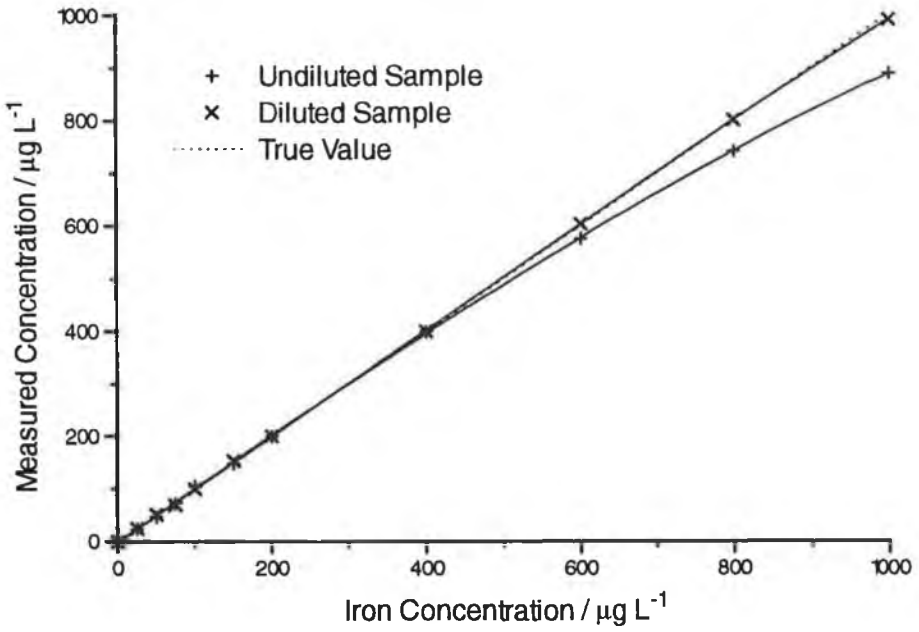

Fig. 6.3.1.b EXAMPLE OF EXTENDED RANGE USING SAMPLE DILUTION FOR IRON CONFIGURATION, YELLOW LED, 3 CM CELL, 1:1 DILUTION RATIO

The lower curve in Fig 6.3.1.b shows the response of the sensor with no sample dilution. For the second curve, the same path length cell was used but a 1:1 dilution ratio was introduced. It can be seen that the system without dilution gave the required response in the 0→400 µg L^{-1} range. The figure shows also that the linear range was extended from 0→400 µg L^{-1} to 0→800 µg L^{-1} with sample dilution. Sample dilution also reduces the sensitivity of the colorimetric test. However, the biggest limitation of sample dilution with this sensor is the additional instrumentation required. The introduction of sample dilution requires the use of an additional channel in the delivery system, and an extra mixing coil.

Sample dilution can also be used to extend the linear range when the sensor is configured to measure turbidity.

6.3.2 Colour Correction

The natural colour of a sample may be measured with this system in the following way. After system calibration, the colour reagent tube (R3) is placed in de-ionised water. Hence no colour is developed in the treated sample and the sample/reagent volume ratio is maintained. A blank sample is inserted and the new blank value measured. The sample is inserted and a measurement made. The difference between the two measurements is the natural colour of the sample. This value can then be subtracted from the measured concentrations to colour-correct the values. Fig 6.3.2.a shows the use of colour correction. Formazine turbidity standard solution was added to de-ionised water to produce blank samples of increasing turbidity. These were then tested with the system in the aluminium configuration. It can be seen that without colour correction the measured aluminium concentration increases dramatically. However, when the values are colour corrected the resulting values remain approximately zero.

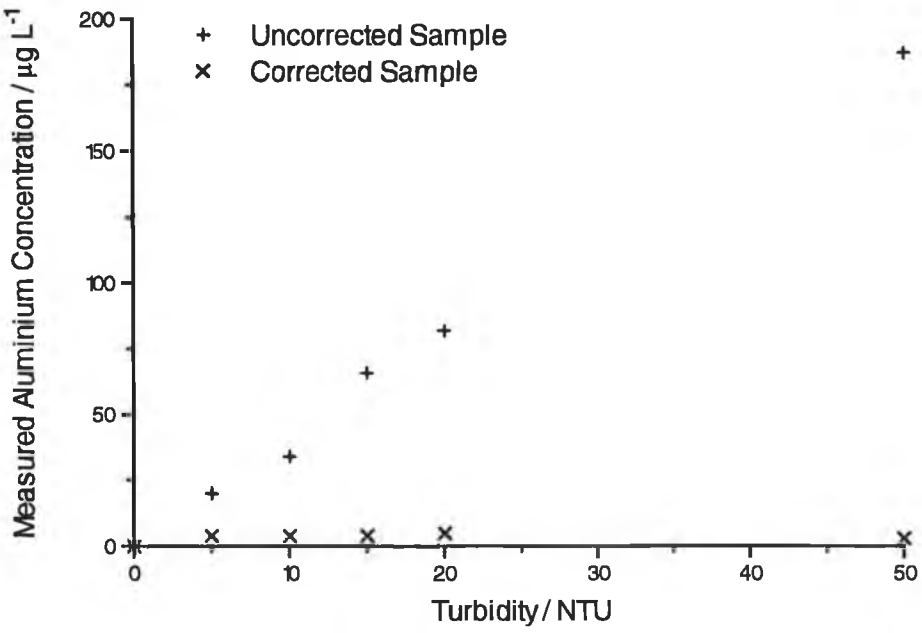

Fig. 6.3.2.a COLOUR CORRECTION OF INCREASINGLY TURBID BLANK SAMPLES

6.4 Summary

Included below is a summary of the performance characteristics of the sensor, based on the terms outlined in section 1.4.3. The sensitivity quoted is the reciprocal of the calibration constant outlined in section 3.2.

Table I

	Al	Colour	Fe	Mn	P (asP)	Turbidity
Path Length /cm	1.5	8	3	3	3	-
Linear Range	0→400 $\mu g\ L^{-1}$	0→80 Hazen	0→500 $\mu g\ L^{-1}$	0→800 ppb	0→1.5 $\mu g\ L^{-1}$	0→50 NTU
Sensitivity	2.5	2.3	1.8	3.1	1.7	200
Resolution %	4	1	3	4	4	3
Repeatability %	3	1	2	3	3	2
Limit of Detection	2 $\mu g\ L^{-1}$	1 Hazen	1 $\mu g\ L^{-1}$	5 ppb	0.05 $\mu g\ L^{-1}$	0.5 NTU
Accuracy %	5	2	4	4	5	4
Response Time /min.	7	2	2	3	12	2

In every case above, the limit of detection is less than the Guide Line concentration and the linear range includes the Maximum Allowable Concentration, as stipulated by the EC Guidelines for Water Quality, (see section 1.3).

6.5 Comparison with Existing Monitors

In section 4.5 a commercial on-line monitor for iron and aluminium, the RC100, was introduced. Aztec Ltd. also produce monitors for the detection of colour and turbidity (CT100), phosphate (P100) and manganese (M100). All of these devices have the piston and optical cell/pump barrel delivery system and they all use an on-board micro-computer for calculations and to control the hardware. An advantage of these monitors compared with the sensor developed here is that they incorporate automatic self cleaning. As it draws samples into the pump barrel, the piston continually wipes clean the sides of the

optical cell. This is essential for long term operation as optical cell fouling is a problem for on-line operation. Another advantage of these monitors is the large number of in-built alarms that constantly check for low reagent levels etc. These alarms aid long term unattended operation. However, these monitors are a considerable size, with dimensions of 1200 mm * 300 mm * 700 mm and 70 Kg weight. The optical disadvantages of the devices have already been covered in earlier chapters in terms of filter delamination and bulb instability. The monitors are also limited to a single path length cell and light source. Hence the advantages of the developed sensor system over these monitors are its versatility, portability and improved optical stability. The following table summarises the performance characteristics of the Aztec monitors as detailed in the respective technical information sheets.

Table II

	Al	**Colour**	**Fe**	**Mn**	**P (as P)**	**Turbidity**
Path Length /cm	2	4	2	3.4	2	-
Linear Range	0→1200 $\mu g\ L^{-1}$	0→250 Hazen	0→2000 $\mu g\ L^{-1}$	0→500 ppb	0→22.5 $\mu g\ L^{-1}$	0→5 NTU
Sensitivity	2.7	0.9	0.7	2	2.7	2700
Repeatability %	2	2	2	2	2	2
Limit of Detection	20 $\mu g\ L^{-1}$	1 Hazen	20 $\mu g\ L^{-1}$	20 ppb	0.3 $\mu g\ L^{-1}$	0.05 NTU
Accuracy %	6	2	5	4	5	4
Response Time /min.	10	1	10	10	10	1

The monitors for aluminium, iron and phosphate incorporate automatic sample dilution and this extends the linear range. The source used for turbidity measurement is a white light bulb without filter. The high intensity of this source gives the high sensitivity and low limit of detection. Apart from these differences, the corresponding table of results, Table I, obtained for the portable sensor system shows that this system has performance characteristics as good as commercially available water quality monitors.

6.6 Conclusion

A portable stand-alone sensor for water quality monitoring was developed. Measurements were made of the concentrations of Al, colour, Fe, Mn, P and turbidity in potable water. The sensor also allowed sample dilution and colour correction. The sensor constructed is easy to use, cheap and versatile. The performance characteristics of the sensor are as good as commercially available systems and a number of problems associated with the sources of these systems have been overcome by the use of LED's.

Chapter 7

Conclusion and Future Work

The work presented in this thesis describes the development of an LED-based, portable sensor unit for monitoring water quality parameters. The measurement procedure is based upon standard colorimetric tests and a nephelometric configuration is used to measure sample turbidity. The sensor response to aluminium, colour, iron, manganese, phosphate and turbidity was determined. In each case the respective limits of detection were below the EC Guide Line concentrations and the linear ranges were within the EC Maximum Allowable Concentrations.

The initial part of the experimental work involved conducting the various colorimetric tests, using LED's as sources, on a specially constructed bench-top system. Investigations were conducted into the sensitivity and linear range of the various tests. The results were then compared with those obtained with the conventional sources, usually an interference filter and an incandescent filament-based white light bulb. In some cases the sensitivity and linear range of the LED was lower than the conventional source. This was usually because the bandwidth of the LED was larger than that of the interference filter used. However, in all the colorimetric (and nephelometric) tests conducted, the performance characteristics of the LED's were as good as those of the conventional sources. The LED's also showed improved stability, versus the incandescent sources, which compensated for the slight loss of sensitivity in certain tests.

A LED was then incorporated into an existing commercial on-line monitor for iron and aluminium, replacing the filter and bulb source. For the colorimetric test employed in this device, the LED has a lower linear range and sensitivity compared with the filter and bulb.

However, with suitable changes to the operating software of the monitor, the performances of the instrument with both sources were approximately the same. These experiments showed that with minimum changes to operating software and design, LED's can be incorporated into existing on-line monitors and that they are suited to long-term continuous operation. Once installed, the LED's overcome a number of problems associated with the previous sources, such as delamination of the interference filter and instability and short lifetime of the bulb.

The next stage of the experimental work was to construct a modular design, miniature flow-through sensor head. This sensor head used LED's as sources and employed miniature optical components and fibre optics to measure sample absorbance and turbidity. The arrangement was tested in a computer controlled system and the configuration used allowed simultaneous measurement of sample colour and turbidity. The miniature sensor head showed positive performance characteristics and the modular design allowed configuration for a number of different colorimetric tests.

The final stage of the project was to miniaturise the rest of the components required for a full system. Sample/reagent mixing and delivery was achieved by use of a peristaltic pump. The miniature sensor head was used and dedicated electronics were designed and constructed. These circuits controlled the LED's and converted signal intensities to analyte concentrations. In this manner, a portable, stand alone sensor for monitoring water quality parameters was produced. Comparisons were made between the performance of existing on-line water quality monitors and the sensor system developed. Future work to this sensor would involve the following:

1. Reduction of the cell and tubing volume. This would decrease the two minute pumping time between samples and reduce reagent consumption.

2. Improvement of the electronics design so as to simplify the configuring of the system, i.e. selecting LED's and checking LED intensity.

3. Investigation of additional colorimetric tests that could be used by this system.

4. Incorporation of some method of self cleaning in the cell, either chemical or mechanical.

References:

1. J. Gardiner and G. Mance, *UK Water Quality Standards Arising from European Community Direcives,* Technical report 204, Wrc, Memenham, 1984.

2. L.S. Clesceri, A.E. Greenberg and R.R. Trussell, *Standard Methods for the Examination of Water and Wastewater,* APHA-AWWA-WPCF, 17th Ed. 1989, p 1-50.

3. R.L. Benson, P.J. Worsfold, F.W. Sweeting, *On-line Determination of Residual Aluminium on Potable and Treated Waters by Flow-Injection Analysis,* Analytica Chimica Acta, 238 (1990) 177-182

4. J.C. Miller, J.N. Miller, *Statistics for Analytical Chemistry,* 2nd Ed. Ellis Horwood Ltd., (1987), p 150

5. B.G. Streetman, *Solid State Electronic Devices*, Prentice/Hall International Editions, 2nd Ed., p 58.

6. J. Wilson and J.F.B. Hawkes, *Optoelectronics: An Introduction*, Prentice/Hall International Series in Optoelectronics, 1983, p. 143.

7. J. Wilson and J.F.B. Hawkes, *Optoelectronics: An Introduction*, Prentice/Hall International Series in Optoelectronics, 1983, p. 52.

8. J.M. Senior, *Optical Fiber Communications: Principles and Practice*, Prentice/Hall International Series in Optoelectronics, 2nd Ed., (1992), p. 304.

9. Ledtronics, California U.S.A., *New Super Bright Blue LED*, Technical Information Sheets

10. J.M. Senior, *Optical Fiber Communications: Principles and Practice*, Prentice/Hall International Series in Optoelectronics, 2nd Ed., (1992), p. 386.

11. B. Culshaw, *Optical Fibre Sensing and Signal Processing*, IEE, p. 37

12. B. Culshaw, *Optical Fibre Sensing and Signal Processing*, IEE, p. 37

13. G. Murtaza and J.M. Senior, *Wavelength Selection Strategies to Enhance Referencing in LED Based Optical Sensors*, Optics Communications, 15th Nov., 112 (1994) 201-213.

14. S.F. Johnson, *Meas. Sci. Technology*, 3 (1992) 191.

15. G. Murtaza and J.M. Senior, *Wavelength Selection Strategies to Enhance Referencing in LED Based Optical Sensors*, Optics Communications, 15th Nov., 112 (1994) 201-213.

16. M.N. Taib and R. Narayanaswamy, *Solid-state Instruments for Optical Fibre Chemical Sensors : A Review*, Analyst, June 1995, Vol 120, 1617-1625

17. R.L. Benson, P.J. Worsfold and F.W. Sweeting, *On-Line Determination of Residual Aluminium in Potable and Treated waters by Flow-Injection Analyis*, Analytica Chimica Acta, 238 (1990) 177-182

18. J.R. Clinch, P.J. Worsfold and H. Casey, *An Automated Spectrophotometric Field Monitor for Water Quality Parameters: Determination of Nitrate*, Analytica Chimica Acta, 200 (1) (1987) 523-531

19. N.J. Blundell, A.Hopkins, P.J. Worsfold and H. Casey, *A Portable Battery-Powered Flow Injection Monitor for the in situ Analysis of Nitrate in Natural Waters*, Journal of Automatic Chemistry, Vol. 15 (September-October 1993), 159-166

20. H. Casey, R.T. Clarke, S.M. Smith, J.R. Clinch and P.J. Worsfold, *Spectrophotometric Field Monitor for the Determination of Nitrate in River Water: Statistical Analysis of the Results from a Nine-Month Field Trial*, Analytica Chimica Acta, 227 (1989) 379-385

21. P.P.R. Kraus, A.P. Wade, S.R. Crouch, J.F. Holland and B.M. Miller, *Portable Double-Beam, Fibre-Optic-Based Photometric Comparator*, Analytical Chemistry, (1988), 60, 1397-1390

22. M. Trojanowicz and J. Szpunar-Lobinska, *Simultaneous Flow-Injection Determination of Aluminium and Zinc using LED Photometric Detection*, Analytica Chimica Acta, 230 (1990) 125-130

23. J. Huang, H. Liu, A. Tan, J, Xiu and X. Zhao, *A Dual-Wavelength Light-Emitting Diode based Detector for Flow-Injection Analysis Process Analysers*, Talanta, Vol. 39, No. 6, (1992), 589-592

24. H.Liu and K. Dasgupta, *Dual-Wavelength Photometry with Light Emitting Diodes. Compensation of Refractive Index and Turbidity Effects in Flow-Injection Analysis.* Analytica Chimica Acta, 289 (1994) 347-353

25. K.T.V. Grattan, Z. Mouaziz and A.W. Palmer, *Dual-Wavelength Optical-fibre Sensor for pH Measurement*, Biosensors, 1987, 3 (1), 17-25

26. P. Bechi, F. Pucciani, R. Falciai, F. Baldini, F. Cosi, A. Bini and F. Milanesi, *Optical Fibre Bile Sensor for Entro-Gastric Reflux Detection*, Sensors and Actuators B, 7 (1992) 775-779

27. B.D. MacCraith, G. O'Keeffe, C. McDonagh and A.K. McEvoy, *LED-Based Fibre Optic Oxygen Sensor using Sol-Gel Coating*, Electronic Letters, 26th May (1994), Vol. 30 No. 11, 888-889

28. R.L. Pecsok, L.D. Shields, T. Cairns and I.G. McWilliam, *Modern Methods of Chemical Analysis*, John Wiley & Sons New York 2nd Ed., (1976), p.138

29. D.A. Skoog and D.M. West, *Fundamentals of Analytical Chemistry*, Saunders Golden Sunburst Series 4th Ed., (1982), p. 492

30. D.A. Skoog and D.M. West, *Fundamentals of Analytical Chemistry*, Saunders Golden Sunburst Series 4th Ed., (1982), p. 494

31. D.A. Skoog and D.M. West, *Fundamentals of Analytical Chemistry*, Saunders Golden Sunburst Series 4th Ed., (1982), p. 495

32. D.A. Skoog and D.M. West, *Fundamentals of Analytical Chemistry*, Saunders Golden Sunburst Series 4th Ed., (1982), p. 496

33. L.S. Clesceri, A.E. Greenberg and R.R. Trussell, *Standard Methods for the Examination of Water and Wastewater,* APHA-AWWA-WPCF, 17th Ed. 1989, p 3-64.

34. L.S. Clesceri, A.E. Greenberg and R.R. Trussell, *Standard Methods for the Examination of Water and Wastewater,* APHA-AWWA-WPCF, 17th Ed. 1989, p 3-68.

35. Aztec Environmental Control Ltd., *Chemical Preparation Instructions for Aluminium*, Part Number 91-0701B

36. Aztec Environmental Control Ltd., *Chemical Quality Assurance Instruction for Aluminium*, Part Number 91-0701

37. L.S. Clesceri, A.E. Greenberg and R.R. Trussell, *Standard Methods for the Examination of Water and Wastewater,* APHA-AWWA-WPCF, 17th Ed. 1989, p 3-64.

38. F. Lazaro, a. Rios, M.D. Luque De Castro and M. Valcarcel, *Simultaneous Multiwavelength Detection in Flow Injection Analysis*, Analytica Chimica Acta., 179 (1986) 279-287

39. Aztec Environmental Control Ltd., *Chemical Quality Assurance Instruction for Iron*, Part Number 92-0601B

40. Aztec Environmental Control Ltd., *Chemical Quality Assurance Instruction for Manganese*, Part Number 92-0803-D

41. J.R. Clinch, P.J. Worsfold and H. Casey, *An Automated Spectrophotometric Field Monitor for Water Quality Parameters: Determination of Nitrate*, Analytica Chimica Acta, 200 (1) (1987) 523-531

42. Aztec Environmental Control Ltd., *Chemical Quality Assurance Instruction for Phosphate*, Part Number 92-0402-C

43. M. Trojanowicz and J. Szpunar-Lobinska, *Simultaneous Flow-Injection Determination of Aluminium and Zinc using LED Photometric Detection*, Analytica Chimica Acta, 230 (1990) 125-130

44. L.S. Clesceri, A.E. Greenberg and R.R. Trussell, *Standard Methods for the Examination of Water and Wastewater,* APHA-AWWA-WPCF, 17th Ed. 1989, p 2-2.

45. E. Hecht, *Optics*, Addison-Wesley Publishing Company 2nd Ed., (1989), p. 294

46. K.S. Shifrin, *Physical Optics of Ocean Water*, American Institute of Physics, Translation Series. pp. 326

47. L.S. Clesceri, A.E. Greenberg and R.R. Trussell, *Standard Methods for the Examination of Water and Wastewater,* APHA-AWWA-WPCF, 17th Ed. 1989, p 2-12.

48. L.S. Clesceri, A.E. Greenberg and R.R. Trussell, *Standard Methods for the Examination of Water and Wastewater,* APHA-AWWA-WPCF, 17th Ed. 1989, p 2-13.

49. Advanced Polymer Systems, Technical Specification Sheet for APS AEPA-1

50. D.G. Walter and V. William, *Handbook of Optics*, McGraw-Hill New York 2nd Ed., (1978), p. 15.5

51. Advanced Polymer Systems, *Technical Specification Sheet for APS AEPA-1*, California 94063, USA.

Appendix A:

Derivation of formulae for two point linear calibration

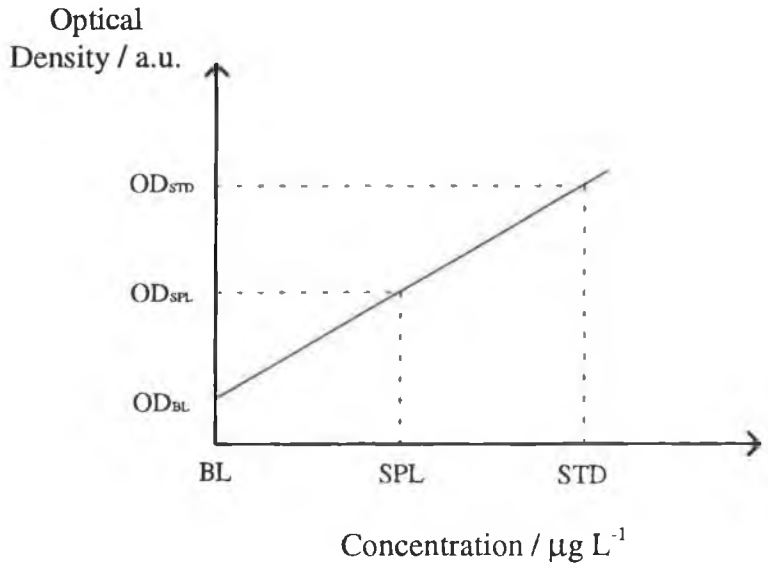

Shown above is a typical calibration curve for a linear two point calibration. The optical density of a de-ionised water blank sample (OD_{BL}) is measured. This point has a concentration of zero on the x-axis. The optical density of the standard sample (OD_{STD}) is then measured. In the case of aluminium, this point has a concentration of 200 μg L^{-1}. Assuming that, for the path length cell used, Beer's Law applies between these two points, a straight line may be drawn between the two. From co-ordinate geometry the equation of this line is given by:

$$\frac{Y - Y_1}{Y_2 - Y_1} = \frac{X - X_1}{X_2 - X_1} \qquad \text{A1}$$

Filling in the values from the above example gives:

$$\frac{Y - OD_{BL}}{OD_{STD} - OD_{BL}} = \frac{X - 0}{200 - 0} \qquad \text{A2}$$

This is rearranged to give:

$$X = \frac{200}{OD_{STD} - OD_{BL}} (Y - OD_{BL}) \qquad A3$$

This equation can be rewritten as:

$$S = K(OD_{SPL} - OD_{BL}) \qquad A4$$

where

$$K = \frac{200}{OD_{STD} - OD_{BL}} \qquad A5$$

and S is the sample concentration in $\mu g\ L^{-1}$, OD_{SPL} is the optical density of the sample and K is known as the calibration constant, the reciprocal of the slope.

Appendix B:

LED Driver Circuit for computer based system

IC1	Voltage to Frequency Converter, (AD654, RS# 637-860)
IC2	Comparator, (LM392N, RS# 308-859)

In the configuration shown, the output from IC1 is a square wave of frequency 950 Hz. The square wave voltage is converted to a square wave current source using field effect transistors. An individual LED is switched on by applying a 5V signal to the base of one of the npn transistors. This control pulse is supplied by the I/O card of the computer. In this way all of the LED's are modulated at the same frequency and by sending the relevant pulse, the computer selects which LED operated at a particular time.

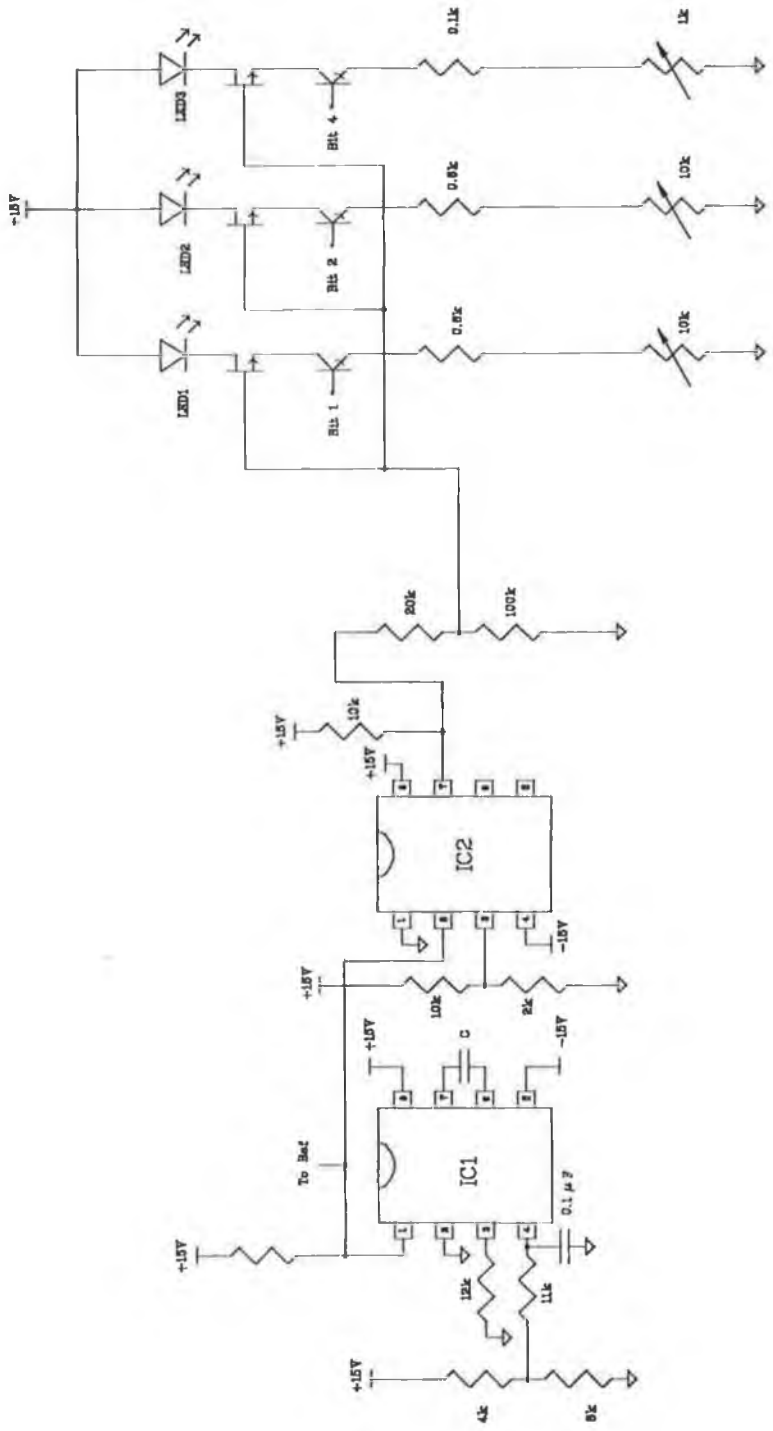
+15V
LED3
LED2
LED1
Bit 4
Bit 2
Bit 1
0.1k
0.6k
0.6k
1k
10k
10k
20k
100k
10k
IC2
10k
2k
IC1
To Bat
0.1 μ F
12k
11k
4k
8k

Appendix C:

Detection Circuit for computer based system

IC1 Balanced Modulator/Demodulator (AD630)

This circuit effectively acts as a lockin amplifier. The photodetector, (RS# 308-067) is a hybrid photodiode and integral amplifier. Combining these two together in a single component reduces the noise pick-up between the detector stage and amplifier. The reference for the lockin chip comes from the square wave generator of the LED driver circuit. The low reference input pin (pin 10) is off-set by 1V and this prevents problems which can be caused by non zero going reference signals. The output from the circuit goes, via a buffer, to the ADC of the I/O card of the computer.

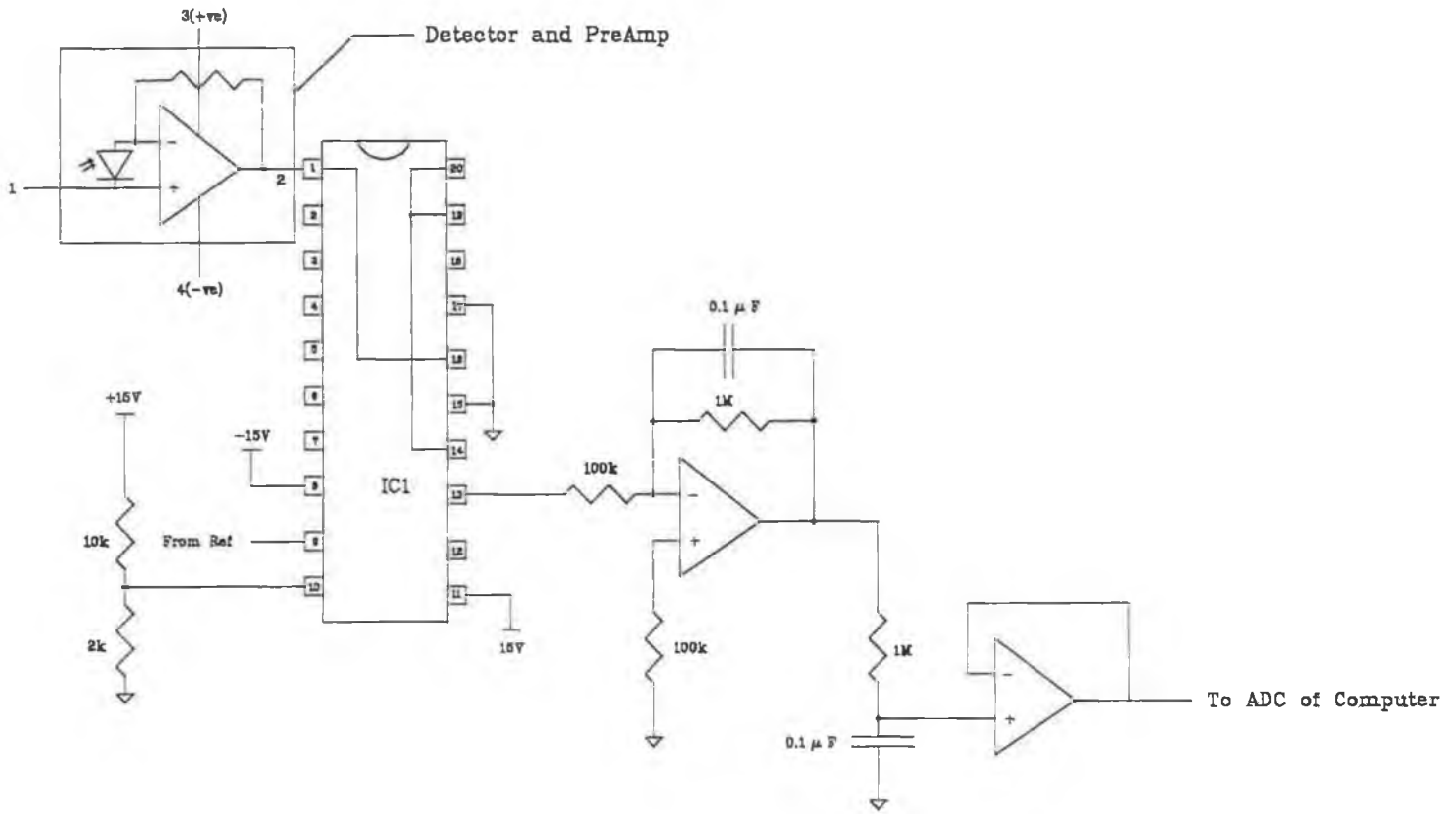
3(+ve)
Detector and PreAmp
1
2
4(-ve)
+15V
-15V
10k
From Ref
2k
IC1
15V
100k
0.1 μ F
1K
100k
1K
0.1 μ F
To ADC of Computer

VI.

Appendix D:

Software listing for computer based system

The software was written in TurboC++ in modular format and using a project file structure. There follows a listing of all the routines used.

Tom.H - Header File for Programs Main.C and Util.C

```
#include <stdlib.h>
#include <stdio.h>
#include <dos.h>
#include <stdlib.h>
#include <stdio.h>
#include <math.h>
#include <conio.h>
#include <graphics.h>
#include <stdarg.h>
#include <alloc.h>
#include <time.h>
#include "smouse.h"
#include <dir.h>

#define base 800
#define IR_LED 4
#define BLUE_LED 2
#define YELLOW_LED 1
#define OFF 0
#define PUMP 8
```

Main.C - Main Control Routine

```
#include "tom.h"
void start_up(void);          /*    Define subroutines        */
void calibrate(void);
float read_adc(float);
void exit_routine();

FILE *fp;

float Kcol;                   /*    Initialise Variables      */
float Ktur;
float Kcorr;
float V1;
float V2;
float xmax1,xmax2;


void main(void)               /*    Start of Main routine     */
```

```
{
int f,c,t,x,y,cc;
float coll,tur,ccoll,colll;

outport((base+7),128);          /*          Initialise I/O card                */

start_up();
scr_draw();
mouseinit();
display_mouse();

calibrate();

setcolor(DARKGRAY);
settextstyle(1,HORIZ_DIR,2);
outtextxy(100,440,"System Running");

for(f=0;f<100;f++){             /*          Main Loop to take 100 points       */


        led_control(BLUE_LED);
        pump(20);
        dellay(6);
        x=430;
        y=350;
        settextstyle(0,HORIZ_DIR,1);
        setcolor(LIGHTGRAY);
        gprintf(&x,&y,"%2.2f",coll);
        coll=read_adc(0);
                colll=coll;
                coll=Kcol*(log10(V1)-log10(coll));    /*          Calculate Colour Value      */
                c=(330-(coll*(300/xmax1)));
                col_plot(f,c);          /*          Plot Colour point on Graph   */
        x=430;
        y=350;
        settextstyle(0,HORIZ_DIR,1);
        setcolor(BLUE);
        gprintf(&x,&y,"%2.2f",coll);

        led_control(OFF);
        led_control(IR_LED);
        dellay(10);

        x=430;
        y=370;
        settextstyle(0,HORIZ_DIR,1);
        setcolor(LIGHTGRAY);
        gprintf(&x,&y,"%2.2f",tur);
        tur=read_adc(0);
                tur=Ktur*(tur-V2);              /*          Calculate Turbidity*/
                t=(330-(tur*(300/xmax2)));
                tur_plot(f,t);                  /*          Plot Turbidity point on Graph          */
        x=430;
        y=370;
        settextstyle(0,HORIZ_DIR,1);
        setcolor(BLUE);
```

```
		gprintf(&x,&y,"%2.2f",tur);
		led_control(OFF);

		x=430;
		y=390;
		settextstyle(0,HORIZ_DIR,1);
		setcolor(LIGHTGRAY);
		gprintf(&x,&y,"%2.2f",ccoll);
		ccoll=Kcol*(log10(V1/colll)-(Kcorr*tur));	/*	Calculate turbidity corrected colour	*/
		cc=(330-(ccoll*(300/xmax1)));
		y=390;
		settextstyle(0,HORIZ_DIR,1);
		setcolor(BLUE);
		gprintf(&x,&y,"%2.2f",ccoll);
		ccol_plot(f,cc);	/*	Plot Turbidity corrected Colour value on graph	*/
		fprintf(fp,"%2.6f  %2.6f  %2.6f\n",coll,tur,ccoll);
		}	/*	End of main for loop	*/


settextstyle(1,HORIZ_DIR,2);
setcolor(LIGHTGRAY);
outtextxy(100,440,"System Running");
setcolor(DARKGRAY);
outtextxy(100,440,"End of Scan");
wait();
exit_routine();

}	/*	End of Main	*/

float read_adc(float channel)		/*	Read value from ADC	*/
{
		float a,b,value;
		int x;
		a=0,b=0,value=0;
		outport ((base+24),channel);

		for(x=1;x<3000;x++){		/*	Average reading 3000 times	*/
			outport ((base +16),channel);
			while (!(inport (base +20) &1));
			a+=inportb (base+19);
			b+=inportb(base+18);
			}
			a/=3000;
			b/=3000;
			value =(a/16)+(b*16);
			value = ((value-2047)/2047)*10;
			return(-value);
}			/*	End of ADC	*/

void start_up(void)		/*	Start-up routine
					Initialises Axis values and file names	*/
{
char file_name[25];
clrscr();

printf("\n\n\n\n\n\n\n\n\n\n\n		Enter file Name...");
```

```
scanf("%s",file_name);
printf("\n\n          Enter X1-Axis Max...");
scanf("%f",&xmax1);
printf("\n\n          Enter X2-Axis Max...");
scanf("%f",&xmax2);

fp=fopen(file_name,"w");
return;
}          /*          End of Start_up     */

void exit_routine(void)                    /*          Exit routine
                                                       Closes files and Returns to DOS    */
{
close(fp);

outport((base+4),0);
cleardevice();
textmode(3);
clrscr();
exit(0);
}

void calibrate(void)          /*          Calibration Routine
                                         Calibrates the system for colour and Turbidity measurement          */
{
int x,y;
float V3,V4,V5;
char ch;

hide_mouse();

settextstyle(0,HORIZ_DIR,1);
setcolor(LIGHTGRAY);

x=200;
y=350;

gprintf(&x,&y,"%4.2f",Kcol);

y=370;
gprintf(&x,&y,"%4.2f",Ktur);

y=390;
gprintf(&x,&y,"%0.4f",Kcorr);



settextstyle(1,HORIZ_DIR,2);
setcolor(LIGHTGRAY);
outtextxy(100,440,"System Running");

setcolor(DARKGRAY);
outtextxy(100,440,"Insert Blank");

ch=getch();
```

```
setcolor(LIGHTGRAY);
outtextxy(100,440,"Insert Blank");

led_control(BLUE_LED);
pump(90);
dellay(15);
V1=read_adc(0);
led_control(OFF);

led_control(IR_LED);
dellay(15);
V2=read_adc(0);

setcolor(DARKGRAY);
outtextxy(100,440,"Insert Colour Standard");

ch=getch();

setcolor(LIGHTGRAY);
outtextxy(100,440,"Insert Colour Standard");

led_control(OFF);
led_control(BLUE_LED);

pump(90);
dellay(10);
V3=read_adc(0);

setcolor(DARKGRAY);
outtextxy(100,440,"Insert Turbidity Standard");

ch=getch();

setcolor(LIGHTGRAY);
outtextxy(100,440,"Insert Turbidity Standard");

led_control(OFF);
led_control(IR_LED);
pump(90);
dellay(15);
V5=read_adc(0);

led_control(OFF);
led_control(BLUE_LED);
dellay(15);
V4=read_adc(0);

led_control(OFF);

Kcol=50/(log10(V1)-log10(V3));      /*      Calculate calibration constants      */
Ktur=5/(V5-V2);
Kcorr=(log10(V1)-log10(V4))/5;


settextstyle(0,HORIZ_DIR,1);
setcolor(BLUE);
```

```
x=200;
y=350;

gprintf(&x,&y,"%4.2f",Kcol);

y=370;
gprintf(&x,&y,"%4.2f",Ktur);

y=390;
gprintf(&x,&y,"%0.4f",Kcorr);

settextstyle(1,HORIZ_DIR,2);
setcolor(DARKGRAY);
outtextxy(100,440,"Insert Sample");

ch=getch();

setcolor(LIGHTGRAY);
outtextxy(100,440,"Insert Sample");
pump(40);
display_mouse();
return;
}       /*      End of Calibrate    */
```

Util.C - Utility Routines for Hardware and Graphics

```
#include "tom.h"

int old_valc;               /*      Initialise Variables */
int old_valt;
int old_valcc;

extern float xmax1;
extern float xmax2;

void graph_set(void);       /*      Initialise Subroutines      */
void icon(char [15],int);
int gprintf( int *xloc, int *yloc, char *fmt, ... );
int icon_select(void);
void wait(void);
void pump(int);
void led_control(int);
void scr_draw(void);
void col_plot(int,int);
void tur_plot(int,int);
void ccol_plot(int,int);
void dellay(int);
void menu(void);

int control=0;

void graph_set(void)        /*      Initialise Graphics         */
{
```

```
        int driver,mode;
        char ch;

        driver=DETECT;
        mode=VGAHI;
        detectgraph( &driver, &mode);
        initgraph( &driver, &mode, "c:\\tc\\bgi");
        return;
}       /*      End of Graph_set   */

int gprintf( int *xloc, int *yloc, char *fmt, ... )   /*      Routine gprintf
                                                      Allows text and variables to be displayed
                                                      on a graphics screen          */
{
 va_list  argptr;                   /* Argument list pointer      */
 char str[140];                     /* Buffer to build sting into  */
 int cnt;                           /* Result of SPRINTF for return */

 va_start( argptr, fmt );           /* Initialize va_ functions    */

 cnt = vsprintf( str, fmt, argptr );    /* prints string to buffer     */
 outtextxy( *xloc, *yloc, str );        /* Send string in graphics mode */
 *yloc += textheight( "H" ) + 2;    /* Advance to next line        */

 va_end( argptr );                  /* Close va_ functions                */

 return( cnt );                     /* Return the conversion count        */

}    /*  End of Graphics Print       */



void icon(char tc[],int t)          /*      Icon Routine
                                    Generates icon boxes on the screen
                                    in pre-determined positions  */
{

int xbox,ybox,xtext,ytext;


xbox=550;
ybox=(t*30)+((t-1)*25);
xtext=580-(textwidth(tc)/2);
ytext=ybox+15;

setcolor(BLUE);
outtextxy(xtext,ytext,tc);
setcolor(RED);
rectangle(xbox,ybox,xbox+60,ybox+30);

return;
}       /*      End of Icon         */
```

```
int icon_select(void)                   /*      Detects which icon has
                                                been selected by the mouse   */
{
int choice,button,xpos,ypos;
mousebuttoninfo(&button,&xpos,&ypos);


if(xpos>550 & xpos<610){
        if(ypos>25 & ypos<55)
                choice=1;
        if(ypos>80 & ypos<110)
                choice=2;
        if(ypos>135 & ypos<165)
                choice=3;
        if(ypos>190 & ypos<220)
                choice=4;
        if(ypos>245 & ypos<275)
                choice=5;
        if(ypos>300 & ypos<330)
                choice=6;
        if(ypos>355 & ypos<385)
                choice=7;
        }       /* end of If */
        else
        choice=0;
return (choice);

}       /*      End of Icon Select  */

void wait(void)                 /*      Halts program execution until mouse press or key press      */
{
while(!kbhit()&&!mousebutton(1)){
        }
return;
}       /*      End of Wait         */



void pump (int x)               /*      Turns on pump       */
{
control=control^PUMP;
outport((base+4),control);
dellay(x);
control=control^PUMP;
outport((base+4),control);
return;
}       /*      End of pump         */

void led_control(int x)         /*      Routine to select specific LED's        */
{
control=controllx;
if(x==0)
        control=0;
outport((base+4),control);
```

```
return;
}       /*      End of led_control */

void scr_draw(void)                     /*      Draw initial graphics screen */
{
float xmin,ymin,xmax,ymax;
int x,y;

xmin=50,ymin=30,xmax=450,ymax=330;

graph_set();
setbkcolor(LIGHTGRAY);
icon("Cal.",1);
icon("Pause",2);
icon("Pump",3);
icon("Exit",4);
setcolor(BLUE);
setlinestyle(0,0,3);
rectangle(xmin,ymin,xmax,ymax);
setcolor(DARKGRAY);
line(0,420,639,420);
settextstyle(1,HORIZ_DIR,2);
outtextxy(10,440,"Message:");
setcolor(BLUE);
setlinestyle(3,0,1);

for(x=130;x<450;x+=80)
        line(x,30,x,ymax);

for(x=60;x<330;x+=30)
        line(50,x,xmax,x);


setcolor(BROWN);
settextstyle(1,VERT_DIR,2);
outtextxy(20,120,"Colour/Hz");
setcolor(YELLOW);
outtextxy(460,120,"Turbidity/NTU");
setlinestyle(0,0,0);

setcolor(BROWN);
settextstyle(0,HORIZ_DIR,1);
x=20;
y=30;
gprintf(&x,&y,"%3.0f",xmax1);
outtextxy(20,330,"0");
setcolor(YELLOW);
x=460;
y=30;
gprintf(&x,&y,"%3.0f",xmax2);
outtextxy(460,330,"0");



setcolor(BLUE);
```

```
settextstyle(0,HORIZ_DIR,1);
outtextxy(50,350,"Colour Constant");
outtextxy(50,370,"Turbidity Constant");
outtextxy(50,390,"Colour Correction");
outtextxy(270,350,"Colour Value/Hz");
outtextxy(270,370,"Turbidity Value/NTU");
outtextxy(270,390,"Corrected Colour/Hz");

return;
}       /*      end of scr_draw     */

void col_plot(int x,int ypos)           /*      Plot Colour Values to Graph */
{
int xpos;

hide_mouse();

xpos=50+(x*4);

if(ypos>330)
        ypos=330;

if(ypos<30)
        ypos=30;

if(x==0)
        old_valc=ypos;

setcolor(BROWN);
circle(xpos+4,ypos,1);

line(xpos,old_valc,xpos+4,ypos);
old_valc=ypos;

display_mouse();

return;
}       /*      End of col_plot     */

void tur_plot(int x,int ypos)           /*      Plot Turbidity Values to Graph      */
{
int xpos;

hide_mouse();

xpos=50+(x*4);

if(ypos>330)
        ypos=330;

if(ypos<30)
        ypos=30;

if(x==0)
        old_valt=ypos;
```

```
setcolor(YELLOW);
circle(xpos+4,ypos,1);


line(xpos,old_valt,xpos+4,ypos);
old_valt=ypos;
display_mouse();
return;
}       /*      End of tur_plot     */

void ccol_plot(int x,int ypos)          /*      Plot Turbidity Corrected
                                                Colour Values to Graph      */
{
int xpos;

hide_mouse();

xpos=50+(x*4);

if(ypos>330)
        ypos=330;

if(ypos<30)
        ypos=30;

if(x==0)
        old_valcc=ypos;

setcolor(GREEN);
circle(xpos+4,ypos,1);


line(xpos,old_valcc,xpos+4,ypos);
old_valcc=ypos;
display_mouse();
return;
}       /*      End of ccol_plot    */

void dellay(int x)  /*      Delay routine, in seconds       */
{
  clock_t start, end;
  start = clock();
  end=start+(x*CLK_TCK);
  while(clock()<end){
        if(mousebutton(1)){
                end=start;
                menu();
                }
        }
return;
}       /*      End of Dellay       */
```

```
void menu(void)    /*          Menu routine, based on mouse selection          */
{
char ch;
int choice;
choice=icon_select();
settextstyle(1,HORIZ_DIR,2);

switch (choice)
        {
        case (1):
                outport((base+4),0);
                delay(500);
                control=0;
                calibrate();
                break;
        case (2):
        setcolor(LIGHTGRAY);
                outtextxy(100,440,"System Running");
                setcolor(DARKGRAY);
                outtextxy(100,440,"System Paused");
                outport((base+4),0);
                delay(300);
                ch=getch();
                setcolor(LIGHTGRAY);
                outtextxy(100,440,"System Paused");
                setcolor(DARKGRAY);
                outtextxy(100,440,"System Running");
                dellay(7);
                break;
        case (3):
        setcolor(LIGHTGRAY);
                outtextxy(100,440,"System Running");
                setcolor(DARKGRAY);
                outtextxy(100,440,"Pump On");
                outport((base+4),0);
                outport((base+4),PUMP);
                delay(300);
                ch=getch();
                outport((base+4),0);
                setcolor(LIGHTGRAY);
                outtextxy(100,440,"Pump On");
        setcolor(DARKGRAY);
                outtextxy(100,440,"System Running");
                dellay(7);
                break;
        case (4):
                outport((base+4),0);
                setcolor(LIGHTGRAY);
                outtextxy(100,440,"System Running");
                setcolor(DARKGRAY);
                outtextxy(100,440,"Exit (Y/N)");
                ch=getch();
                if(ch=='y')
                        exit_routine();
                setcolor(LIGHTGRAY);
                outtextxy(100,440,"Exit (Y/N)");
```

```
                setcolor(DARKGRAY);
                outtextxy(100,440,"System Running");
                delay(7);
                break;
        }       /*      End of Choice switch        */
return;
}       /*      End of Menu     */
```

Smouse.H - Header file for Mouse Controller. Written by Dr. Simon Mc Cabe

```
int  mouseinit(void);
void display_mouse(void);
void hide_mouse(void);
void mouseshape(int);
void mousemaxmin(int,int);
void mousesetpos(int,int);

int readcharacter(void);
int mousebutton(int);
void mousebuttoninfo(int *,int *,int *);
```

Smouse.C - Routine to Control Mouse. Written by Dr. Simon Mc Cabe

```
/*
;       Mouse handling routines....using interrupt 33h
;               note must install mouse to use
;
;       pass value in ax as below
;
;       ax      0               :get mouse status and initialise
;                               :status returned in ax  0 => not installed
;                                                       0ffffh=> otherwise
;                               :number of buttons returned in bx
;
;               1               :show mouse cursor
;
;               2               :hide mouse cursor
;
;               3               :get mouse position and button status
;                               :xpos in cx
;                               :ypos in dx
;                               :buttons pressed returned in bx as follows
;                                       left - 01b
;                                               right- 10b
;                                               both - 11b
;
;               4               :put mouse at defined pos
;                               :xpos - cx
;                               :ypos - dx
;
;               8               :set limits to mouse movements (vertical)
;                               :min  - cx
```

```
;                                   :max  - dx
;
;           9                       :assign a shape to the mouse
;                                   :es - contains array data segment
;                                   :dx - segment offset to data
;                                   :bx - xpos hot spot
;                                   :cx - ypos hot spot
*/


#include <dos.h>
#include <math.h>
#include <bios.h>


void mousebuttoninfo(int *button, int *xpos, int *ypos) {
        _AX = 3;
        asm int 33h;
        asm mov ax,bx;
        *button=_AX;  /*1 = left  2 = right 3 = both  */
        *xpos  =_CX;
        *ypos  =_DX;
}


int mousebutton(int button) {
        _AX = 6;
        _BX = button;
        asm int 33h;
        return(_AX);
}



void display_mouse(void)  {
        _AX = 1 ;
        asm int 33h;
}

int mouseinit(void) {
        _AX = 0;
        asm int 33h;
        return (_AX);
}

void hide_mouse(void) {
        _AX = 2 ;
        asm int 33h;
}


void mousemaxmin(dsply *display) {
        _AX = 7;
        _CX = 0;
        _DX = MAXX;
        asm int 33h;
```

```
        _AX = 8;
        _CX = 0;
        _DX = MAXY;
        asm int 33h;
}

void mouseshape(int type) {
        static unsigned hand[32]={0xF9ff,0xE1FF,0xE9FF,0xE9FF,
                                  0xE9FF,0xE849,0xE800,0x8924,
                                  0x0924,0x0986,0x0DFC,0x2FFC,
                                  0x3FFC,0x3FFC,0x0000,0x8001,
                                  0x0C00,0x1200,0x1200,0x1200,
                                  0x1200,0x13B6,0x1249,0x7249,
                                  0x9249,0x9001,0x9001,0x8001,
                                  0x8001,0x8001,0x8001,0x7FFE
                                  };

        static unsigned check[32]={0xFFF0,0xFFE0,0xFFC1,0xFF83,
                                   0xFF07,0x060F,0x001F,0x8037,
                                   0xC07F,0xE0FF,0xF1FF,0xFBFF,
                                   0xFFFF,0xFFFF,0xFFFF,0xFFFF,
                                   0x0003,0x0006,0x000C,0x0018,
                                   0x0030,0x0060,0x70C0,0x3980,
                                   0x1F00,0x0E00,0x0400,0x0000,
                                   0x0000,0x0000,0x0000,0x0000
                                   };

        static unsigned larrow[32]={0xFE3F,0xFC7F,0xF87F,0xF0FF,
                                    0xE0FF,0xC000,0x8000,0x0000,
                                    0x8000,0xC000,0xE0FF,0xF0FF,
                                    0xF87F,0xFC7F,0xFF3F,0xFFFF,
                                    0x0080,0x0100,0x0300,0x0600,
                                    0x0E00,0x1C00,0x3FFF,0x7FFF,
                                    0x3FFF,0x1C00,0x0E00,0x0600,
                                    0x0300,0x0100,0x0080,0x0000
                                    };

        unsigned far *ptr;

        hide_mouse();
        _AX = 9;
        _BX = 1;
        _CX = 1;
        if(type==1) ptr=hand;
        if(type==2) ptr=check;
        if(type==3) ptr=larrow;

        if(type==4) mouseinit();
        else {
         _ES = (unsigned)FP_SEG(ptr);
         _DX = (unsigned)FP_OFF(ptr);
         asm int 33h;
        }
        display_mouse();
        display_mouse();
```

```
}

void mousesetpos(int x, int y) {
        _AX = 4;
        _CX = x;
        _DX = y;
        asm int 33h;
}
```

Appendix E:

Photograph of Portable Sensor, Sensor Head in Fore-Ground

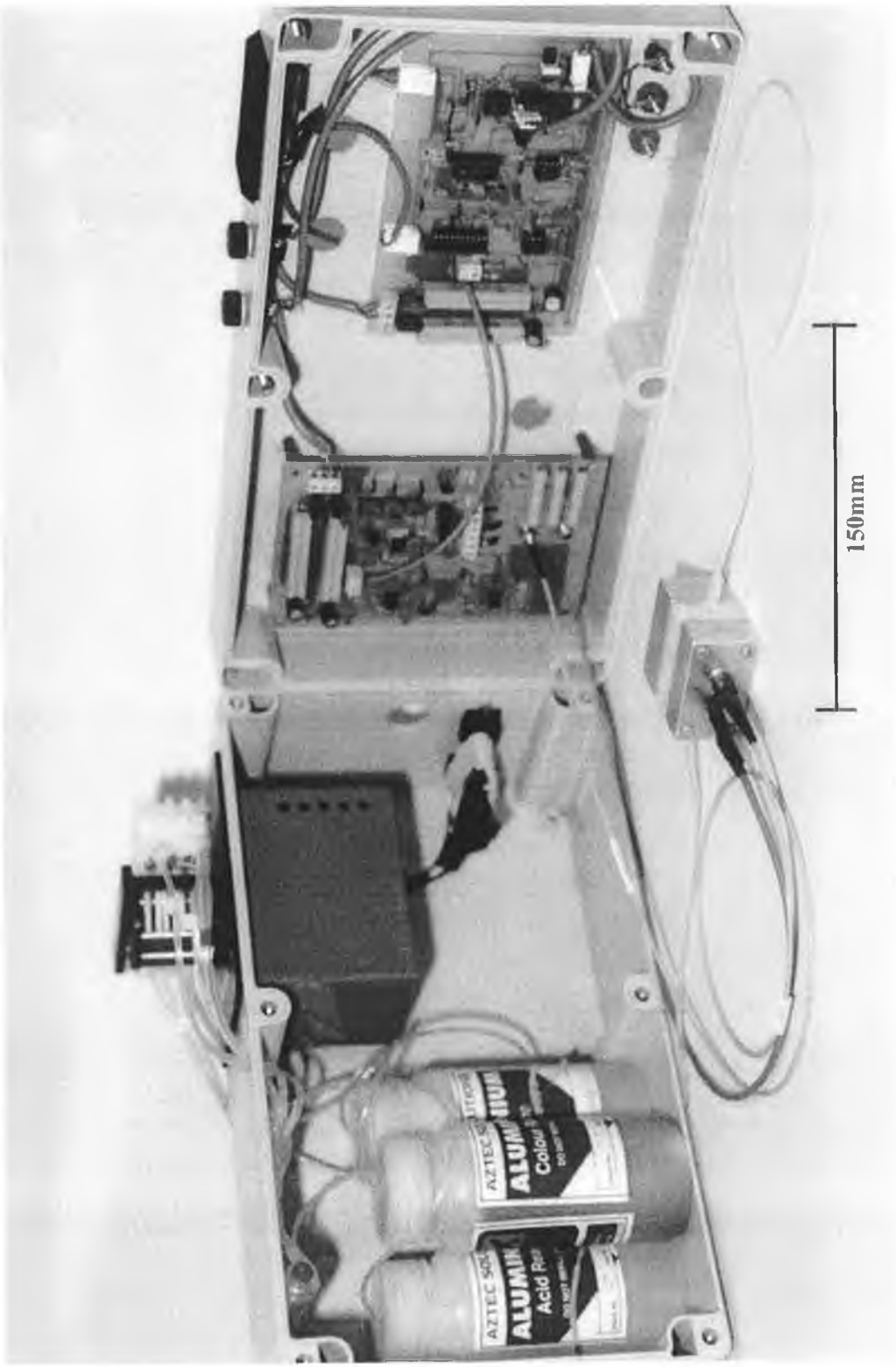

Appendix F:

LED Driver Circuit for portable system

IC1	Voltage to Frequency Converter, (AD654, RS# 637-860)
IC2	Comparator, (LM392N, RS# 308-859)

This circuit is similar to the circuit outlined in Appendix B. The op-amp is used to provide feedback and hence regulate the LED current. The main difference to this circuit is that this time the operator manually switches between the various LED's by placing a jumper connection at S1, S2, or S3 and by positioning a jumper at the feedback switch S4. The RC filter at the op-amp output 'slows' down the output waveform and prevents ringing in the LED drive current.

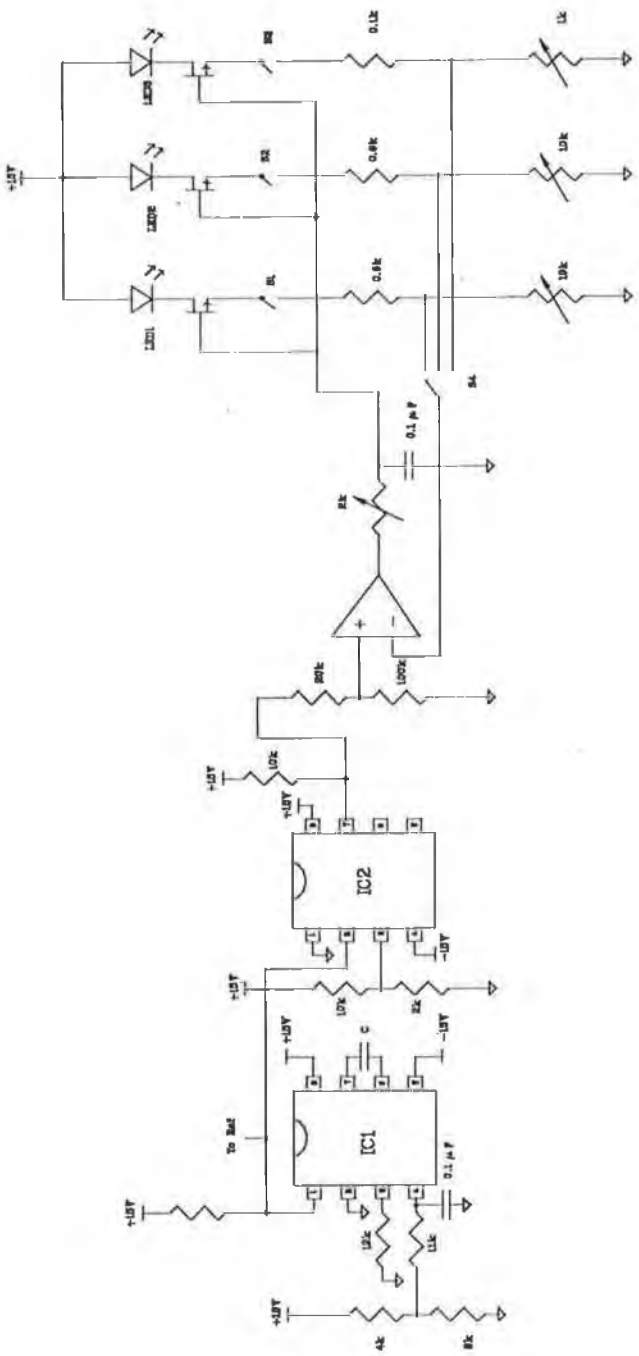
IC1
IC2
+15V
-15V
0.1 μ F
To Rad

Appendix G:

Detector and Log-Amp Circuit for portable system

IC1	Balanced Modulator/Demodulator (AD630)
IC2	ICL8048 Log Amplifier

The initial part of this circuit is similar to the circuit outlined in Appendix C. The inverter is used to change the signal from the detector to a positive voltage. This is necessary for the log-amp operation. The output from the log-amp goes to a voltage adder. The other input to this adder is a variable voltage determined by Pot#1, or the Zero Adjust. In this way the blank signal is effectively subtracted from subsequent readings. The output from the voltage adder then goes to a variable gain amplifier. The gain of this amplifier is determined by Pot#2, or the Gain Adjust. The gain range was set for 0.2→3.2. The output from the final amplifier goes to the panel meter, a 3½ digit LCD display, (DPM 700 RS# 255-979). The switch S1 by-passes the log-amp and is used to switch between absorption and turbidity measurements. S2 connects the output from the detector directly to the panel meter, and it is used to check signal intensities.

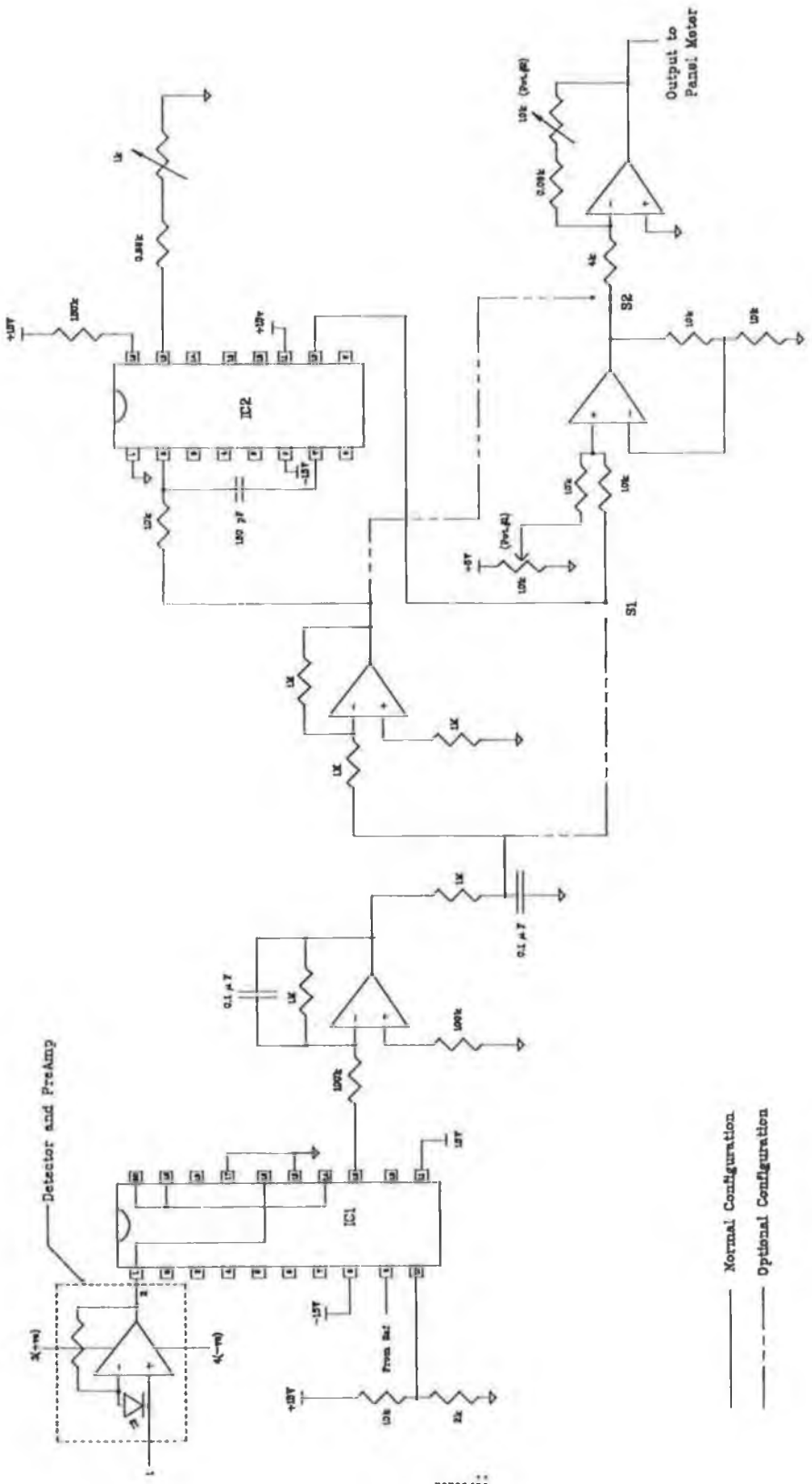
Output to
Panel Meter
IC2
IC1
S1
S2
Detector and PreAmp
Normal Configuration
Optional Configuration

Appendix H:

User instuctions for portable system

Included is a copy of a set of user instruction written independently for the portable system. Included with the actual instructions are the following figures: Fig. 5.2.5.a, Fig. 6.2.a, Fig 6.2.1.a and the circuit diagrams from Appendices F &G.

Instructions for use of LED Based Portable Sensor for Monitoring Water Quality Parameters

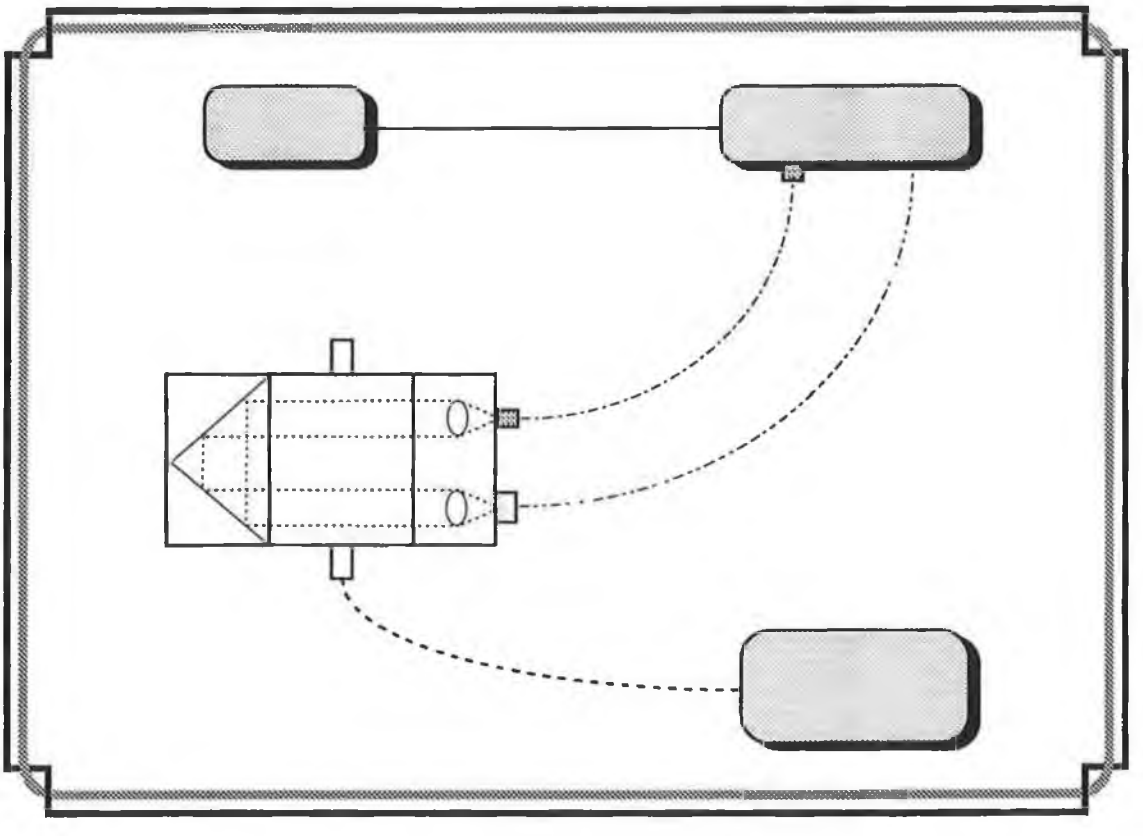

August 95' - Thomas Murphy

Measurement Procedure

- Assemble the cell for the required path length using the necessary modules.
- Select the required LED on the LED driver circuit. Connect the fibre cable to the relevant SMA connector or, for turbidity measurements, install the IR-LED in the LED holder.
- Configure the detector and log-amp circuit for absorption or turbidity measurements.
- Pump de-ionised water through the system and adjust the LED intensity to just below full scale for the detector circuit, (i.e. ~-0125 on the panel meter).
- Insert the required reagents.
- Prime the sample delivery system.
- Insert a blank sample and turn on the pump for ~2 minutes.
- Change the Gain Adjust to roughly half maximum. After colour has been allowed to develop in the cell, change the Zero Adjust until the panel meter reads 0000.
- Insert a standard sample and turn on pump for ~2 minutes
- Again, once colour has been allowed to develop in the cell, change the Gain Adjust until the panel meter reading corresponds to the concentration of analyte in the standard. For example, when using a 200 $\mu g\ L^{-1}$ standard to calibrate the system, the panel meter should read -0200. The system is now calibrated and ready for use.
- A sample is tested by pumping it through the system for ~2 minutes and allowing colour to develop. The panel meter reading corresponds to the concentration of analtye in the sample. For example, using the above example of a 200 $\mu g\ L^{-1}$ standard, a reading of -0034 would correspond to a analyte concentration of 34 $\mu g\ L^{-1}$.

Colour Correction

- After calibration and without changing the Zero Adjust or Gain Adjust, place the colour reagent tube (R3) in de-ionised water.
- Pump a blank sample through the system and record the new blank value

- Pump the sample through the system. The difference between the sample value and new blank value is the natural colour of the sample. This can be subtracted from the measured concentration in the sample.

Following is a set of user instructions for each of the components involved in the system.

Modular Cell

The recommended path lengths for the various tests are as follows:

	Aluminium	**Colour**	**Iron**	**Manganese**	**Phosphate**
Path Length /cm	1.5	8	3	3	3

Rubber O-rings on either side of the glass windows seal the sample cell. The outlet should be placed above the inlet so the any air bubbles in the system rise to the outlet and are ejected from the cell.

Electronics

A layout diagram of the electronic circuits is included.

List of Components

LED Driver

IC1	-	LM351N, Comparator, (RS# 308-843)
IC2	-	AD654, Voltage to Frequency Converter, (RS# 637-860)
IC3	-	CA3140E, FET Op-Amp, (RS# 308-130)
C1	-	Connector, Reference output to Detector Circuit

Detector & Log-Amp

IC1	-	AD630 Balanced Modulator/Demodulator
IC2	-	ICL8048 Log Amplifier
IC3→IC6	-	CA3140E, FET Op-Amp, (RS# 308-130)
C1	-	Connector, input from Detector
C2	-	Connector, output to Panel Meter
C3	-	Connector, input from Zero Adjust
C4	-	Connector, input from Gain Adjust
C5	-	Connector, Reference input from LED Driver

Changes to Electronics

Selecting LED's

The LED Driver circuit can switch between one of three LED's. The connectors for these LED's are shown in the layout diagram. LED1 is the connector for the infra-red LED. On the driver board two switches must be changed to select an LED. For example to select LED3, position a jumper link at S3 in both switches. The fibre would then be connected to SMA#3.

Setting Detector Circuit for Attenuation Measurements

On the Detector & Log-Amp circuit, remove jumper link from J1. Place jumper links at position 1 of switches S1 and S2.

Setting Detector Circuit for Turbidity Measurements

On the Detector & Log-Amp circuit, place a jumper link at J1. Place jumper links in position 2 at switch S1 and position 1 at S2.

Checking Signal Intensities

Reduce Gain Adjust to minimum value. On the Detector & Log-Amp circuit, position a jumper link at position 2 of switch S2. On the LED Driver circuit the potentiometers, Pot#1, 2 &3, are used to adjust the LED intensities. Pot#3 corresponds to LED3 and so on. The adjustment screws are turned clockwise to increase signal intensity and vice versa. The full scale of the detector circuit corresponds to -0130 on the panel meter. LED intensities should be adjusted to just below this value, i.e. (~-0122).

Reagents and Sample Delivery System

The following reagents and LED's are required for the various tests.

	R1	R2	R3	LED
Aluminium	Acid	Buffer	Colour	Yellow
Iron	Acid	Buffer	Colour	Yellow
Manganese	Alkali	Buffer/Complexing	Colour	Blue (450 nm)
Phosphate	Acid	Conditioning	Colour	Red
Colour	-	-	-	Blue(420nm)
Turbidity	-	-	-	IR

Immerse the free ends of the labeled pumps tubes in the required reagent reservoir. Immerse the sample tube in the required sample. Turn on the pump in the forward direction and tighten the eccentric cams until sample and reagents are pumped through the system.

No reagents are required for the colour or turbidity configurations. A single sample tube to the cell is required.

Occasionally air bubbles become trapped in the cell. These can often be removed by reversing the direction of the pump, emptying the cell, and then changing back to pumping in the forward direction. It is advisable to carry out this procedure when initially setting up the system.

When using pre-acidified standards, as in the case of aluminium/iron, the acid reagent tube (R1) should be placed in de-ionised water while the standard in being pumped through the system.

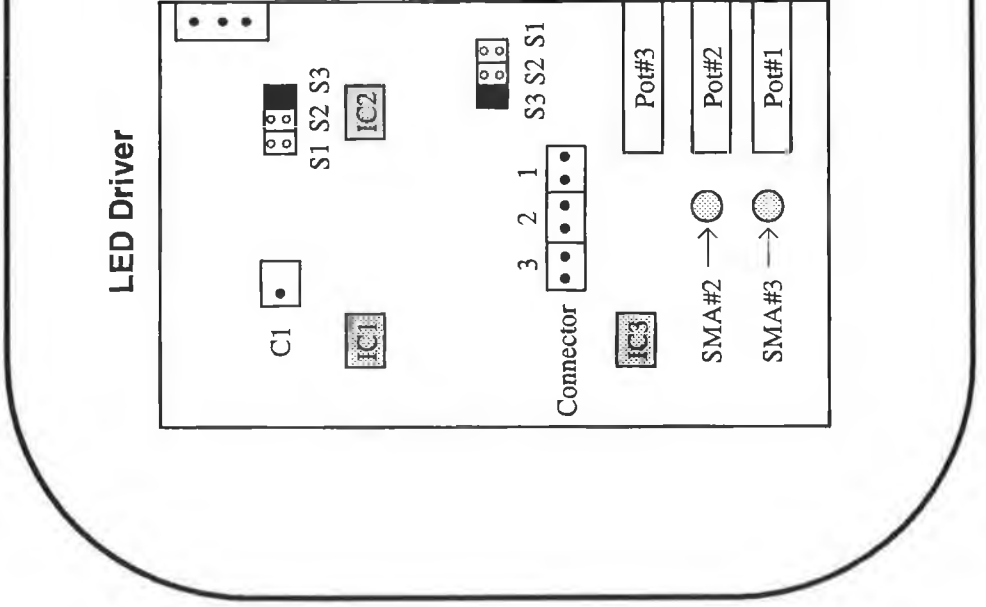

Fig. 1 LAYOUT DIAGRAM OF ELECTRONICS

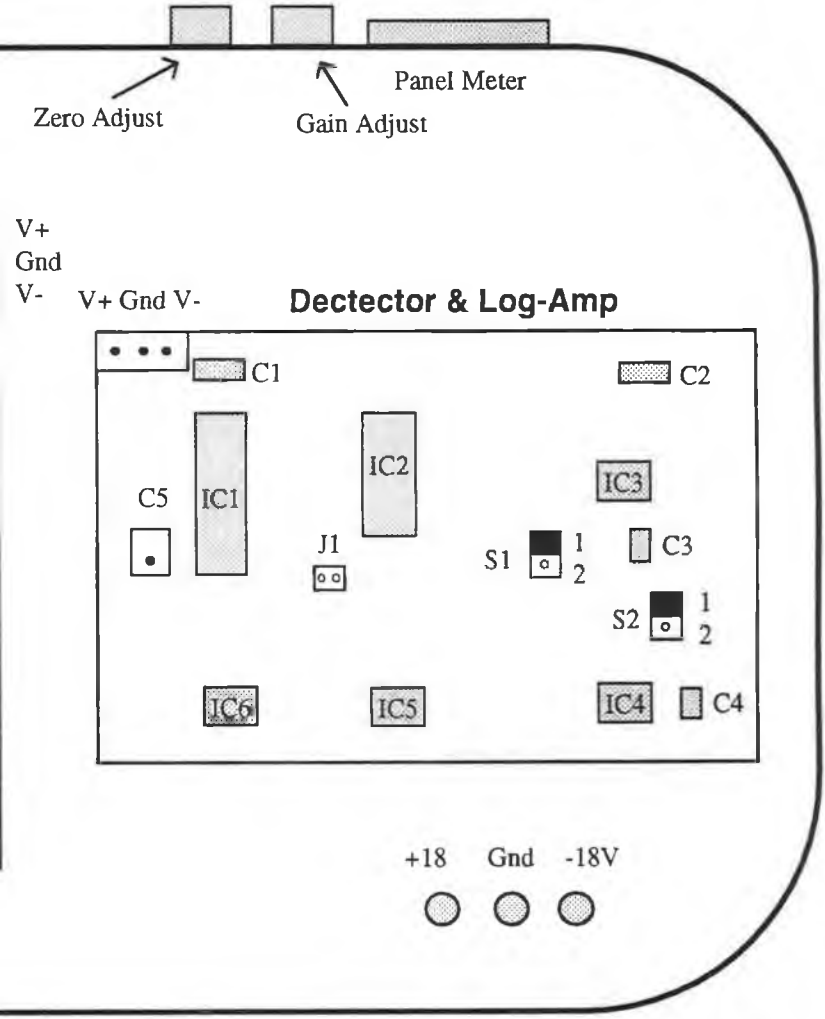
Zero Adjust
Gain Adjust
Panel Meter
V+
Gnd
V-
V+ Gnd V-
Dectector & Log-Amp
C1
C2
C5
IC1
IC2
IC3
J1
S1
1
2
C3
S2
1
2
IC6
IC5
IC4
C4
+18
Gnd
-18V